https://doi.org/10.59761/RCR5176

Nanoemulsions: composition, properties, production methods, and prospects for oil recovery

Andrey V. Minakov, Olesya P. Stebeleva

Siberian Federal University, 660041 Krasnoyarsk, Russian Federation

The global demand for energy necessitates an increase in the oil production efficiency in oil fields by means of enhanced oil recovery methods. Nanoemulsion technologies attract attention in the oil and gas industry as a way for improvement of the existing enhanced oil recovery methods. Nanoemulsion flooding is promising owing to the properties of nanoemulsions such as kinetic stability, controlled interfacial behaviour, and tunable rheology. However, nanoemulsion flooding is not widely used in oil fields as yet. There are only a few known pilot studies, which are described in this review. Nanoemulsion systems continue to rapidly develop: new generations of compositions with modified architectures and improved stability appeared in the last four years, but have not yet been systematized. This review is meant to fill this gap in the field of enhanced oil recovery, including analysis of alternative methods for the synthesis of nanoemulsions, by considering the benefits of fundamental and engineering aspects as well as drawbacks that hamper further development of this area and addressing the data unification issue.

The bibliography includes 273 references.

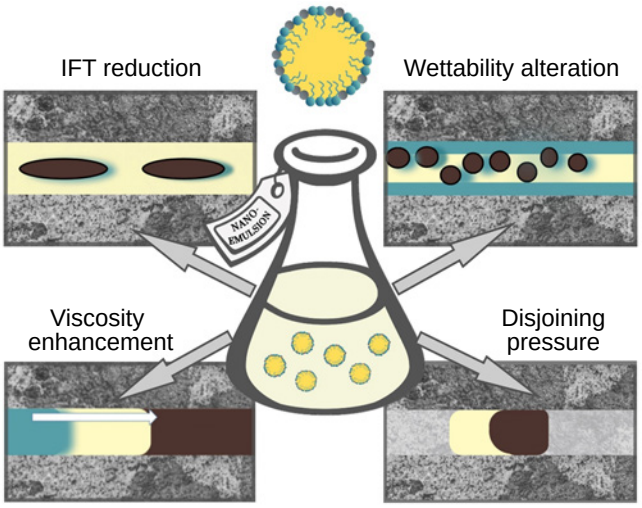

Keywords: nanoemulsion flooding, enhanced oil recovery methods, nanoparticles, nanoemulsions, surfactants, polymers, rheology, interfacial tension.

Contents

1. Introduction

Recent decades have witnessed declining oil recovery in oil-producing regions. The global demand for energy has necessitated enhancement of the oil production efficiency in old fields. As of 2024, Russia has the fifth largest oil reserves [10.9 billion tons according to the data of the US International Energy Agency (IEA) and 31.4 billion tons according to the

A.V.Minakov. Doctor of Physics and Mathematics, Professor, Director of the Institute of Engineering Physics and Radioelectronics, and Head of the Laboratory of Physico-Chemical Technologies for Hard-to-Recover Hydrocarbon Reserves of the Siberian Federal University. E-mail: tov-andrey@yandex.ru
Current research interests: heat and mass transfer in nanofluids, numerical modeling of thermophysical processes in fluids for the oil industry.

O.P.Stebeleva. Candidate of Technical Sciences, Senior Researcher at the Laboratory of Physico-Chemical Technologies for Hard-to-Recover Hydrocarbon Reserves, Associate Professor at the Department of Thermophysics and Hydrogasdynamics of the Polytechnic Institute of the Siberian Federal University.
E-mail: opstebeleva@mail.ru
Current research interests: high-energy synthesis of nanoemulsions, suspensions, processing of liquid fuels, including oil.
Translation: Z.P.Svitanko

Received 21 March 2025

estimates of the Russian Federal Agency on Subsoil Use, which includes hard-to-recover reserves], being inferior to Venezuela, Saudi Arabia, Canada, and Iran.[1–3] According to IEA, the global oil production from mature fields is declining by 5–8% every year, while the global energy demand will grow by 25% by 2040.[1] International investigations[2] and public data of the Russian Federal Agency on Subsoil Use[3] indicate that the primary methods using artificial lift and natural flow provide the recovery of 10–20% of reserves, while secondary methods (liquid/gas injection) can increase the total oil recovery factor to 20–40%. The remaining 30% of oil can be recovered using tertiary, that is, enhanced oil recovery methods (EOR), which involve heating or injection of gases and/or liquids. It is noteworthy that EOR methods are applicable at any stage of field development, despite the fact that in most cases, these techniques are utilized when primary and secondary methods have been exhausted. Therefore, EOR methods should be reasonably classified as methods that follow the primary oil production.

The enhanced oil recovery methods can be thermal,[4] microbiological,[5] electromagnetic,[6] gas,[7] water/gas,[8] and chemical. The goal of chemical methods is to enhance oil recovery by injection of special chemicals into the oil reservoir, which either decrease the water mobility (by decreasing the phase permeability) or change the capillary forces thus enhancing the oil displacement.

Chemical flooding is one of the most popular and important methods directed towards enhanced oil recovery from oil reservoirs. This method includes surfactant flooding technologies, polymer flooding, foam flooding, alkaline flooding, and so on. Among these methods surfactant flooding is used most widely; it decreases the interfacial tension of capillary trapped oil and enhances the production owing to variation of the physicochemical properties of the injected fluid, resulting in decreasing oil viscosity and increasing rock permeability.[9,10] The decrease in the interfacial tension (IFT) and formation of oil-in-water macroemulsions during the surfactant flooding are the major factors for enhanced oil recovery.[11,12]

The use of polymer flooding increases the viscosity of injected water, which in turn reduces the mobility ratio. This effect is beneficial for the oil recovery because it increases the swept area of the reservoir. The introduction of a polymer into these systems produces a very stable displacement front, which increases the overall efficiency of the displacement process by up to 90% *in situ*.[13]

Foam flooding provides diversion of the fluid from absorption zones to lower permeability areas. A critically important factor for the practical use of foam is the foam stability, that is, the ability to retain the initial structure for a specified period of time; therefore, apart from foaming agents, compositions should contain stabilizing agents (surfactants, polymers), which ensure compatibility of the solution with oil and thermodynamic conditions of the reservoir.[14]

In the case of alkaline flooding, the oil recovery is enhanced owing to emulsification of trapped residual oil, that is, a decrease in the oil–water interfacial tension as a result of formation of natural surfactants upon the reaction between the alkali and acidic components of oil and change in the rock wettability.[15] The alkaline reagent usually consists of a mixture of an alkali, surfactant, and polymer (ASP), compatible with the reservoir oil.

The described chemical flooding methods are generally aimed at increasing the macroscopic efficiency (sweep efficiency) and/or microscopic efficiency (pore level displacement efficiency). The use of such compositions increases the oil recovery *via* several mechanisms: (1) decrease in the interfacial tension between oil and the flooding solution ($<10^{-3}$ mN m^{-1}); (2) spontaneous emulsification of trapped oil; (3) change in the interfacial rheological properties at the oil–flooding solution interface; (4) control of the rock wettability for optimization of oil displacement.

However, these methods are not free from drawbacks. For example, surfactant flooding generates an unfavourable mobility ratio between the crude oil and injected fluid, which allows the surfactant solution to enter highly permeable layers of the oil reservoir. In the case of polymer flooding, the polymer hampers penetration into the pores due to generation of selective barriers: the polymer plugs capillaries and generates low-permeability layers due to the difference between the sizes of polymer and oil molecules.[16] In the case of flooding with ASP solutions, the presence of an alkali promotes the formation of salt deposits, which contaminate the oil reservoir. Many of these contaminations and damages are persistent and have a pronounced adverse effect on the subsequent operation of oil fields.[17] Thus, at high temperatures and high salinity of the formation water (brine) in complex reservoirs, the foam becomes unstable, the bubblies coalesce, the alkaline reagent and the surfactant are adsorbed on the reservoir rock, and polymers decompose thus restricting the oil production.

Nanotechnology is attracting attention in the oil and gas industry as a way to improve the existing methods of enhanced oil recovery. As a strategy of implementation of such methods, the use of nanofluids, nanoemulsions, and nanoparticles of various sorts and in various combinations has started to be extensively investigated. The use of nanoemulsion flooding on the laboratory and pilot scales has shown a significant increase in oil recovery due to the integrated effect on the key physicochemical processes.[18,19] This technology shows high efficiency owing to the ability to optimize oil emulsification processes directly under reservoir conditions, while eliminating the mobility imbalances and smoothing the displacement front. A considerable contribution to the increase in the oil displacement efficiency is made by the decrease in the surface tension at the interface between the reservoir oil and the injected fluid. An additional effect is attained because of alteration of the rock wettability and improvement of the reservoir porosity and permeability characteristics *via* increase in the effective permeability. This multifactorial approach provides the full implementation of the potential of nanoemulsion technologies for enhanced hydrocarbon production.

Like other emulsions, nanoemulsions can be of two types, oil-in-water (O/W) and water-in-oil (W/O) ones. In the literature emulsions are commonly classified into nanoemulsions, microemulsions, and macroemulsions. All types of emulsions are usually stabilized by surfactants. In O/W systems, water is the continuous phase, while the hydrophobic tails of the surfactant are directed inside the oil droplets. In the W/O system, the oil phase is continuous and the hydrophilic heads of the surfactants are directed towards the inner part of the water droplets.

Before the mid-20th century, emulsions were classified in terms of the dispersed phase (O/W or W/O) and practical properties rather than the droplet size. The cause for this is obvious: the techniques for measuring nanoscale sizes (10–100 nm) such as electron microscopy and dynamic light scattering appeared only in the 1930s–1970s. To our knowledge, the term ‘microemulsion’ was used for the first time in 1961 to denote the droplet size of 10–60 nm,[20] while the term

'nanoemulsion' appeared in 1996[21] for the 200–250 nm range of droplet size and then for 300 nm size.[22] The International Union for Pure and Applied Chemistry (IUPAC)[23] gives a clear criterion only to distinguish between micro- and macroemulsions:

— microemulsions (10–100 nm, thermodynamically stable),

— macroemulsions (1–100 μm, kinetically slightly stable, thermodynamically unstable).

Despite numerous publications including reviews,[18,24–26] there is no commonly accepted particle size that could be used as the final criterion to distinguish between nanoemulsions and microemulsions. A variety of droplet size ranges for nanoemulsions can be found in the literature: ~100 nm,[27–29] 10–100 nm,[30,31] 10–500 nm,[32–34] and 10–600 nm.[35] Nanoemulsions are usually defined as systems with droplet size of up to 200 nm, but some sources extend the upper limit to 600 nm. It follows from the presented sources that the limit of 200 nm is the commonly accepted theoretical standard, while a greater limit is acceptable for real applications (most often, for dosage forms) if the emulsion preserves the kinetic stability (does not separate into layers) and the droplets possess properties typical of the nanoscale range. Thus, in practice and in industry, the droplet size range for nanoemulsions is extended to 600 nm if the system meets the key criteria including stability and functionality. The absence of a common definition reflects the integrated nature of the phenomenon. As applied to EOR, the critical factor is not the size of emulsion droplets, but their ability to penetrate into pores, reduce the interfacial tension, and remain stable in the reservoir rock.

The performance characteristics of emulsions are determined by their resistance to various destabilization mechanisms: thermodynamic stability (the ability of the system to maintain a minimum free energy is characteristic only of microemulsions), kinetic stability, including aggregative resistance to flocculation and coalescence provided by van der Waals forces (*i.e.*, electrostatic, steric, and other forces), and sedimentation stability, *i.e.*, the ability to resist gravitational phase separation determined by the balance between gravity, Brownian motion, and viscosity of the dispersion medium. These types of stability can vary independently of each other as functions of the system composition and conditions, as they are determined by different physicochemical mechanisms.[25]

There are important differences between nanoemulsions and microemulsions. Nanoemulsions are thermodynamically unstable systems that are kinetically stable against phase separation and require energy expenditures for the formation. This means that a nanoemulsion will be stable for a certain period of time, but will undergo irreversible phase separation after a sufficient period of time. Microemulsions are thermodynamically stable and are spontaneously formed at optimal component ratios and at high concentrations of surfactants (usually 15–25%).[36] Conversely, nanoemulsions are kinetically stable systems that require external impacts for the formation, but can achieve stability at much lower surfactant concentration. Recent studies have shown that optimization of the composition and preparation method makes it possible to generate nanoemulsions with surfactant concentration of only 1–10%, which is a significant practical advantage over microemulsions.[37] In turn, macroemulsions remain thermodynamically unstable systems with limited kinetic stability. The stability of nanoemulsions is mainly provided by the interfacial adsorption of surfactants on the droplet surface and depends on the preparation method. Meanwhile, microemulsions are formed spontaneously and show a more complex pattern of surfactant distribution, since micelle formation processes take place in the medium apart from the interfacial adsorption.

The small droplet size in nanoemulsions makes them resistant to physical destabilization *via* gravity separation, flocculation, and/or coalescence. Nanoemulsions are resistant to phase separation because the Brownian motion in them is sufficient to overcome the low gravitational separation force. They are also resistant to flocculation due to highly effective steric stabilization.

The resistance to precipitation is provided by the Brownian motion of the nanodroplets, which counteracts the gravity sedimentation, but for particle size approaching the upper limit (500 nm), the gravity separation can take place, especially if the difference between the densities of the phases is high or the viscosity of the medium is low. Flocculation and coalescence can be prevented by steric or electrostatic stabilization; the stability is provided by not only small droplet size, but also the presence of stabilization agents that generate an electrostatic and steric barrier. In the absence of stabilizing agents, even nanoemulsions can aggregate upon the change in the conditions (pH, ionic strength, temperature). Thus, the stability of nanoemulsions is determined not only by the droplet size, but also by the composition of the system and external factors.[34] For the use in oil production, the key factor is not the stability of an emulsion at rest, but its behaviour during filtration through the rock under reservoir conditions (temperature, pressure, mineral composition). The small size of droplets helps them to penetrate into the pores, but the long-term stability depends on composition of the formation water, temperature, and pressure.

The interest in the development and in oil and gas application of nanoemulsions is growing. This is related to their unique properties such as low interfacial tension, large surface area of the droplets with respect to the total volume, change in the surface wettability, stability to the environmental and reservoir conditions, and high ability to bind and emulsify reservoir oil.[38–42] According to modern studies, the stability period of model nanoemulsions under typical reservoir conditions (temperature of 60–120°C, salinity of 50 000–200 000 ppm, and a pressure of 10–50 MPa)[43] varies from one week to a few months. Model microemulsions, although show storage stability of up to a year, require large volumes of expensive thermally stable surfactants and are sensitive to the composition of reservoir water.[44] The reservoir medium has a considerable effect on the long-term stability of nanoemulsions: for example, the destabilization rate of nanoemulsions in carbonate reservoirs is 30–40% higher than that in sandstones.[45,46] This directly affects the nanoemulsion production method, requiring development of formulations with adaptive properties: thermal stability of up to 150°C, salinity tolerance above 250 000 ppm, and rheological characteristics (50–500 MPa s viscosity) tailored to particular reservoir conditions.[47,48]

Nanoemulsion systems continue to be actively developed: new generations of compositions with modified architecture and enhanced stability have appeared over the last four years, but they have not been systematized. This review fills this gap in the field of enhanced oil recovery by analyzing the benefits of fundamental and engineering aspects as well as drawbacks that hamper further development of this area and addressing the data unification issue. Many concepts developed for other fields[49–53] have been adapted for the application in oil and gas industry. However, the research related to oil exploration and production must take into account a wide range of physicochemical conditions that are rarely found in other areas, such as high temperature and high salinity. In addition, EOR methods usually

require injection of hundreds of tons of various chemicals. In this respect, nanoemulsion systems have a considerable advantage over microemulsions. In the large-scale flooding operations, even a few percent difference in the required amounts of active components for nanoemulsions and microemulsions makes it possible to save tens of tons of expensive surfactants. These features emphasize not only the necessity of rational design of nanoemulsions, but also the importance of economic optimization of these design products.

In this review, we give examples of application of nanoemulsions in the basic production operations in the oil and gas industry and emphasize the unique properties of nanoemulsions that are applied or are potentially applicable in these processes, analyze methods for the synthesis to attain these properties, identify particular problems related to large-scale use of nanoemulsions in EOR processes, and consider the potential and promising lines for the future research.

2. Mechanisms of nanoemulsion flooding

Emulsions increase the recovery of both residual and heavy oil through a variety of mechanisms,[47] including the reduction of the interfacial tension to low or ultralow values (Fig. 1 *a*); change in the rock wettability (Fig. 1 *b*); improvement of the sweeping efficiency of the displacing fluid due to increase in its viscosity (Fig. 1 *c*); and the disjoining pressure effect (Fig. 1 *d*). The stability of nanoemulsions under reservoir conditions allows them to perform more efficiently than other flooding systems.

High IFT values and low capillary numbers (10^{-7}–10^{-6}) in the reservoirs are due to immiscibility of water and crude oil during flooding. This fact restricts the displacement efficiency, which results in a poor oil recovery and high water cut. As opposed to water flooding, in the case of nanoemulsion flooding, the greater surface area and interfacial activity of nanoemulsion droplets during flooding enhance the interaction between nanoemulsion droplets and residual oil spots and allows the nanoemulsion droplets to form a film on the crude oil surface. As a result, capillary forces (with reduced IFT and increased capillary number) would provide enhanced recovery.

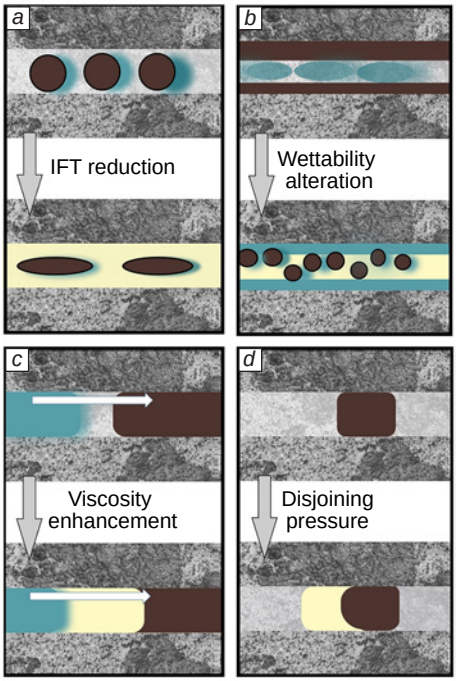

Figure 1. Mechanisms of emulsion interaction during oil production from reservoirs: (*a*) reduction of the interfacial tension to low or ultralow values, (*b*) alteration of the rock wettability, (*c*) enhancement of the sweeping efficiency by increasing the viscosity of the displacing fluid and/or decreasing the viscosity of the phase being displaced, and (*d*) disjoining pressure effect. IFT is the interfacial tension.[47]

The EOR efficiency depends also on the rock wettability, which is determined by heterogeneous composition of minerals. The wettability of reservoir rock surfaces can range from completely oil-wet to completely water-wet. The wettability alteration is shifting of the starting reservoir rock wettability towards wetting with water in order to increase the oil recovery. The mechanism of nanoemulsion flooding is that nanoemulsion droplets easily enter the pores and are adsorbed on the rock surface, thus coating the surface and altering the wettability.[54] The nanoemulsion injection gives rise to ion-pair (cationic/anionic) and electron polarization (non-ionic) interactions between the oil phase adsorbed on the rock surface and surfactant monomers present in the continuous phase of the nanoemulsion.[55,56] This is followed by pulsed absorption of water into the rock matrix in low-permeability zones followed by oil displacement. In addition, easy migration of nanosized droplets in porous media alters the wettability of reservoir rocks to the completely water-wet state.[57] Thus, crude oil is separated and released into the injected medium, resulting in increased oil production.

The adsorption of a nanoemulsion on the rock surface depends on hydrophobic interactions between the oil-wet surface and the surfactant molecules in the nanoemulsion (Fig. 2).[58] A stable nanoemulsion effectively breaks the adhesive bonds between reservoir oil and rock, that reducing the separation energy through synergistic effects on the interfacial tension and wettability. The observed decrease in the energy of oil separation from the rock with time is due to the migration of nanoemulsion droplets towards the oil–rock interface, the subsequent reorientation of surfactant molecules at the interface, and the formation of hydrophobic domains due to the adsorption of nanoparticles. This process caused by increasing local hydrophobicity of the contact surface leads to effective detachment of the oil phase from the rock.[58]

The rheological properties of nanoemulsions influence their infiltration into reservoir capillaries and control the migration in pore channels, pore plugging, and displacement efficiency in porous media. The non-Newtonian behaviour of nanoemulsions is an indication that they represent a suitable chemical component (plug) for mobility control. The injection of nanoemulsions into the reservoir affects the capillary forces, which hold crude oil in the reservoir pores.[59] Under shear conditions during injection, the structure of the nanoemulsion is distorted and then it is restored owing to viscoelastic properties as soon as the nanoemulsion enters the reservoir capillaries containing residual oil. Due to the fact that nanoemulsions usually have higher effective viscosity and are more prone to exhibit non-Newtonian properties than microemulsions, they provide a better oil recovery, owing to the ability to smooth down the displacement profile by directing the liquid flow from high-permeability to lower-permeability zones.

The nanoemulsion droplets are adsorbed at the interface between oil sand and water in various zones because of variable adsorption rates. The adsorption of nanoemulsion droplets at the interface generates spatially inhomogeneous IFT distribution, *i.e.*, gives rise to high-IFT and low-IFT regions.

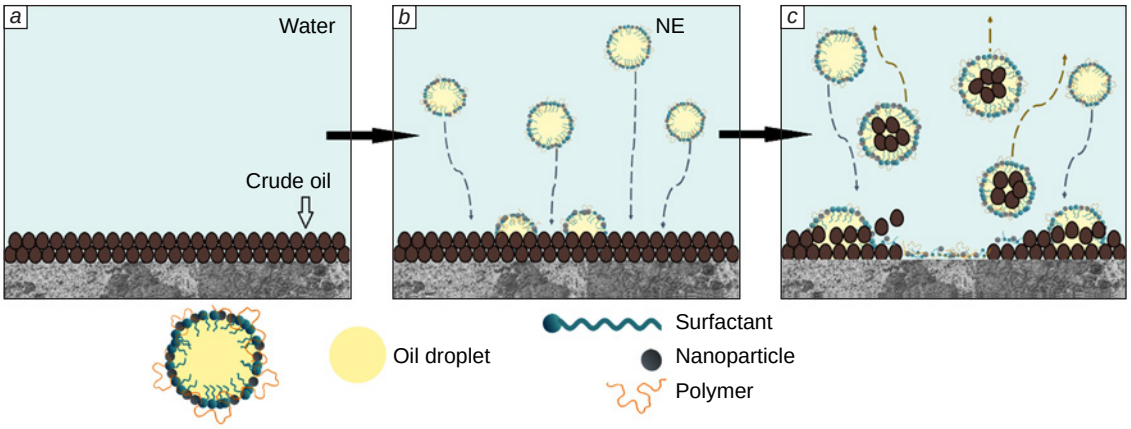

Figure 2. Mechanism of action of nanoemulsions on the rock wettability: (*a*) oil-saturated state; (*b*) nanoemulsion (NE) as O/W phase injected into the reservoir; interaction between nanoemulsion droplets and crude oil deposited on the rock surface; (*c*) displacement of crude oil by emulsifier molecules and oil sweeping by the nanoemulsion.[58]

This induces interfacial turbulence, that is, liquid flow from low-IFT to high-IFT region; as a result, the oil film on the reservoir rock is stretched to form oil droplets. Due to anisotropy of interfacial energy, the oil droplets and water are emulsified to form an emulsion, which decreasies the viscosity of crude oil and, hence, improves the sweep, that is, the percentage of pore volume involved in the oil production. The role of the Marangoni effect in heavy oil production has been investigated.[47,60,61] The Marangoni effect is manifested as a non-uniform distribution of nanoemulsions at the oil–water interface due to different nanoemulsion adsorption rates. In this case, the IFT of the oil–water interface is different in some local areas. A surface characterized by higher IFT pulls the surrounding liquid more intensively than a lower-IFT surface. As a result, oil nanodroplets generate a surface tension gradient, which allows for both the interfacial turbulence and mass transfer. Finally, crude oil droplets are pulled out of the oil phase and form emulsions with water, which thus increases the mobility of crude oil.[62]

The disjoining pressure is defined as an excess liquid pressure in the film between reservoir oil and rock as this film becomes sufficiently thin. A narrow layer is formed upon injection of the nanoemulsion into the interface between the oil and the reservoir rock. If the thickness of this layer is fairly small, intermolecular forces (van der Waals interactions) start to play a predominant role. These forces give rise to a pressure that exceeds the capillary or hydrostatic pressure of the bulk fluid. Exactly this excess pressure arising in a compressed nanoemulsion film is defined as the disjoining pressure. This pressure disjoins, that is, it generates local forces capable of detaching oil from the rock surface. This helps to overcome the adhesive forces between oil and rock and, hence, improves the oil recovery. The key issue is that the interlayer between oil and rock should be sufficiently thin. As the thickness of this interlayer decreases, the force effects become much more pronounced, and the arising pressure may considerably exceed the liquid phase pressure outside this narrow range. In the pores, nanoemulsion droplets are arranged as well-ordered layers. The very high freedom of movement of the droplets leads to increasing entropy and generates additional disjoining pressure at the interface, which detaches the oil film from the rock surface and mobilizes (detachment and movement) the film.

In the case of water flooding, viscous fingering effect arises because of reservoir inhomogeneity, considerable mobility difference between the displacing fluid and crude oil, which decreases the displacement efficiency (Fig. 3).

Nanoemulsions enhance the displacement through the Jamin effect: the droplets entrapped in the pores selectively block the most permeable paths, thus forcing water to move through low-permeability zones and displace residual oil. In oil production, this helps to stabilize the displacement front and improves the reservoir sweep, which increases the efficiency of oil recovery.[63] That is, the cause is the appearance of additional counter-pressure in the porous medium generated by the movement of droplets or bubbles through capillaries of variable radius and shape. The unequal radii of curvature of the menisci r_1 and r_2 at the interfaces give rise to capillary forces, which hinder the movement of the gas–liquid mixture by blocking pore channels and increasing the flow resistance (Fig. 4).[45] There are three ways of blocking caused by emulsion droplets in the pores and channels: (1) one large droplet plugs a pore (Fig. 4*a*); (2) a few emulsion droplets form a bridge in a pore or channel (Fig. 4*b*); (3) ultrafine droplets are adsorbed in a pore or channel, thus reducing the channel or pore diameter and causing blockage (Fig. 4*c*).[45]

3. Composition of nanoemulsions

Discussion of the components of a nanoemulsion provides understanding of the scientific fundamentals for the nanoemulsion behaviour, which is ultimately a function of their composition. A typical nanoemulsion consists of two immiscible liquids, *i.e.*, a nonpolar phase (oil phase) and a polar phase

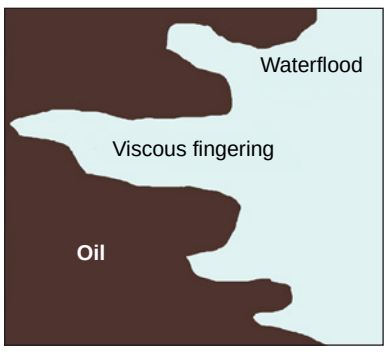

Figure 3. Viscous fingering effect upon water flooding of an oil formation.

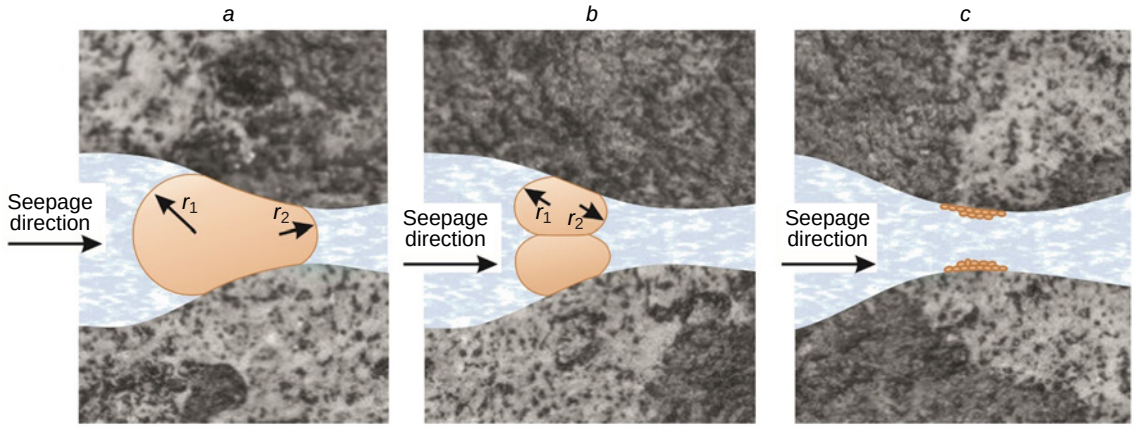

Figure 4. Basic diagram of emulsion plugging of pore channels: (*a*) one large droplet, (*b*) a few droplets, (*c*) ultrafine emulsion droplets.[45]

(water) stabilized by emulsifiers/surfactants, polymers, and, in some cases. solid nanoparticles.[64]

3.1. Water and oil phase

The oil phase is usually a nonpolar oil, including vegetable and mineral oils based on short-chain hydrocarbons and long-chain triacylglycerols, because they are readily available and inexpensive, monoacylglycerols, diacylglycerols, *etc*. The method of synthesis, stability, and functional characteristics of a nanoemulsion depend on the properties of the oil component, such as density, viscosity, and interfacial tension.

The formation of nanoemulsions for oil and gas applications requires thorough selection of the hydrocarbon phase, because the industrial process implies injection of considerable amounts of fluid into the reservoir. Stability of the nanoemulsion under reservoir conditions, prevention of reservoir damage by using an appropriate droplet size distribution, environmental compatibility, economic feasibility, and high efficiency are crucial factors for the selection of the hydrocarbon phase. Considering these factors, various authors used different products as the oil phase (Table 1). The listed oils do not exhaust the available options, but these are oils of choice due to their ready availability, economic feasibility, and environmental friendliness (*e.g.*, the use of secondary raw materials).

Generalization of the results (see Table 1) is complicated by the data diversity and lack of a unified approach to the preparation and testing of emulsions. To increase the comparability and practical applicability, it is necessary to use standard procedures and take into account particular oil deposit conditions to select the compositions of emulsion systems. The chosen oil type and volume fraction in a nanoemulsion determine the nanoemulsion characteristics in terms of stability, migration behaviour, and, hence, the ability to plug pores. Effective plugging takes place if viscous oil is used, since it increases the frictional resistance. However, if the viscosity is too high (> 10 000 cP), oil droplets begin to behave as solid particles, which can lead to demulsification and formation damage.[80,81]

The properties of a nanoemulsion are strongly dependent on the oil volume fraction, which determines the mechanisms of action in the EOR processes. When the oil content is low (5–15 vol.%), a nanoemulsion has a high stability and good mogration behaviour. These systems are effective for reservoir oil displacement by reducing the interfacial tension, microdestruction of oil films, and selective plugging of fractures. These emulsions are readily injected into a reservoir and effectively penetrate into small pores, but have a moderate ability to displace viscous reservoir oil.[67,75,76] Nanoemulsions with an intermediate oil content (15–30 vol.%) show balanced properties. They combine a moderate viscosity with good displacing and plugging performance. These systems effectively displace oil by altering the rock wettability and simultaneously provide controlled blockage of highly permeable zones. This makes these systems a versatile solution for most EOR processes.[71,74,79] A high content of oil (more than 30 vol.%) endows nanoemulsions with specific properties. In particular, increased viscosity and strong plugging ability result in the formation of mobile 'oil plugs' for the displacement of reservoir oil and deep blockage of water channels. These systems are particularly effective for viscous oils, but can cause complications during injection due to the risk of pore clogging.[62,78]

The choice of the optimal oil content depends on the operating mechanism of EOR. Systems containing 10–20 vol.% oil are more appropriate for reducing the interfacial tension and enhancing the displacement. Concentrations of 25–35 vol.% are more efficient for water channel plugging. Dealing with high-viscosity and ultrahigh-viscosity oil deposits may require systems containing 30–40 vol.% oil, but thorough selection of emulsifiers is needed in this case to ensure stability. The particular composition depends on reservoir characteristics, reservoir oil properties, and used surfactants.

The rheological properties, interfacial tension, polarity, and ionic strength of nanoemulsions are mainly determined by the polar phase. The polar phases used most often in laboratory studies include deionized water,[82] distilled water,[70] and sea water with a salinity of 5 to 300 g L^{-1}.[76] The destruction of nanoemulsions with separation of oil and water phases may follow three main mechanisms: coalescence (irreversible droplet merging upon contact), flocculation (reversible aggregation without merging, which may but does not always lead to phase separation), and Ostwald ripening (isothermal growth of large droplets *via* dissolution of small ones). Each mechanism is characterized by particular droplet growth kinetics, critical stability factors, and degree of reversibility of the process.[83]

The polar components of crude oil such as asphaltenes, resins, and fatty acids, being located at the oil–water interface, behave as surfactants and promote the formation of W/O emulsions *in situ*.[12,84,85] Among all oil components, asphaltene molecules play a particularly important role in the formation of emulsions.[86] On contact with salt water, asphaltene molecules diffuse to the oil–water interface and form strong bonds with cations of the aqueous phase, especially Mg^{2+} and Ca^{2+}. Other

Table 1. Some examples of nonpolar phase of emulsions for enhanced oil recovery methods.

Nonpolar phase	Emulsion type, droplet size	Concentration of the nonpolar phase	Components	Properties	Ref.
Sunflower oil	Nanoemulsion, average size of 190 nm	10 vol.%	No additional components[a]	Kinetic stability: two weeks of storage at room temperature and at 4°C without phase separation	65
Pine oil	Microemulsion, average size of 100 nm	50 vol.%	Surfactant: fatty acid sodium salts	Thermodynamic stability Viscosity of 32 mPa s Oil recovery: 87.5%	66
Palm oil	Microemulsion, 10–100 nm	10 vol.%	Surfactant: a mixture of alkyl polyglycoside (APG) and glyceryl monooleate (GM) Salt: NaCl	Thermodynamic stability IFT 0.0002 mN m^{-1} Oil recovery: 71.8 %	67
Kerosene	Nanoemulsion, 70–100 nm	0.0186 mass %	Surfactant: a mixture of sodium dodecylbenzene-sulfonate (SDBS), ethoxylated alkylphenol (OP), and n-butanol	Kinetic stability IFT 0.091 mN m^{-1} Oil recovery 33.2 % Alteration of rock wettability	68
Heptane oil (n-heptane)	Nanoemulsion, average size of 148 nm	10 vol.%	Surfactant: 1-methyl-3-hexadecylimidazilium bromide Salt: NaCl Alkali: Na_2CO_3	Kinetic stability for up to 7 days Oil recovery: 79% (in sandstone) and 77.3% (in carbonate rock) Alteration of rock wettability	39
	Nanoemulsion, average size of 98 nm	10 vol.%	Polymer: PEG 6000 Surfactant: Tween 40 Nanoparticles: SiO_2	Kinetic stability for 20 days Additional oil recovery: 27.82%	69
Decane oil (n-decane)	Nanoemulsion, average size of 192 nm	10 vol.%	Surfactant: α-olefin sulfonate (AOS) Salt: NaCl	Kinetic stability IFT 26.42 mN m^{-1} Additional oil recovery: 23.97% Alteration of rock wettability	70
	Nanoemulsion, average size of 172 nm	10 vol.%	Surfactant: AOS Nanoparticles: Al_2O_3 Salt: NaCl	Kinetic stability IFT 13.89 mN m^{-1} Additional oil recovery: 17.71% Alteration of rock wettability	
Crude oil	Nanoemulsion, average size of 35 nm	5 vol.%	Surfactant: a mixture of bioemulsifiers, mono- and dirhamnolipids	Kinetic stability for 30 days IFT 3.4 mN m^{-1} Viscosity: 1.2–1.5 mPa s Demulsification upon addition of HCl	62
	Nanoemulsion, average size of 183 nm	20 vol.%	Surfactant: SDBS Salt: NaCl	Kinetic stability for 30 days Viscosity: ~20–40 mPa s at low shear rates (10–100 s^{-1}) Demulsification upon addition of 0.5 M HCl	71
	Nanoemulsion, 160–650 nm	50 vol.%	Surfactant: imidazolium bromide dimer [$C_n$im–C4–imC_n][Br_2] Salt: NaCl and $MgCl_2$	Kinetic stability for 7 days IFT 0.0032 mN m^{-1}	72
Transmission oil (EPX 90)	Macroemulsion, average size of 5 μm	5 vol.%	No additional components[b]	Kinetic stability for 6 h Additional oil recovery: 23%	73
Lubricating oil (Hindustan Petroleum Corporation Ltd)	Macroemulsion, 2–7 μm	25 vol.%	Polymer: polyacrylamide (PAA) Surfactant: sodium dodecyl sulfate (SDS)	Stability in the formation brine Thermal stability 318–334 K IFT 1.1 mN m^{-1} Viscosity: 0.19 Pa s at a shear rate of 1 s^{-1}	74
			Polymer: PAA Surfactant: SDS Nanoparticles: SiO_2	Stability in the formation brine. Thermal stability: 346–371 K IFT 0.13 mN m^{-1}	74
			Polymer: PAA Surfactant: SDS Nanoparticles: CuO	Stability in the formation brine Thermal stability: 331–360 K IFT 0.2 mN m^{-1}	74
			Polymer: PAA Surfactant: SDS Nanoparticles: clay Salt: NaCl	Stability in the formation brine Thermal stability: 356–384 K IFT 0.09 mN m^{-1} Viscosity: 0.19 Pa s at a shear rate of 1 s^{-1}	74

Table 1 (continued).

Nonpolar phase	Emulsion type, droplet size	Concentration of the nonpolar phase	Components	Properties	Refs
Synthetic mineral oil (Nice Chemicals)	Nanoemulsion, average size of 22.8 nm	5 vol.%	Surfactant: Tergitol 15-S-12 Salt: NaCl	Kinetic stability IFT ~ 10^{-3} – 10^{-2} mN m^{-1} Pseudoplastic behaviour Additional oil recovery: 23.3%	75
Biodiesel	Macroemulsion, 1–2 μm	10 vol.%	Surfactant: cetyltrimethylammonium bromide (CTAB) Nanoparticles: SiO_2 Salt: NaCl	Kinetic stability for several months Pseudoplastic behaviour Additional oil recovery: 50.01%	76
Liquid paraffin	Nanoemulsion, 2.7–43.8 nm	21 mass %	Surfactant: a mixture of Span-80 and Tween-80	Kinetic stability for 25 days at 50°C Salt stability at 100 g L^{-1} of NaCl or $CaCl_2$ Oil recovery: 82.92%	77
Medicinal grade white oil Marcol 52	Nanoemulsion, average size of 86 nm	50 vol.%	Surfactant: copolymer of oxypropylene and oxyethylene esters of fatty acids Salt: NaCl	Kinetic stability for up to 12 months Thermal stability at 5–55°C IFT 2 mN m^{-1}	78
Waste cooking oil	Nanoemulsion, average size of 262 nm	20 vol.%	Surfactant: a mixture of Tween 80 and Span 80	Kinetic stability for 4 days IFT less than 0.001 mN m^{-1} Oil recovery: 63.89%	79

[a] Synthesis by a combination of membrane emulsification and ultrasonic dispersion methods without surfactants; [b] synthesis by mechanical stirring (up to 3000 rpm) without surfactants.

physical properties of the aqueous phase, such as ionic strength, viscosity, pH, and density and the operating conditions such as temperature and pressure are important factors that should be considered to study the formation of emulsion systems.[87,88]

The effect of water salinity on the stability of emulsions has been addressed in many studies, according to which a decrease in the salinity/ionic strength of water to a certain level can improve the stability of W/O emulsions by reducing the interfacial tension.[89,90] Hence, there is an optimal range of salt concentrations (50–80 g L^{-1}), in which emulsions are stable, but outside this range they are separated into layers.[91,92] The stability of W/O emulsions is controlled[89] by the ionic strength of the aqueous phase: an increase in the salinity decreases the stability of emulsions due to salting-out of natural stabilization agents and is determined by the types of ions the contribution of which to the stabilization decreases in the series: $Mg^{2+} \geqslant Ca^{2+} > SO_4^{2-}$ (cations are bound more actively to the polar components of crude oil). The simultaneous presence of SO_4^{2-} with Mg^{2+} or Ca^{2+} increases the stability as a result of balanced interaction; however, an excess of sulfates with deficiency of the cations leads, on the contrary, to fast phase separation of emulsions. The optimal stability was found for a narrow range of water salinity in the Persian Gulf (about 5 g L^{-1}), in which a moderate ionic strength is combined with a balanced concentration of potential-determining ions. High temperature (~80°C) accelerates[93] the phase separation of emulsions, with divalent cations being more beneficial for emulsion stability than monovalent cations. Detailed analysis of hydrogen bonds, distribution of water and ions, and change in the average size of water droplets in W/O crude oil nanoemulsions suggests[94] the existence of different degrees of ion hydration in small and large droplet systems: small water droplets with a radius of 1. 86 nm have a large surface area to volume ratio and, therefore, they cannot provide a strong ion hydration, while large droplets with a radius of 3.10 nm are capable of pronounced hydration of ions, which leads to a decrease in the attraction between model asphaltenes and water. Thus, the control of ion hydration by varying the salt concentration and the size of water droplets may provide a stable W/O nanoemulsion and controlled demulsification.

However, the formation of thick W/O emulsions during water flooding of heavy oil reservoirs may induce pronounced pressure variation or block the reservoir channels.[95,96] The rock wettability is a highly important parameter for maintaining the emulsion phase. The water-to-oil ratio defines the discontinuous and continuous phases; therefore, small changes in the phase ratio can change the interaction mechanism of additives (surfactants, polymers, nanoparticles), resulting in a change in the type of nanoemulsion. In addition, the volume ratio of water and oil in the nanoemulsion affects the viscosity of the whole system and, hence, the droplet formation kinetics, stability of the nanoemulsion, and hydrodynamics of the liquid flow.

For the selection of injection parameters (pressure, flow rate), O/W emulsions are preferred, while W/O emulsions are better for well stimulation.[97] This is due to the fact that O/W emulsions have a moderate viscosity, similar to the viscosity of water, which accounts for good injection and flow behaviours, whereas W/O emulsions have a higher viscosity compared to that of crude oil, which complicates the injection and causes a considerable pressure drop in the displacement profile.[98] An increase in the viscosity of the oil phase and interfacial tension improves the displacement control in parallel sandpacks with a permeability ratio of 4.57. The fractional flow of the low-permeability sandpack exceeds that of the high-permeability sandpack during injection of the emulsion. An increase in the reservoir oil viscosity enhances the resistance to the flow of emulsion droplets in the pores, thus increasing the pressure differential (Fig. 5).[99] The interfacial tension equal to 0.24 mN m^{-1} simultaneously increases the plugging effect and maintains the system mobility. An additional control is attained by adjustment of emulsion droplet size and fractional composition.[99]

Oil-in-water nanoemulsions allow effective control over the filtration *via* controlled pore plugging in high-permeability

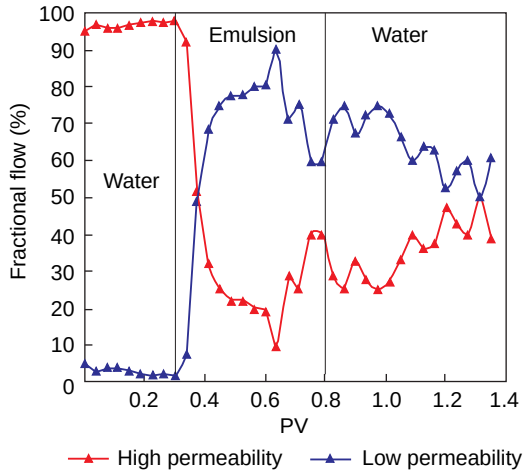

Figure 5. Fractional flows of O/W emulsion with IFT = 0.24 mN m^{-1} in sandpacks depending on the pore volume (PV).[99] Copyright belongs to Elsevier.

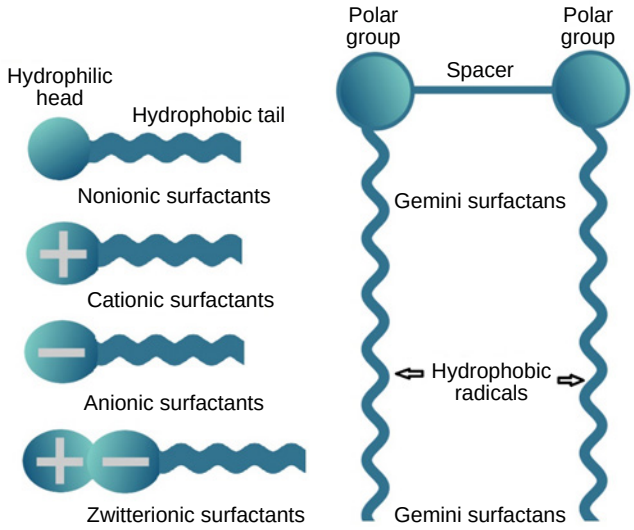

Figure 6. Schematic picture of various types of surfactants and structure of dimeric (gemini) surfactants. In reality, there are also surfactants with two or more hydrocarbon tails; the Figure depicts a simplified classification to provide basic understanding of surfactant structures and action mechanisms.

zones. The droplet size polydispersity provides a wide range of penetration and selective decrease in the permeability.[42]

3.2. Surfactants and polymers

Phase separation in nanoemulsions can be prevented by addition into the aqueous phase of a stabilizing agent, a surfactant, which is a chemical compound that reduces the interfacial tension between two phases by being adsorbed on the surface or at the interface between the liquids. The surfactants are widely used in various methods for oil recovery enhancement, as they are capable of decreasing the interfacial tension and changing the wettability. Surfactants are amphiphilic molecules, which contain a polar part (hydrophilic) and a nonpolar (hydrophobic or lipophilic) part. The term 'amphiphilic' implies that all surfactant molecules are composed of two parts: hydrophilic, which is soluble in a certain liquid, for example in water, and a hydrophobic part, which is water insoluble. Surfactants are adsorbed on the droplets of the oil phase, thus decreasing the interfacial energy per unit area (decrease in the interfacial tension between the oil and water phases) and preventing the oil droplets from coalescence and collisions *via* electrostatic repulsion or steric hindrance. This gives rise to oil droplets with a small size and high kinetic stability. In terms of the charge of the molecule head, surfactants are subdivided into anionic, cationic, nonionic, and zwitter-ionic[100] (Fig. 6).

Anionic surfactants are often used in enhanced oil recovery processes for several reasons: (1) their production is relatively inexpensive; (2) they have relatively low adsorption on sand rocks, the surface of which is also negatively charged; (3) they effectively reduce the interfacial tension; and (4) they are stable at high temperatures. The anionic surfactants can be classified in terms of the nature of polar head groups into carboxylates, sulfates, sulfonates, and phosphates.[101,102]

Cationic surfactants have a limited applicability in EOR processes. However, they can be used to switch the wettability of carbonate reservoirs from oil-wet to water-wet.[103] Examples of cationic surfactants include benzalkonium, benzethonium, methylbenzethonium, cetylpyridinium, alkyl dimethyl dichlorobenzene ammonium, dequalinium, and phenamylinium chlorides and cetrimonium and cethexonium bromides.[104]

Nonionic surfactants are much more stable to high salinity. However, their ability to reduce the interfacial tension is inferior to that of anionic surfactants, which limits their use as primary surfactants in enhanced oil recovery applications; they are mainly used as auxiliary agents to increase the salinity resistance of anionic surfactants. The nonionic surfactants used most often for emulsion flooding include polyglycerol alkyl ethers, glucosyl dialkyl ethers, crown ethers, polyoxyethylene alkyl ethers, and ester-based polysorbates Span® and Tween®.[104]

Zwitter-ionic (amphoteric) surfactants can be anionic, nonionic, anion-cationic, or nonion-cationic. The positively charged group is always ammonium, while the negatively charged group is, most often, carboxylate.[105] These surfactants are stable to high temperatures and salinity. However, their high cost is a limiting factor. The following amphoteric surfactants are often used: phospholipids, alkyl betaines, and alkyldimethylimidazoline derivatives such as alkylampho-acetates.[†,106]

There are also dimeric surfactants, called gemini surfactants, the molecules of which consist of two ionic or nonionic diphilic moieties connected by a bridge (spacer), which can be hydrophobic or hydrophilic, flexible or rigid[107] (see Fig. 6). Some of these molecules are superior to similar monomeric surfactants in decreasing the surface tension and also tend to form micelles at lower concentrations. The synthesis of cationic gemini surfactants is relatively simple, while the degree of adsorption and the Krafft temperature (solubility at the reservoir temperature) are lower than those of monomeric analogues.[108] In addition, cationic gemini surfactants show viscoelastic properties at low concentrations. Therefore, they have an

[†] Amphoacetate surfactants, *e.g.*, those marketed under the registered trademark Miranol, are usually prepared by the reaction of long-chain fatty acids, for example, a mixture known as coconut fatty acids, with aminoethylethanolamine followed by the reaction of the product with haloacetic acid or its salt in the presence of alkali (see, for example, *Kirk-Othmer's Encyclopedia of Chemical Technology*, 3rd Edition (Wiley & Sons), vol. 22, pp. 385, 386 and US Patent 2528378 or 2773068).

extensive potential for application in oil recovery enhancement processes.[109]

One more classification of surfactants is based on their hydrophilic-lipophilic balance (HLB),[110] according to which surfactants with HLBs below six are soluble in the oil phase and stabilize W/O emulsions. Conversely, surfactants with HLBs above eight are soluble in water and form O/W type emulsions.

Nanoemulsions can be stabilized both due to electrostatic repulsive forces of surfactants and due to steric hindrance arising when polymers are added to the composition, *i.e.*, stabilization is attained by a combination of electrostatic repulsion and steric effects.[58] Rheological properties play a key role in determining characteristics of nanoemulsions. The non-Newtonian behaviour and rheological properties imparted to emulsions by polymers make the emulsions useful for EOR applications. The addition of polymers to surfactant-stabilized nanoemulsions improves the rheological behaviour and forces the displacing fluid to penetrate into unswept parts of the reservoir and into low-permeability areas by blocking areas with high permeability. Thus, the enhancement of oil recovery on treatment with nanoemulsions is due to dual functionality: interfacial tension and viscosity.[111] Also, polymer nanoemulsions proved to be useful for facilitating flow in pipelines that transport multicomponent fluids containing oil, water, gas, and solid particles, as they reduce friction and resistance. Acrylamide-based polymers such as polyacrylamide, partially hydrolyzed polyacrylamide, xanthan gum, and guar gum are widely used in oil industry, as they improve the rheological behaviour during displacement of oil, can flush the well, and retain solid particles in drilling fluids.[112]

Polymer systems are characterized by viscoelasticity, which implies the ability of the material to exhibit both viscous and elastic properties. This behaviour is described by the loss modulus, which characterizes the viscous component, and the storage modulus, which is responsible for the elastic component of the response to the applied shear stress. To be effectively transported through a complex system of pore channels in the reservoir, polymer solutions should maintain a balance between viscosity and elasticity and a clear-cut elastic component (capability of reversible deformation), which is of prime importance for overcoming pore restrictions, decreasing hydrodynamic resistance, and effective oil displacement.[113] According to investigations, traditional polymers based on acrylamide show moderate elastic properties, which are achieved only at high concentrations above1000 ppm and considerably decrease (by 60–80%) at a shear rate of $\gamma > 200$ s^{-1}. Conversely, polymeric surfactants possess a wider range of elasticity owing to hydrophobic association effects;[114] therefore, they can influence oil recovery not only by controlling the mobility, but also *via* viscoelastic mechanisms at the microscopic level. However, conventional acrylamide-based polymer systems are subject to mechanical degradation at higher shear rates.

In a dilute state, when the concentration is lower than the 'overlap threshold concentration', which is the critical concentration at which polymer coils come in physical contact (C^*), the polymer molecules virtually do not interact with one another ($C < C^*$).[115] As the 'overlap threshold concentration' is reached ($C = C^*$), the coils start to come in touch with one another, and the initial intermolecular interactions arise, but no stable network is formed as yet. In a semi-dilute solution ($C > C^*$), polymer chains begin to interpenetrate and entangle, which leads to the formation of a dynamic network (Fig. 7).[115] Upon further increase in the concentration, the system can reach the gelation state in which a pronounced elasticity appears. The

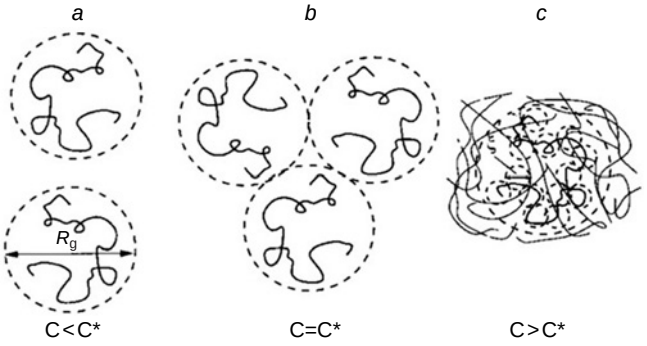

Figure 7. Polymers in solution: (*a*) polymer chains are isolated in a dilute polymer solution ($C < C^*$); (*b*) polymer chains contact one another at the 'overlap threshold concentration' ($C = C^*$); (*c*) polymer chains entangle and form a dynamic network in a semi-dilute polymer solution ($C > C^*$), where R_g is a hydrodynamic radius.[115] Copyright belongs to the Royal Society of Chemistry.

described mechanism of phase behaviour is characteristic of both polymer solutions and polymeric surfactant solutions.

Polymeric surfactants are typical viscoelastic liquids combining both viscous and elastic properties. This is exemplified by copolymer of acrylamide, sodium allylsulfonate, allyl glycidyl ether, and ethylhexyl acrylate; a hydrophobic associative polymeric surfactant, that is, copolymer of acrylic monomers with hydrophobic and anionic moieties; and a copolymer of acrylic acid and polyethyleneoxylated fatty alcohol. Their rheological dynamic characteristics, including storage modulus and loss modulus, are markedly influenced by factors such as salinity, concentration, and temperature. When a critical concentration is reached, these systems undergo a phase transition to a gel state,[116] with the critical concentration value being dictated by the copolymer composition and architecture. An example of polymeric surfactant is the anionic copolymer of fatty acid methyl ester sulfonate and acrylamide (PMES) in which polyacrylamide is the polymer backbone, while side groups containing sodium sulfonate endow this system with surfactant properties. This structure ensures simultaneously a decrease in the interfacial tension and an increase in the viscosity, which makes PMES an effective stabilizing agent for nanoemulsions for EOR, which is widely used for oil recovery applications.

The concentration of a polymeric surfactant plays a key role for certain properties of nanoemulsions such as interfacial activity and emulsification capacity. Varying the concentration from 0.02 to 0.5 mass% demonstrated[117–119] that even minor amounts can markedly influence the efficiency: IFT decreased to ultralow values (down to 3.16×10^{-3} mN m^{-1}), while oil recovery increased by 18% after water flooding.

However, in the case of low- and medium-permeability reservoirs, high concentrations of polymeric surfactants ($C > C^*$) inducing a considerable increase in the viscosity and formation of gel structure, are not the optimal conditions, since this may generate too high pressure drops in the reservoir.[120] Nanoemulsions stabilized with polymeric surfactants or by compositions of polymers and surfactants exhibit stable viscoelastic behaviour at lower concentrations. Thus, in rheological tests, an increase in the elastic and viscous moduli with increasing angular frequency was observed, indicating the presence of a stable internal structure in the system. In particular, nanoemulsions stabilized by polymeric surfactants such as PMES exhibit typical pseudoplastic behaviour at shear rates of

up to 100 s^{-1}: a decrease in the viscosity is caused by weak interaction between the droplets of the dispersed phase and polymer components. At higher rates, shear thickening takes place due to increased interfacial interactions between polymer chains of the surfactant and emulsion droplets.[116]

3.3. Nanoparticles

In the enhanced oil recovery methods, nanoparticles (NPs) are used as parts of nanofluids, Pickering nanoemulsions, and nanofoams. The emulsion stability is ensured by high surface tension at the interface and by adsorption of nanoparticles, which form a protective barrier on a droplet. The particle hydrophilicity/hydrophobicity balance and size determine their arrangement on the droplet surface, thus preventing coalescence.

A nanoliquid (colloidal nanoliquid) is a liquid containing dispersed nanoparticles with an average size of <100 nm forming a stable colloidal dispersion, which is however potentially prone to aggregation and sedimentation when there is no effective surfactant stabilization. When a nanoemulsion is stabilized by solid nanoparticles adsorbed at the interface, it is called a Pickering nanoemulsion (but not all Pickering emulsions are nanoemulsions).[64] Nanofoams are dispersions of gas bubbles (<100 nm) in a liquid. In this case, the nanosize of bubbles is a critical feature, while stabilization by nanoparticles is a possible but not obligatory mechanism. The key advantages of using Pickering nanoemulsions over conventional EOR methods include their ability to withstand high pressures and temperatures up to 70°C in an oil reservoir or formation, long-lasting kinetic stability for up to several months, and, as a result, an increase in the oil recovery to 26% after secondary methods.[121,122]

The selection of nanoparticles is a complex issue requiring thorough investigation, with active research being underway in this field. The nanoparticle shape, charge, concentration, and surface nature are the key parameters determining the properties of nanoemulsions and, hence, their suitability for particular applications. These factors altogether determine the nature of interaction of nanoparticles with one another and with phases of the emulsion. The nanoparticle shape influences their adsorption at the interface: for example, plate-like particles (clays, metal hydroxides) form denser barriers against coalescence than spherical particles. The nanoparticle charge controls the electrostatic repulsion forces: high zeta (ζ)-potential prevents aggregation, but it can hinder the adsorption at the interface if the charge is not balanced with the hydrophobicity. The concentration determines the coverage of the droplet: when the particles are present in excess, secondary aggregation is possible, while insufficient amount of particles may lead to incomplete stabilization. The relationship between the shape and charge is manifested in the fact that, due to the non-uniform charge distribution over the surface, anisotropic particles (rods, sheets) can have areas with different adsorption activity, which enhances their binding at the interface. The stability of nanoparticles in emulsions is determined by the chemical nature of the nanoparticle surface. Hydrophilic nanoparticles are stabilized in polar solvents and form colloidal dispersions, whereas lipophilic nanoparticles are dispersed in nonpolar media; amphiphilic NPs are also used.[123] It is noteworthy that under different conditions (type of the phase: polar or nonpolar; phase composition: different polar or different nonpolar phases; temperature; pressure; and so on), nanoparticles with the same characteristics may give nanoemulsions with completely different properties. Over the last decade, various types of NPs such as metal and metal oxide nanoparticles, carbon nanoparticles, and polymers have been used to obtain Pickering nanoemulsions; the promising results of these studies are discussed in the next Section. The general classes of NPs that are potentially applicable for EOR are briefly discussed below (Table 2).

Unlike surfactants, which provide ultralow IFT values, solid nanoparticles show a different behaviour while stabilizing emulsions: most often, they cannot considerably (by more than 5 mN m^{-1}) reduce the interfacial tension.[42] The nature of the nanoparticle surface is an important factor influencing stabilization of emulsions. The ability of particles to be adsorbed at the oil–water interface is the driving force for the formation of Pickering emulsion droplets. Like surfactants, nanoparticles may possess hydrophilic, hydrophobic, or amphiphilic properties, which provides an effective stabilization of emulsions. For the effective stabilization, the particles should have contact angles (θ) differing from 90°. When $\theta < 90°$ (more hydrophilic), oil-in-water emulsions are stabilized; when $\theta > 90°$ (more hydrophobic), water-in-oil emulsions are stabilized. The highest stability is achieved if the θ angle deviates from 90° by 10–30° depending on the system, which ensures strong particle binding at the interface (Fig. 8).[130] The type of emulsion is determined, first of all, by the relative wettability of the immiscible liquids, as indicated by the θ angle. These particles act as steric hindrances, which effectively prevent the coalescence of droplets over a long period of time.

Table 2. Characteristics of NPs used for Pickering emulsions.

NPs	Particle shape and average size	Effect	Emulsion type	Ref.
Fly ash	Spherical nanoparticles, 150 nm	Kinetic stability Salinity tolerance Additional oil recovery: 40%	O/W	124
Nanocrystalline cellulose	Nanorods, 76 nm long, 3.4 nm in diameter	Stability for 2 weeks	O/W	125
Starch	Spherical nanoparticles, 30 nm	Stability for a few months	O/W	126
Halloysite nanotubes	Nanocylinders, 0.5–1.5 mm long, 30–70 nm in diameter	Stability for 5 h IFT ~3 mN m^{-1} Additional oil recovery: 25.2% Alteration of rock wettability	O/W, W/O	127
Cloisite organoclay 15A	Plate-like nanoparticles, 50 nm	Stability for 30 days at 60°C IFT 20 mN m^{-1}	W/O	128
Chitin nanocrystals (ChiNC)	Nanoneedles, 200–800 nm long, 20–80 nm in diameter	Kinetic stability Pseudoplastic behaviour	O/W	129

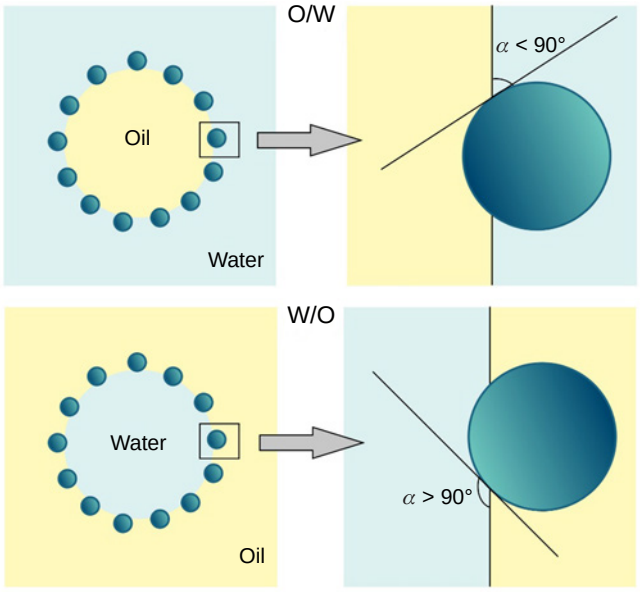

Figure 8. Effect of particle wettability on the formation of Pickering emulsions of either O/W or W/O type.[130]

3.3.1. Silica nanoparticles

Silica (SiO_2) nanoparticles are widely used for the formation of nanoemulsions. The concentration of silanol groups in nanoemulsions containing silica nanoparticles substantially affects wetting of the rock. An increase in the concentration of silanol groups on the surface enhances the hydrophilic properties of nanoemulsions and thus promotes the formation of stable O/W nanoemulsions. Conversely, a surface concentration of silanol groups of less than 10% gives rise to hydrophobic properties and promotes the formation of W/O emulsions.[64,131] This makes it possible to design particular types of nanoemulsions by controlling the interaction of nanoparticles with phases of various polarity.

Silica particles possess exceptional benefits for stabilization of emulsions. Pickering nanoemulsions stabilized by SiO_2 NPs, showed longer stability than surfactant-stabilized nanoemulsions (see Table 1) under drastic reservoir conditions, owing to the formation of a solid interfacial barrier, which prevents coalescence of droplets.[132–134] A comparison of the stability of classic emulsions and emulsion systems modified with SiO_2 nanoparticles with different wettability (hydrophilic or hydrophobic) demonstrated[118] that the thermal stability of modified systems exceeds that of conventional emulsions by more than 100%.

Janus particles with amphiphilic properties (half hydrophilic and half lipophilic nanoparticles) are also promising for EOR applications. Owing to asymmetrical structure, the amphiphilic Janus nanoparticles have a better interfacial activity and stability; they are readily adsorbed at oil–water interface, which leads to a decrease in IFT. Wu *et al.*[135] recently reported the synthesis of a Pickering emulsion with Janus nanoparticles responding to the presence of CO_2 (Fig. 9): SiO_2 NPs were modified with 3-aminopropyltriethoxysilane, which afforded NH_2 groups on the surface and, therefore, the whole particle surface became hydrophilic. Then a half of the SiO_2–NH_2 particle was concealed by immersing it into a water–paraffin–surfactant emulsion. The hydrophilic side (–NH_2) remained in water, while the opposite side was hidden in paraffin. After removal of paraffin, the bare NH_2 groups reacted with dodecanal, which imparted hydrophobicity to the second side of the particle. Emulsions based on Janus particles remained stable at room temperature for 120 h, but injection of CO_2 induced phase separation within 1.5 min. The authors believe that nanoparticles have lost their amphiphilic nature, which induced a substantial decrease in the interfacial activity and the loss of surfactant properties by sodium oleate. Cconsequently, the particles started to be desorbed from the droplet surface. This study offers a convenient and simple approach to the preparation of Pickering emulsions that rapidly respond to CO_2. This approach using the CO_2-responsive Janus particles provides control over emulsions and offers a solution to the pore clogging problem, which is critically important for oil production.

Jia *et al.*[136] investigated the stability of multiple O/W/O Pickering emulsions synthesized using amphiphilic Janus-SiO_2 nanoparticles under reservoir conditions (Fig. 10). The obtained emulsions effectively blocked the pore throats and increased the flow resistance. This led to fast pressure build-up and considerable increase in the swept reservoir area, which in turn provided an additional oil recovery of 27.2% in core flooding tests. The Janus-SiO_2-stabilized multiple O/W/O Pickering emulsion system, combining the benefits of O/W emulsions providing high displacement efficiency and W/O emulsions responsible for high sweeping efficiency, may become a promising flooding fluid in EOR methods.

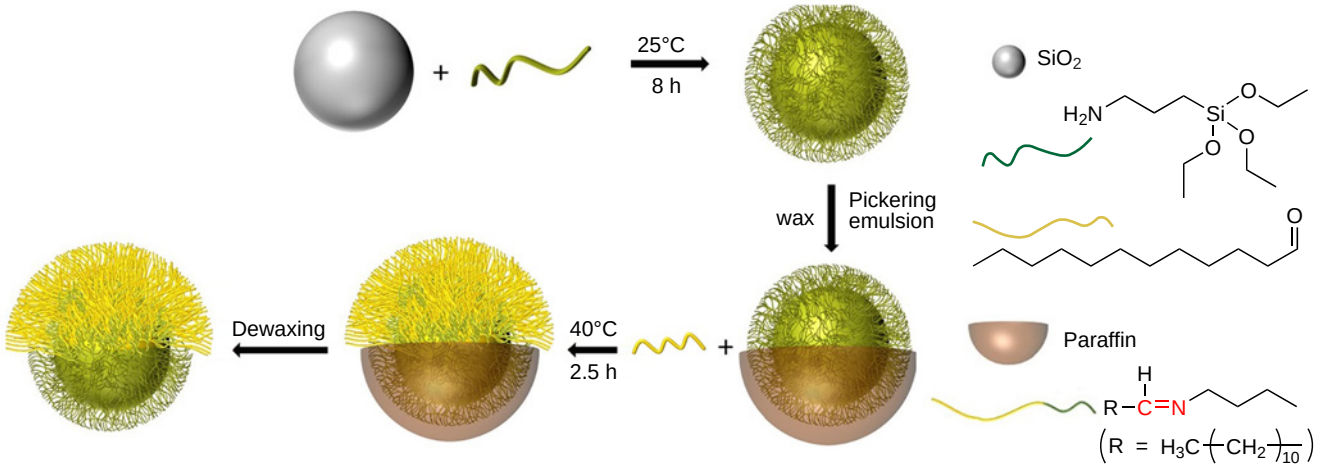

Figure 9. Diagram of the synthesis of SiO_2-based Janus nanoparticles.[135] Copyright belongs to the ACS Publications.

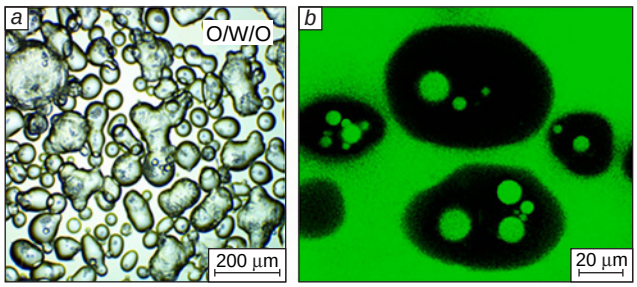

Figure 10. Images of Janus-SiO_2-stabilized multiple Pickering emulsions recorded 72 h after the preparation at 25°C (nanoparticle concentration of 5000 mg L^{-1}): (*a*) optical microscopy, (*b*) confocal laser scanning microscopy.[136] Copyright belongs to Elsevier.

3.3.2. Metal oxide and hydroxide nanoparticles

The ZnO, TiO_2, Fe_3O_4, γ-AlOOH, and other nanoparticles can be used as highly effective emulsifying agents.[137–140] The γ-AlOOH nanoscales have a large specific surface area, abundant surface hydroxyl groups and high sorption capacity.[141] Jia *et al.*[142] modified hydrophilic γ-AlOOH nanoparticles with amphiphilic sodium benzenesulfonate (SBS) molecules through electrostatic adsorption. Emulsions, the stability of which was markedly improved due to the 3D network formed by modified nanoparticles, provided plugging of high-permeability channels and expansion of the sweep area, which resulted in satisfactory (18.87%) tertiary oil recovery in artificial core flooding and in microfluidic models.

Titania nanoparticles also proved to be useful for EOR applications. Nourafkan *et al.*[143] synthesized a nanoemulsion stabilized by TiO_2 NPs and a mixture of anionic (alkylarylsulfonic acid) and nonionic surfactants (ethoxylated alcohol, EA, C12–13/7EO), which exhibited good stability as regards the retention of surfactants while passing through a core. However, the efficiency of this approach may be limited by the difficulty of controlling the mobility of NPs in the fluid injected into the formation. The total oil recovery increased by 7.81% of original oil in place to reach 91.66% upon flooding with a surfactant- and TiO_2 NP-stabilized nanoemulsion compared to surfactant flooding.

Dibaji *et al.*[144] synthesized the MgO@CNT nanocomposite comprising carbon nanotubes (CNTs) completely coated by crystalline MgO phase (Fig. 11), which provided an IFT decrease and high oil recovery (60%). The emulsifying role of the MgO@CNT nanocomposite was studied at various salinities and temperatures and at various nanocomposite concentrations. High stability of the emulsion, which lasted for more than a week, was observed when the concentration of MgO@CNTs was 0.1 mass% and the NaCl concentration was 2 mass%.

3.3.3. Carbon nanoparticles

For obtaining emulsions with smaller droplet sizes and controlled colloidal behaviour, it is preferable to use carbon materials of up to 100 nm in size.[145,146] Carbon materials (quantum dots, CNTs, graphene) are chemically inert and withstand high temperatures and harsh media in the reservoir, unlike polymeric or SiO_2 stabilizers.

Graphene is a monolayer of carbon atoms that form a hexagonal lattice possessing excellent optical, mechanical, thermophysical, and electronic properties.[147,148] Modified graphene (graphene oxide, hydrophobic graphene, and graphene

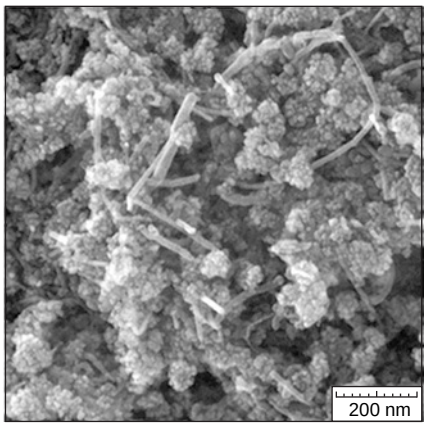

Figure 11. FESEM (field emission scanning electron microscopy) image of the MgO@CNT nanocomposite.[144] Copyright belongs to Elsevier.

with covalently grafted functional groups) can increase the viscosity of an aqueous system, decrease the surface tension at the interface between oil and water, and increase the stability of the O/W emulsion, thus increasing the efficiency of EOR.[149–152] AfzaliTabar *et al.*[153] used nanoemulsions containing a nanohybrid system based on covalently bound graphene quantum dots and molybdenum sulfide nanoparticles, which can alter the wettability of reservoir rock from oil-wet to water-wet; therefore, the reservoir oil trapped in the porous area of the rock can be easily extracted. This is accompanied by a slight increase in the density and viscosity of the nanoemulsion for core flooding, with oil recovery being high (22%).

Graphene oxide (GO) is formed upon graphite oxidation giving rise to oxygen-containing functional groups (carboxyl, epoxy, and hydroxyl groups) on the surface of graphene layers. This process endows GO with amphiphilic properties provided by combination of a hydrophobic sheet and hydrophilic edges; this accounts for good dispersibility in water and polar solvents. The formation of oxygen groups upon graphite oxidation is a key factor determining the unique colloidal and chemical properties of graphene oxide.[154,155] In view of easy production and relative stability of liquid dispersions, graphene oxide is used in emulsion flooding of reservoirs more often than other carbon nanomaterials, graphene or CNTs.[156,157]

It was shown[158] that for emulsions stabilized by 0–4 mg g^{-1} of GO, the salts and asphaltenes present in reservoir oil in low concentrations (0–10 and 0–2 mass%, respectively) are two beneficial factors that make it possible to decrease the size of emulsion droplets down to 0.6 μm and increase the emulsion stability. An increase in the GO concentration up to 7 mg g^{-1} does not affect the emulsion type, whereas increase in the water/oil (reservoir oil) ratio causes inversion of the emulsion. It is well known that asphaltenes stabilize W/O emulsions *via* the formation of interfacial films, usually called rigid or skin-like, around dispersed water droplets.[159] On the other hand, GO tends to stabilize O/W emulsions. At higher concentrations of asphaltenes (>1.5 mass%), O/W emulsion is inverted to give a W/O emulsion (Fig. 12).[158]

It was shown that the combined use of carbon nanoparticles, such as nanotubes, graphene, and graphene oxide, and metal nanoparticles can prevent particle aggregation and coagulation to stabilize the Pickering emulsions.[64,144,160–64] Tang *et al.*[165] used the Ag-NP/GO nanocomposite, which was easily obtained by redox reaction between $AgNO_3$ and GO, to stabilize Pickering

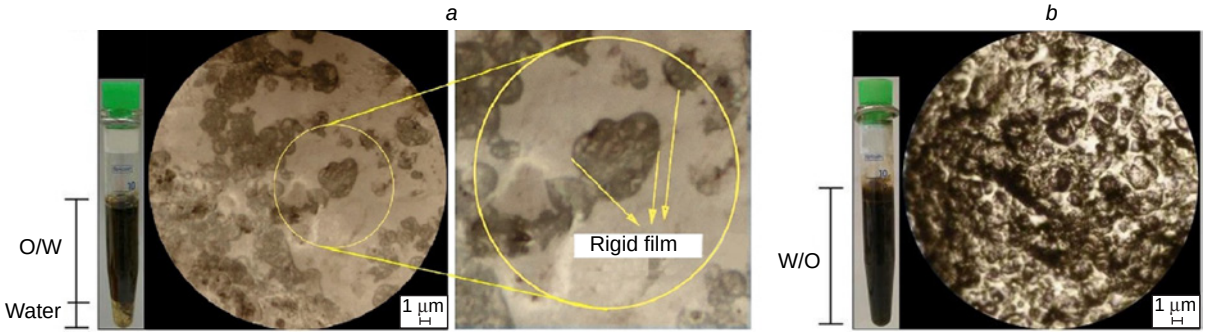

Figure 12. Optical micrographs of GO-stabilized Pickering emulsions with asphaltene concentrations in the organic phase of (*a*) 1 mass%, (*b*) 1.5 mass%. GO concentration: 1 mg mL^{-1}, oil/water ratio: 1 : 1. The inset shows an enlarged microscopic image of an oil phase droplet with the rigid film.[158] Copyright belongs to Elsevier.

emulsions in benzyl chloride as a non-polar phase (Fig. 13). An increase in the particle surface roughness enhances the stability of Pickering emulsions. As the $AgNO_3$/GO weight ratio increases to 0.75, the Ag NP layer formed on GO sheets becomes less uniform, which makes the sheets rough. When the $AgNO_3$/GO weight ratio is 1.5, the nanoparticles coalesce, thus reaching a size of 100 nm and giving rise to rough GO sheets. Thus, the increase in the surface roughness in the Ag-NP/GO composite may be responsible for the increased stability of the Pickering emulsion and the diversity of droplet shapes.

The performed studies attest to good prospects of carbon nanoparticles for stabilization of Pickering emulsions in EOR applications. However, additional laboratory experiments are needed to investigate the influence of important factors such as temperature, pH, salinity, and the interaction between carbon NPs and the reservoir, in order to further confirm this statement. In conclusion of this Section, we would like to note that nanoparticles that stabilize the Pickering nanoemulsions should possess a number of characteristics to ensure emulsion stability (Table 3). The first one is amphiphilicity, which is followed by the surface charge and a moderate particle size (which should be smaller than the expected droplet size, but insufficient for particles to be fully attached to the interface).

Thus, the choice of nanoparticles is determined by their properties and the intended application of the resulting nanoemulsion.[18,182] When SiO_2 NPs of 5–12 nm in diameter are used, the resulting Pickering nanoemulsions[183] with 100–300 nm droplets were retained without signs of coalescence for more than 30 days, while an increase in the size of SiO_2 NPs to 80 nm resulted in the stability decrease to a few days. The enhanced stability can be attributed to the increase in the specific surface area, formation of several dense layers of particles at the interface, and effective suppression of drainage of the interfacial film. Zan *et al*.[184] showed that montmorillonite nanosheets (~1–100 nm) form a Pickering nanoemulsion with ≈200 nm droplets, which is retained without coalescence for 30 days. The increased stability is attributable to the anisotropic shape of the sheets where the sharp edges and small radii of curvature attach the particles to the interface, thus generating a strong multilayer barrier. Luo *et al*.[185] used ion-pair gold nanoparticles (5–10 nm), that is, the particles decorated with a stoichiometric pair of oppositely charged organic ligands (6-mercaptohexanoate anion and tetrapentylammonium cation), which formed an electrically neutral complex. This design made it possible to study the influence of electrostatic forces on the reversible adsorption of particles at the oil–water interface and the particle assembly. By increasing pH of the aqueous solution, it is possible to achieve control of the emulsion stability *via* controlled desorption of nanoparticles from the interface upon increase in the electrostatic repulsion between them. Kaptay[186] demonstrated that particles with contact angles of approximately 70–86° are the best candidates for the development of typical O/W emulsion systems. For stabilized W/O emulsions, the optimal θ_w value should be between 94° and 110°.

Aveyard *et al*.,[187] who studied the effect of concentration of SiO_2 NPs on the droplet size in O/W emulsion, reported that at low particle concentrations (below 3 mass%), the size of emulsion droplets would decrease with increasing particle concentration. A tenfold increase in the particle concentration induced an approximately eightfold decrease in the droplet size. When the NP concentration was above 3%, the droplet size did not change with increasing particle concentration, while additional particles tend to disperse in the continuous phase, instead of being adsorbed at the droplet interface. The use of a mixture of nanoparticles can reduce the required surface coverage of nanoemulsion droplets. When a mixture of SiO_2 NPs and hydroxypropyl cellulose is used for stabilization,[188] the stability of nanoemulsions is attained when the droplet surface coverage is only 29%.

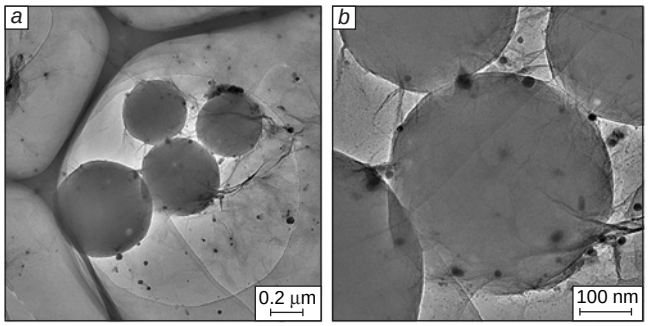

Figure 13. TEM images of Pickering nanoemulsion stabilized by the Ag-NP/GO composite: (*a*) emulsion nanodrop, (*b*) Ag-NP/GO nanocomposite.[165] Copyright belongs to Elsevier.

4. Preparation of nanoemulsions

The understanding of processes involved in the preparation of nanoemulsions is critical for the control over the droplet size. Most methods include two stages: (1) preparation of macroemulsion, (2) conversion of the macroemulsion to nanoemulsion. Methods for the fabrication of nanoemulsions

Table 3. Nanoparticle characteristics that determine the properties of Pickering nanoemulsions.

Characteristics	Mechanism of the effect	Ref.
Size	Nanometre-size particles (1–100 nm) have exceptionally high specific surface area, which allows them to be effectively adsorbed at the interface and form a tight mechanically strong interfacial film. They generate a nonuniform distribution of capillary pressure, caused by a change in the local curvature of particle meniscus, and steric barriers due to close packing and hydrate/solvate shells. These factors prevent droplets from approaching one another, hinder drainage of the interfacial film, and effectively suppress coalescence. This provides a considerable increase in the kinetic stability of the emulsion (although the system remains thermodynamically unstable).	166–168
Shape	The stabilization energy of Pickering particles at the water–oil interface depends on the contact angle. For anisometric particles, the irregular geometry gives rise to regions with extremely small radii of curvature of the meniscus: 1–10 nm at sharp edges; 5–20 nm at rod bending points; and 2–20 nm at angular bulges. This leads to a local increase in the capillary pressure up to 130 Pa and enhancement of the attraction between the particles. Due to these effects, in combination with a greater number of atoms accessible for the interaction compared to that in spherical analogues, the attractive forces predominate over the repulsive forces; this increases the probability of aggregation between the particles (but not with the emulsion droplets) and stabilizes the emulsion through the mechanical binding to the interface.	169–173
Charge	The charge of nanoparticles that stabilize the Pickering nanoemulsions enhances the electrostatic repulsion, thus preventing the particle aggregation in the bulk phase and improving the dispersibility. However, at the water–oil interface, the crucial role is played by capillary forces that promote attachment of the particles. The surface modification (surfactants, polymers) add steric stabilization by maintaining the balance between the degree of dispersion in the bulk and mechanical strengthening of the interface. A charge indirectly increases the emulsion stability by preventing too early coagulation of particles before they are adsorbed on the droplets.	174, 175
Wettability	Hydrophilic particles form an oil-in-water emulsion, whereas hydrophobic nanoparticles stabilize aqueous droplets in an oil phase. This behaviour is described by the Young–Laplace equation: $\cos\theta_w = \frac{\gamma_{s/o} - \gamma_{s/w}}{\gamma_{o/w}}$, where θ_w is the contact angle in the aqueous phase, and $\gamma_{s/o}$, $\gamma_{s/w}$, and $\gamma_{o/w}$ are the interfacial tensions at the solid–oil, solid–water, and oil–water interfaces, respectively. This equation makes it possible to predict and control the type of the formed emulsion by analyzing the wettability of nanoparticles and interfacial energies. The control of the nanoparticle amphiphilicity *via* surface modification and adjustment of interfacial energy allows for exact control of NP distribution at the interface and, as a consequence, stability of the whole system.	176–178
Concentration	The size of nanoemulsion droplets can be determined by the concentration of nanoparticles: a large number of NPs completely cover the droplet, thus ensuring the stability of the whole emulsion. Excess amount of NPs can induce additional stabilization of the major phase of the emulsion and lead to the formation of a network structure around emulsion droplets.	178–181

are mainly subdivided into two types: high-energy methods and low-energy methods, with the choice of the preparation method depending on the specific requirements to the final product, including droplet size, stability, and the production cost.[189–192]

Low-energy methods imply the use of chemical and physical processes that do not require considerable energy consumption. These methods are based on the natural properties and interactions of emulsion components. In low-energy methods, smaller droplets are formed when the system undergoes a phase inversion in response to a change in the composition or temperature and passes through a state with a low interfacial tension. These methods require a much lower input energy density: $\varepsilon \sim 10^3 - 10^5$ W kg^{-1}.[31] Spontaneous emulsification takes place upon a sharp change in the of surfactant solubility, *e.g.*, upon the addition of water into an oil solution of the surfactant. This process requires little energy, but critically depends on the accurate selection of components and component ratios. The phase inversion method uses temperature-induced change in HLB of nonionic surfactants. On gradual heating, the system passes through the phase inversion point, which gives rise to nanodroplets during the subsequent cooling. Although this method is more energy efficient than mechanical dispersion, it requires strict temperature control.

The input energy density in high-energy methods is approximately $\sim 10^{10}$ W kg^{-1}.[193] High-energy methods are processes that require considerable external impacts for droplet breakup. The ultrasonic treatment makes use of the cavitation phenomenon: the formation and collapse of bubbles generate local pressure drops sufficient for the rupture of large droplets. Although this method is effective in laboratory, it is associated with high energy costs and the risk of system overheating. High-pressure homogenization is based on the generation of intense turbulent flows as the emulsion is squeezed through narrow slits under a pressure of 10–150 MPa. Despite high energy intensity, this method is widely used in industry due to its scalability. However, multiple treatment cycles and wear of equipment are still considerable limitations. The main drawback of high-energy methods is the large loss of energy dissipated as friction losses caused by high shear rates. The energy is thus converted to heat, which can easily raise the emulsion temperature. Thus, these devices often require a cooling system.[194, 195]

4.1. High-energy methods

The high-energy treatment results in effective disintegration of phases to a nanoscale state followed by the formation of a stable emulsion. Methods of this treatment are characterized by high efficiency, but require thorough control of the treatment parameters to achieve the optimal characteristics for the resulting nanoemulsion. Additionally, it is possible to use systems meant to overcome the IFT effect and reach a Laplace pressure sufficient for obtaining nanoscale droplets by fragmentation of microscale droplets.

The Laplace pressure is determined by IFT on the droplet surface and the droplet radius and describes the pressure difference between the inner and outer sides of the interface:

$$\Delta P = 2\gamma/R, \quad (1)$$

where γ is the interfacial tension at the droplet interface, and R is the droplet radius. Thus, a decrease in the droplet size by a few nanometres leads to increase in the Laplace pressure by a large factor. If a surfactant is used in the system, the surface of newly formed droplets is coated by the monomers that are present in the aqueous phase as micelles, thus preventing the droplet coalescence caused by the induced shear.

High-pressure homogenization, direct stirring, and ultrasonic treatment are three widely used high-energy methods for the formation of nanoemulsions (Fig. 14).

In the case of direct mixing, which can also be called hydrodynamic shear, the preparation of O/W nanoemulsions starts with the formation of a coarse O/W emulsion by mechanical mixing of oil and water phases in the presence or in the absence of surfactants for a period of time sufficient for the preparation of a stable emulsion. This method implies the use of mixing devices: rotor stator disperser, mixer, or homogenizer, which operate at high speeds of 1000 to 30 000 rpm to generate an external power. This power destroys IFT between the continuous and dispersed phases, which is favourable for the formation of nanoemulsion droplets. A major advantage of mechanical emulsification is that it splits large and highly viscous oil droplets into smaller ones, which in turn results in the fabrication of a more stable emulsion. However, an obvious drawback of this method is that the resulting droplets of the dispersed phase tend to aggregate, which may result in phase separation irrespective of how thorough the emulsion components have been mixed.[196] Also, the stability of emulsions fabricated by mechanical mixing is influenced by certain factors such as type and concentration of the emulsifer, phase ratio, mixing speed and time, geometry of the stirrer, and temperature of the process.[197] Hence, the appropriate choice of the emulsification conditions and the use of suitable emulsifers are key factors for the preparation of stable emulsions. Furthermore, a lot of heat is lost during stirring, being spent for viscous friction; therefore, the energy efficiency of this method is low. Nevertheless, due to the easy spreading of the technique and equipment, direct mechanical emulsification is the most popular approach for the *ex situ* enhancement of oil recovery using emulsions and for enhacing the fluidity and reducing the pumping cost of heavy crude oil.[198,199]

Using a high-speed rotary mixer, it is possible to produce very small droplets down to 1 nm in diameter. However, due to the high shear rate, long-chain molecules (such as polymers, surfactants, and so on) can be cleaved; therefore, the use of macromolecular components should be avoided in this method. The results reported by Al-Sabagh *et al.*[200] demonstrate the applicability of emulsifier blends for stabilization of water-in-diesel fuel nanoemulsions upon treatment in a high-speed homogenizer. It was shown that the stability of nanoemulsions depends considerably on the emulsifer concentration and the content of the aqueous phase. The maximum stability (15 days) is achieved with an optimal combination of parameters such as sufficient surfactant concentration for complete coating of the interface and a limited content of water to prevent redistribution of the emulsifer in the bulk system. An important factor is the revealed synergistic effect arising if a mixture of emulsifers is used. Span 80 and Emarol 85 used separately are insufficiently efficient as they have non-optimal HLB and a moderate ability to form dense adsorbed layers. Meanwhile, a combination of these surfactants shows clear-cut synergistic effect, providing a considerable decrease in IFT and formation of stable interfacial structures. The stability of the obtained systems is caused by integrated effect of several factors: electrostatic barrier (for ionic components of the mixture), steric factor (owing to the bulky hydrophobic moieties), and the geometrical conformity of the molecular structure of the emulsifers to the curvature of the nanosized droplets (Fig. 15).[200]

In the ultrasonic approach, the turbulence generated by the ultrasound shock waves breaks the droplets of O/W micro- or macroemulsions, and this process continues until droplets of equal size are formed.[201] It is believed[18,202] that the formation of nanoemulsions under ultrasonic treatment can follow two mechanisms: (1) high-frequency acoustic waves break interfaces in emulsions; (2) pressure oscillations in ultrasonic waves give rise to cavitation in emulsions. In other words, numerous microbubbles are formed and then collapse, which generates strong turbulence at the oil–water interface. As a result, large

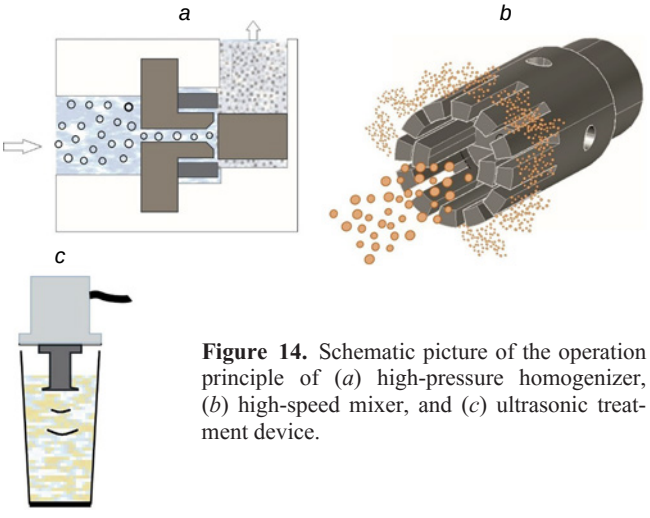

Figure 14. Schematic picture of the operation principle of (*a*) high-pressure homogenizer, (*b*) high-speed mixer, and (*c*) ultrasonic treatment device.

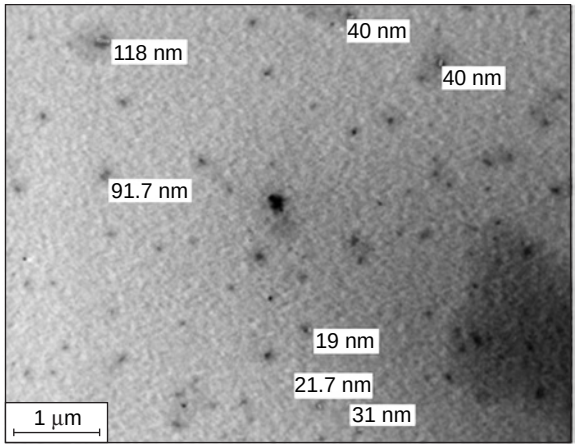

Figure 15. TEM image of water–Span 80+Emarol 85–diesel fuel nanoemulsion at a total surfactant concentration of 8 mass% and a water content of 10 mass%, prepared by high-speed homogenization method at 20000 rpm for 2 min.[200] Copyright belongs to the Egyptian Petroleum Research Institute.

droplets of reservoir oil dissipate in the nanoemulsion.[203,204] Pal *et al*.[205] showed, on a laboratory scale, that stability of n-heptane droplets in water upon ultrasonic treatment is determined by the fact that the inertial stress generated by cavitation microjets exceed the interfacial stress and depends on the localized viscous stresses inside the droplets. The addition of PAA (~0.1 mass%) increases the viscosity of the aqueous phase several-fold and, hence, the viscous resistance around the droplets increases, the inertial contribution no longer predominates, and the droplet breakup substantially slows down, resulting in an increase in the average size of droplets from 4–25 nm to 0.13–0.36 μm. This method has two drawbacks: it is inefficient for high-viscosity systems and has low feasibility for industrial application.

Using ultrasound, Kumar and Mandal[116] fabricated nanoemulsions with dispersed oil droplets of less than 200 nm in size that showed long-term kinetic stability. Enhanced nanoemulsion stability was achieved, first, by introducing SiO_2 nanoparticles with a zeta-potential above –30 mV, and, second, by adding polymeric surfactant (PMES), which prevented the droplet coalescence owing to the electrostatic repulsion and steric hindrance generated by the 3D network structure of the surfactant located on the surface of oil droplets. In Fig. 16*a*, one can clearly see a uniform dispersion of nanosized oil droplets (black spots) in a continuous aqueous medium (white background). Figure 16*b* shows accumulation of SiO_2 nanoparticles (bright dots) on nanoemulsion droplets.

In the high-pressure homogenization,[206–208] the initial coarse O/W emulsion is pumped many times through a narrow slit a few micrometres high with a high-pressure pump. As this takes place, the droplets become smaller, being subjected to pronounced vibrations, shear stress, and elongation.[209] In the case of Pickering nanoemulsions, the pressure levels are usually in the range from a few tens to a few hundreds of MPa. In addition, nanoemulsion can be passed through the homogenizer once again to further reduce the droplet size. Gupta and Rousseau[210] passed the initial coarse emulsion through a high-pressure homogenizer at 100 MPa five times, and the resulting nanoemulsion with an average droplet diameter of 460 nm was stabilized by solid lipid NPs based on glyceryl stearyl citrate with an average particle size of 150 nm. This is a complex polar lipid with a melting point of 59–63°C (solid at 4–25°C); therefore, the particles remain crystalline and form a rigid barrier around the oil droplets. This Pickering nanoemulsion was kinetically stable for 12 weeks and showed no visible phase separation for 24 weeks. Destabilization of the emulsion was caused by dissolution of lipid NPs. Nevertheless, the high shear used in this method and the requirement for thorough control of the preparation conditions still limit the widespread use of high-pressure homogenization, especially in EOR.

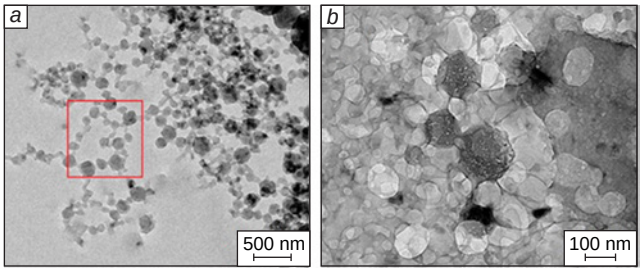

Figure 16. TEM images of a nanoemulsion prepared without (*a*) and with (*b*) the addition of SiO_2 nanoparticles.[116] Copyright belongs to Elsevier.

4.2. Low-energy methods

Low-energy methods of phase inversion by changing the temperature (PIT) and composition (PIC) consist of the stage of formation of a W/O macroemulsion by simple mixing and the subsequent stage of macroemulsion conversion to nanoemulsion. For example, for nanoemulsions obtained using PIT, the initial macroemulsion is prepared at a temperature above PIT of the mixture; then the emulsion is cooled down to a temperature below PIT and is transformed into an O/W nanoemulsion.[211] In the PIC method, the initial macroemulsion is slowly diluted with an aqueous medium to induce phase inversion giving an O/W nanoemulsion.[212] Both PIT and PIC methods make use of changes in the spontaneous curvature of the interface related to HLB and surface tension during phase transitions at the inversion points, which allows the formation of oil phase nanodroplets with minor energy expenditure. Unlike HLB, the hydrophilic-lipophilic deviation (HLD), which describes the deviation of the real surfactant behaviour from the ideal behaviour, related to the change in the balance between the hydrophilic and lipophilic properties of molecules depending on the external conditions (temperature, concentration, composition of the solution), is widely used for ionic surfactants, correctly predicts the type of the resulting emulsion (O/W or W/O), and determines the applicability and efficiency of a surfactant for a nanoemulsion. A change in a variable (temperature or composition) affects HLD, thus making it possible to form a nanoemulsion *via* either gradual shift of the emulsification process away from the optimal formation region (HLD = 0) or crossing the optimal formation region and slightly shifting the formulation from the optimal range. When the temperature (PIT) or composition (PIC) is changed, the system passes through a region with minimal IFT (HLD ≈ 0), where nanodroplets are formed spontaneously. After departure from this region, a thermodynamically unstable, but kinetically stable nanoemulsion is formed.

In the spontaneous emulsification method based on weak perturbation of the interface, the oil pseudophase prepared in advance with surfactants (sometimes, auxiliary surfactants) is diluted with an excess of the aqueous phase to form nanoemulsion at a constant temperature. The oil phase is slowly added dropwise with stirring to the aqueous phase, the surfactants diffuse from the oil phase into water, which induces local changes in the surface tension by 0.1–1 mN m^{-1} and results in spontaneous droplet breakup down to a nanosize.[32,63,213] A spontaneous emulsification formulation consisting of the alkyl polyglycoside surfactant (0.4 mass%) and alkali (NaOH, 0.1 mass%) reducing the surface tension down to 0.0035 mN m^{-1} was proposed for effective use in low-permeability reservoirs.[214] Nanoemulsions with an average droplet size of 0.2 μm formed spontaneously in a single dilution cycle, with the size of formed droplets being smaller than the pore channels (0.2–4.0 μm). Visual core flooding experiments using micromodels demonstrated that small residual oil drops can be easily displaced in porous media. Another nanoemulsion[215] consisting of anionic and cationic surfactants in 6:4 molar ratio in a total concentration of 3000 mg L^{-1} was also proposed for EOR in low-permeability reservoirs. The strong electrostatic attraction between the anionic and cationic surfactants resulted in an ultralow surface tension of $<10^{-3}$ mN m^{-1} and, as consequence, in the spontaneous emulsification. According to core flooding experiments, an optimal EOR system can simultaneously effectively increase the oil recovery by 14.14% and markedly reduce the well injection pressure.

In recent years, low-energy emulsification techniques such as microfluidics and membrane emulsification have been actively developed, and they offer significant advantages over traditional high-energy approaches. These methods open up new prospects for the fabrication of high-quality nanoemulsions with controlled parameters, although their industrial implementation is still facing limitations regarding the production capacity.

Membrane emulsification is an energy-efficient way to fabricate micro- and nanoemulsions with precisely controlled droplet size. In the direct membrane emulsification process, the dispersed phase is forced under pressure through a porous membrane into the continuous phase to form droplets. Low shear rates (10^5 s^{-1} to 2×10^5 s^{-1}) are used at the boundary between the membrane and the continuous phase to overcome capillary forces and to separate the droplets from the membrane pores. In addition, droplets can also be formed without external shear, in the dripping mode. This is due to the Laplace pressure gradient resulting from the difference in the curvature of the interface. This imbalance arises when the forming droplets crowded on the membrane surface squeeze each other or detach from irregularly shaped pores.

Premix membrane emulsification (premix-ME) implies a decrease in the droplet size of a pre-synthesized macroemulsion (pre-emulsion) by passed the pre-emulsion through a membrane or a tight microparticle layer (Fig. 17).[216] The droplet breakup is due to an internal shear in the pores, which is generated by the transmembrane flow without the need of using external shear.

A recent study[217] demonstrated the possibility of implementing premix-ME by pumping a dispersed and continuous phase (pre-emulsion) simultaneously through a membrane without the preliminary emulsification stage to give O/W and W/O/W macroemulsions with a droplet size <1 μm and a high content of the dispersed phase at a high production capacity. Alliod *et al*.[218] were able to reach the nanoscale droplet size using the same premix-approach by successive passing of a pre-emulsion through a cascade of membranes with pore size of $0.5\rightarrow0.4\rightarrow0.3\rightarrow0.2$ μm, which gave rise to a monodisperse O/W nanoemulsion with an average droplet diameter of 335 nm. Thus, obtaining <500 nm droplets by the premix-ME method requires either a cascade decrease in the pore size or further improvement of the design of the membrane assembly and hydrodynamic conditions. Wetting of the pore walls by the dispersed phase may induce phase separation or phase inversion in the initial emulsion. Therefore, hydrophobic membranes are used to introduce an aqueous solution or O/W emulsion into an external oil phase, while hydrophilic membranes are used to introduce an oil phase or W/O emulsion into an external aqueous phase.[219,220]

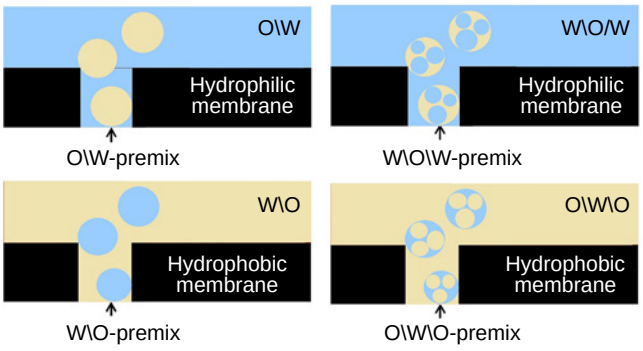

Figure 17. Emulsions obtained by premix membrane emulsification and required wettability of the membrane.[216]

Track-etched polymer membranes with isolated straight pores formed *via* ionic irradiation followed by chemical etching are less efficient in droplet breakup than porous glass membranes because of their non-crossing straight pores and the short residence time of the emulsion inside the relatively thin membrane. In most cases, a single pass through a porous glass membrane is sufficient to obtain a small droplet size, whereas in the case of track-etched polycarbonate membranes, repeated extrusion is required in most cases. The droplet size in premix-ME critically depends on the wettability of the membrane surface by the continuous phase. The better the wettability of the membrane wall by the liquid in the continuous phase, the smaller the droplet size that can be achieved. The pre-emulsion quality has no effect on the quality of the nanoemulsion after five premix-ME cycles.[221] The design of experiments (DoE) demonstrated that an increase in the flow rate is of secondary importance, whereas increase in the number of cycles has a pronounced effect on the decrease in the particle size. The most appropriate combination includes a hydrophilic alumina membrane and saccharose laurate as a surfactant, which causes the lowest interfacial tension of 2 mN m^{-1}. A smaller particle size (~100 nm) can be achieved by using an alumina membrane with a pore size of 100 nm.

In recent years, microfluidic emulsification methods have been actively developed as a promising alternative to traditional high-energy approaches. Microfluidic systems are based on the use of micrometre channels of complex geometry in which droplets are formed under the action of laminar flows and capillary forces. The key benefit of these devices is the possibility of precisely controlling the size and monodispersity of the resulting droplets with minimized energy expenditure.

Microfluidic systems implement several principles of droplet generation. In T-junction devices, the dispersed phase is introduced through a side channel into a perpendicular flow of the continuous phase in which an emulsion is formed under the action of shear stress. Toprakcioglu *et al*.[222] used a microfluidic device manufactured by two-step photolitography, in which microchannels with a width of up to a few tens of micrometres were integrated with ~800 nm wide nanochannels of 400 ± 30 nm height, which provided the formation of nanoemulsions with sizes from 2500 to 51 ± 6 nm (Fig. 18).

More sophisticated flow-focusing devices generate a thin jet of the dispersed phase, which is then broken up into monodispersed droplets under the action of two counter-flows of the continuous phase. Of particular interest are terrace-like devices in which the Laplace pressure drop upon the passage through a terrace-like channel widening causes spontaneous droplet detachment without the need to precisely control the flow velocities.[223] These methods are particularly valuable for the fabrication of Pickering nanoemulsions stabilized by solid particles.

Microfluidic systems not only allow for precise control of the droplet size, but also ensure uniform distribution of stabilizing particles at the interface. For example, in flow focusing devices, it is possible to successively form an oil droplet in an aqueous medium and then adsorb hydrophobic nanoparticles on its surface, thus forming a stable emulsion system.[224]

Despite the obvious advantages, that is, high monodispersity, mild process conditions, and the possibility of handling nanosystems, microfluidic methods still have limitations related to production capacity and scaling up of the process. Current studies address these problems by designing new chips and

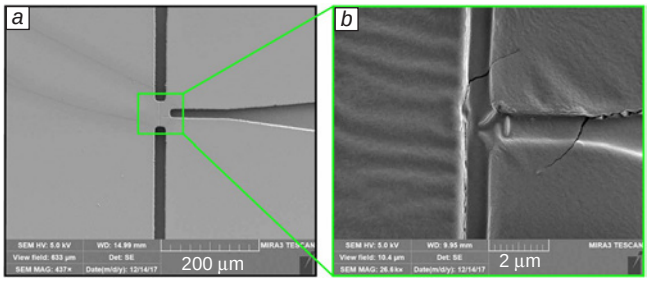

Figure 18. Nanochannel region with T-junction of a microfluidic device: (*a*) SEM micrograph of the nanodroplet-generating T-junction of nanochannels, (*b*) magnified SEM image of the same T-junction demonstrating a ≈800 nm wide nanochannel.[222] Copyright belongs to the American Association for the Advancement of Science.

hybrid systems that combine the benefits of microfluidics and other emulsification methods.[225]

4.3. Alternative methods for the preparation of nanoemulsions

A new method for the synthesis of nanoemulsions by water vapour condensation on mixtures of oil phases and surfactants was recently reported.[226] The fabrication of W/O emulsions by condensation is caused by various interfacial phenomena that act in combination upon immersion of water droplets that have arisen at the oil–air interface: water droplets condense at the oil–air interface *via* heterogeneous nucleation and then grow *via* vapour diffusion and coalescence. This process depends on the rate of nucleation and the behaviour of oil on water (in the presence of air), which is thermodynamically described as the spreading coefficient.

$$S_{ow} = \gamma_{wa} - \gamma_{oa} - \gamma_{ow}, \quad (2)$$

where γ_{wa}, γ_{ow}, and γ_{oa} are water–air, oil–water, and oil–air interfacial tensions, repectively. The spreading coefficient shows whether the oil phase would spontaneously spread over the surface of condensed water droplets at the water–air interface, thus coating the water droplets with a thin film of oil. A positive spreading coefficient indicates that oil will spread, while a negative spreading coefficient predicts that the oil is not going to spread. If the oil contains a sufficient concentration of surfactants and/or nanoparticles, they can be rapidly absorbed on the immersed water droplets, thus preventing their coalescence and naturally leading to the formation of stable nanoemulsions.

Guha *et al*.[226] reported a simple method for water emulsification in a mixture of dodecane and Span 80 surfactant (M = 428.6 g mol^{-1}, HLB = 4.3). An oil bath was placed into a high humidity atmosphere with controlled temperature and then cooled below the dew point. Water droplets spontaneously condensed from the vapour phase on the surface of the oil phase (Fig. 19). The optical image shows W/O emulsions formed 10 minutes after the start of condensation. (Fig. 19, inset). It was found that for obtaining stable nanoscale emulsions, the amount of surfactant in the oil must be quite high (not less than 1 mM), *i.e*., it should be at least ten times as high as the critical micelle concentration.

Anand *et al*.[227] solved the problem of surfactant depletion during the synthesis of nanoemulsions by upgrading the experimental setup: water droplets condensed on an

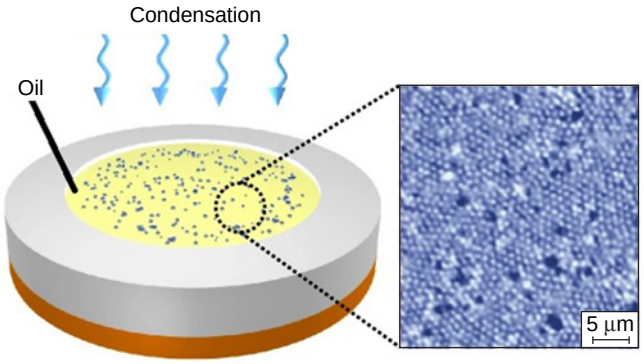

Figure 19. Experimental setup for the fabrication of W/O nanoemulsion by vapour condensation ($T_{surface} < T_{dew\ point}$); the inset shows the resulting nanoemulsion.[226] Copyright belongs to the Nature Research.

oil–surfactant solution that moved in one direction in a channel located on a Peltier element.‡

The same publication demonstrated the applicability of this method for the synthesis of O/W nanoemulsions: the oil evaporation and condensation on a water surface can occur even on heating to 30°C. The vapour condensation to obtain W/O emulsions is implemented rather simply, while the preparation of oil-in-water nanoemulsions or complex emulsions (oil/water/oil or water/oil/water) by vapour condensation is associated with difficulties: the formation of W/O emulsions is based on the fact that water is not spread over oils (*i.e*., the spreading coefficient of water over oil in the presence of air $S_{wo} < 0$) because of high surface tension. This is also an obstacle to the preparation of O/W emulsions, since water does not show a natural tendency to cover condensed oil. In addition, there is a fundamental difference in the vapour condensation on an aqueous or oil surfactant solution. Low thermodynamic efficiency of the adsorption of oil-soluble surfactants at an oil–air interface is due to the fact that the initial surface tension of oils is relatively low ($\gamma_{oa} \approx 25$ mN m^{-1}), and its further decrease does not provide any significant benefit for the free energy of the system. Additionally, this process is limited by high hydrodynamic resistance: the diffusion transport of surfactant molecules in the organic phase is difficult; therefore, their movement toward the interface in question is slow. Water-soluble surfactants show the opposite behaviour. The high initial surface tension of water on air ($\gamma_{wa} \approx 72$ mN m^{-1}) generates a considerable thermodynamic stimulus for their adsorption: when the hydrophobic tail is displaced to the gas phase and the hydrophilic head remains in water, the free energy of the molecule sharply decreases, while a dense surface layer is formed. The condensation of water vapour on a surfactant solution in oil affords W/O nanoemulsions because of the enveloping effect: water droplets are rapidly covered by a stabilized oil film. Conversely, condensation of oil vapour on a water surface gives O/W emulsion only in the case of preliminary adsorption of a hydrophilic surfactant, which reduces γ_{wa} to a level providing a positive spreading coefficient S_{wo} and thus stable existense of the condensed oil layer.[227]

‡ Peltier element is a thermoelectric module that uses the Peltier effect: an electric current passes through a circuit of p- and n-semiconductors connected in pairs and induces heat transfer. One side of the module absorbs heat (being cooled) and the opposite side releases heat (being heated), giving rise to a stable temperature gradient.

Other methods for the formation of nanoemulsions include evaporating ripening and bubble bursting at an oil–water interface. Fryd and Mason[228] proposed evaporative method for the formation of small droplets of O/W nanoemulsions using high-viscosity oils. Initially, the droplets obtained by high-pressure homogenization consist of a mixture of high-molecular-weight (non-volatile) and low-molecular-weight (volatile) oils or components. On heating, volatile components are evaporated, which leads to decreasing droplet size and enrichment of the oil phase with non-volatile macromolecular components.

Feng *et al*.[229] proposed the bubble bursting method to prepare small droplets of the oil phase by gas bubble bursting at the interface in an aqueous mixture with a surfactant. The formation of relatively small droplets includes the following stages: a gas bubble formed in the lower part of the system rises and reaches the interface, being located under oil and water layers. A hole appears on the cap of the bubble, as shown by the white oval in Fig. 20*a*. The oil film located above water is thinned and ruptures before the water film does (Fig. 20*b*). This deformation propagates along the interface. The rupture of the water film produces a cavity or a hole (Fig. 20*c*). As the deformation propagates further, splashes consisting of oil droplets appear on the walls of the cavity (Fig. 20*d*). It is noteworthy that the water film is drawn in a direction different from the direction of the oil film withdrawal. The bubble bursting method is based on the use of energy released when a gas bubble bursts at the oil–water interface. The bubble generates local perturbations leading to the film rupture and formation of small oil droplets, while surfactants present in the aqueous phase stabilize the arising droplets, preventing them from coalescence. This method produces nanoemulsions with small droplets (average size of 59.8 nm) without the use of high energies compared to high-pressure homogenization. It is particularly useful for systems where energy consumption needs to be minimized.

The above analysis of alternative methods for the formation of nanoemulsions (bubble bursting, evaporative ripening, vapour condensation) showed their basic applicability to the enhancement of oil recovery. The major advantage of these approaches is the control of droplet size at the nanolevel. Unlike conventional methods, alternative processes minimize the energy consumption and enable adjustment of the composition of emulsions to specific reservoir conditions. However, the industrial implementation of these methods is hampered by the need to optimize process parameters for field conditions, as well as by the limited production capacity compared to conventional emulsification methods. The prospects for the application of these methods for enhanced oil recovery are related to the development of hybrid technologies that would combine their advantages with the scalability of conventional approaches, including laboratory synthesis of reference nanoemulsions, point application in wells, and simulation of reservoir processes on microfluidic chips. The integration of advanced methods with industrial processes is particularly important, since this allows for optimization of the development of hard-to-recover reserves while reducing the operating costs.

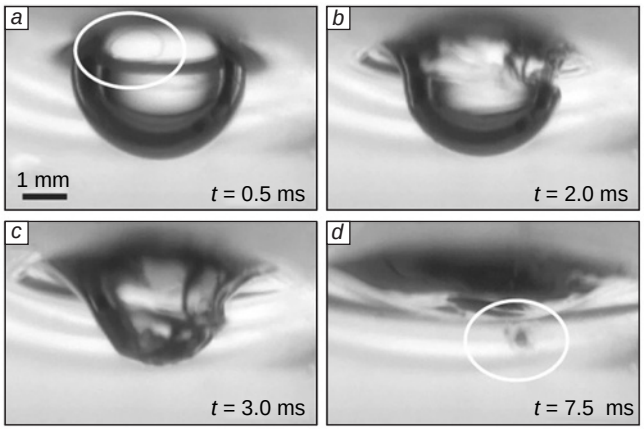

Figure 20. Photo images of burst bubble at the air–hexadecane–water interface during the preparation of a nanoemulsion by the bubble bursting method at the oil–water interface: (*a*) a hole nucleates on top of the bubble (white oval in the image); (*b*) surface of the cavity is deformed; (*c*) the deformation propagates further along the interface; (*d*) a spray of droplets (white oval) appears on the wall of the cavity.[229] Copyright belongs to the Nature Publishing Group.

5. Properties of nanoemulsions in the context of oil production

The discussion of the unique properties of nanoemulsions, such as long-term stability (kinetic stability), low IFT, wetting, and rheological characteristics provides the understanding that the behaviour of a nanoemulsion depends not only on the composition, but also on the preparation method and mixing concentration.

5.1. Stability

The emulsion stability is a crucial factor for oil industry applications. Nanoemulsions contain lower amounts of surfactants than microemulsions and are relatively insensitive to physical or chemical media. Low demand for surfactants and high stability inherent in nanoemulsions are caused, in particular, by their nanoscale structure: small droplet size leads to large specific surface area and a minor content of stabilizing agents, and the Brownian motion suppresses sedimentation. However, their stability is limited: even nanoemulsions can break upon critical impacts (temperature > 150°C, high concentrations of demulsifers or extreme salinity); hence, thorough selection of the composition for particular reservoir conditions is required.[24,25] In addition, being surfactant-containing solutions, nanoemulsions can decrease the surface tension, emulsify reservoir oil, and change the wettability. The oil phase of the nanoemulsion experiences hydrophobic attraction to the hydrophobic part of the surfactant molecule, which endows nanoemulsion with the ability to reduce the adsorption of surfactants. The hydrophobic attraction between the oil phase and the hydrophobic parts of surfactant molecules can actually promote the selective adsorption of surfactants on the droplet surface, thus reducing their losses on rock surfaces. This is one of the reasons why nanoemulsions can remain stable even at relatively low surfactant concentrations.

During the formation of emulsions, surfactants are adsorbed at the oil–water interface, thus forming a stable interfacial film. This film increases the initial interface viscosity, giving rise to a repulsive barrier between oil droplets. This barrier is caused by electrostatic interactions or steric hindrances arising between oil droplets.[230,231] As a result, drainage of the interfacial film during coalescence of droplets is retarded and the rate of oil droplet breakup also decreases.

Al-Sakkaf and Onaizi[231] stabilized O/W nanoemulsions by rhamnolipid biosurfactant at various pH values. The resulting systems had an average droplet size of 72 nm in highly alkaline medium (pH = 10, zeta-potential of ~54 mV), low IFT, and

long-term (14 days) kinetic stability without phase separation. The viscosity of nanoemulsions increased with increasing pH (4–12), but still remained low (2.2–4.2 mPa s) compared to the viscosity of crude oil; heating resulted in a considerable decrease in the viscosity. Despite the long-term stability, nanoemulsions were completely broken within 75 min upon the addition of 0.01 M NaOH or HCl, which corresponded to pH of 10.3 and 4.1.

Nanoemulsions[37] have high kinetic stability, which is confirmed by small droplet size in the range of 18–31 nm and a negative zeta-potential (~–35 mV). Cryo-TEM data revealed a uniform morphological structure, indicating the system stability. An important characteristic is thermal stability, manifested as invariable viscosity properties in the temperature range from 30 to 70°C. The interfacial stability is expressed as a pronounced decrease in IFT with increasing surfactant concentration and temperature. The practical efficiency was confirmed by flooding results in which the use of a nanoemulsion provided a 28.94% additional oil recovery.

Oil-in-water nanoemulsions[232] obtained by ultrasonic treatment of SDBS surfactant (4 mass%), crude oil (5–25 vol.%), and deionized water have an average droplet size of ~63 nm, zeta-potential of –62 mV, and low IFT (~0.45 mN m^{-1}). The nanoemulsion viscosity increased with increasing crude oil content: when the oil content was 5 vol.%, it was approximately 1.3 mPa s, while at 25 vol.% crude oil, it reached 2.45 mPa s at a shear rate of 100 s^{-1} (pseudoplastic behaviour). Although viscosity increased, it still remained lower than the viscosity of crude oil, which ensured good mobility in porous media. The nanoemulsions retained stability for more than 30 days without the signs of coalescence or phase separation and underwent pH-induced breakdown upon the addition of 0.01 M HCl or NaOH, despite the fact that SDBS does not formally refer to pH-sensitive surfactants.

A study of the effect of the terminal carboxyl groups of asphaltenes on the aggregation of crude oil droplets[233] revealed molecular mechanisms that are important for heavy oil field development. Two molecular systems of asphaltenes, with and without carboxyl groups, were simulated to perform a comparative analysis of their behaviour. According to the results, anionic asphaltenes show increased adsorption capacity at the water–oil interface compared to neutral analogues. The key conclusion of the study is that carboxyl groups substantially enhance intermolecular interactions in the crude oil system. Anionic asphaltenes not only stabilize the water–oil interface more effectively, but also promote the formation of a stronger spatial network between oil molecules, while enhancing their interaction with the aqueous phase. These fundamental data open up new opportunities for optimization of heavy oil production techniques, in particular, using targeted modification of the surfactant properties of asphaltene components. These results can underlie the development of more effective and environmentally sustainable methods for increasing oil recovery, especially for hard-to-recover reserves.

High stability of O/W nanoemulsions is characteristic of emulsifers with HLB of 10 to 12. In general, smaller droplet sizes are achieved with higher HLB values and lower molecular weights of the surfactant.[234] The authors prepared W/O nanoemulsions by spontaneous emulsification and high-speed rotor dispersion using a surfactant mixture (Span 80 + Tween 80) possessing a low HLB (9.864). The influence of homogenization parameters such as treatment time and rotation speed on the formation of nanoemulsions with kerosene as the oil phase was also established experimentally. The key results of the study indicated than narrow polydispersity increases the stability of the system. The authors were also be able to prepare nanoemulsions with droplet size of 20–45 nm which had low interfacial (0.138–0.312 mN m^{-1}) and surface (23.656–26.342 mN m^{-1}) tensions. Analysis of destabilization mechanisms revealed the predominance of Ostwald ripening over coalescence. Additional studies of surface properties demonstrated an inverse relationship between the droplet size and the interfacial tension. The prepared nanoemulsions possessed a number of benefits such as narrow particle size distribution and enhanced kinetic stability. The nanoemulsions with a droplet size of up to 30 nm prepared using low-energy emulsification methods at a surfactant : decane mass ratio of 15 : 85 by Porras *et al*.[28] showed a high kinetic stability for nearly 400 h without phase separation, sedimentation, or creaming; however, the droplet size gradually increased to 300 nm.

A number of publications describe[82,235,236] the use of the zeta-potential as the main tool for analysis of nanoemulsion stability. This value can be used to evaluate the stability of nanoemulsions, check the accuracy of determination of the droplet size, and explain the rate of oil phase aggregation and coalescence. The optimal stability is attained when the absolute value of the zeta-potential is $\geqslant$ 30 mV (for either positive or negative potentials), which provides for the electrostatic repulsion between the droplets. The critical instability occurs at potentials between –30 and +30 mV, when van der Waals forces inducing aggregation predominate. However, when polymers are added, steric repulsion becomes the major stabilization mechanism. In these systems, the zeta-potential may be in the region of $|\zeta| < 30$ mV, but the emulsion would remain stable due to the formation of a dense polymer layer on the droplet surface and the entropic barrier. Nanoemulsions stabilized by surfactant–polymer–NP systems were prepared by a high-energy method,[205] and the initial zeta-potential of +42.7 mV decreased to approximately 15 mV over a period of 168 h because of increasing number of oil droplets and continued to gradually decrease down to +11 mV over a period of one month, with the nanoemulsion stability being preserved. Thus, the results of zeta-potentiometry prove that the stability of nanoemulsions cannot be perfectly described by the electrostatic barrier effect alone, but it is also necessary to include the effect of bulk steric hindrance. A detailed study by Pal *et al*.[237] elucidated the temporal dynamics of the zeta-potential in various systems (surfactant, surfactant–polymer, surfactant–polymer–NPs) by demonstrating that the decrease in the zeta-potential with time is attributable to the coalescence of droplets and decrease in the interfacial surface area. Mention should be made of the authors' conclusion about limited applicability of zeta-potential measurements for assessing the stability of complex systems containing polymer stabilizers where steric effects play a predominant role. In addition, the authors confirmed that measurement of the zeta-potential is not an accurate method for evaluating the stability of nanoemulsion systems containing a polymer and a surfactant. These studies highlight the need for an integrated approach to evaluation of the stability of nanoemulsions taking account of both electrostatic and steric stabilization mechanisms.

5.2. Interfacial activity

The interfacial tension describes the attractive force between molecules at the interface of two phases. In the general case, it is called surface tension at the air–liquid interface in which

cohesive forces predominate. However, there are also adhesive forces that act between a liquid and a solid, a liquid and a gas, or between liquids in different phases. The interfacial tension is an important factor for oil recovery: a decrease in IFT between reservoir oil and nanoemulsion down to values of approximately 0.001 mN m^{-1} and below is favourable for increasing oil recovery.[47] In addition, IFT provides valuable information for optimizing the concentrations of emulsifiers and co-emulsifiers, as well as for appropriate correction of the formulation.

Surfactants containing a benzene ring can decrease IFT of an O/W nanoemulsion. The benzene ring tends to interact with hydrophobic molecules, thus forming a thin hydrophobic barrier upon the adsorption of such surfactant at the oil–water interface. Higher hydrophobicity leads to lower IFT.[238] In addition, the benzene ring has a planar regular hexagonal structure and is sufficiently large to form a stable film at the interface between the liquids. For example, a nanoemulsion[68] with an average particle size of 60–90 nm was prepared by diluting a microemulsion with deionized water down to concentrations of 0.05–1 mass% (for the indicated size, respectively); the microemulsion was composed of a mixture of SDBS and alkylphenol ethoxylate OP-11 (25.58 mass%), n-butanol (9.31 mass%), water (46.51 mass%), and kerosene (18.60 mass%). At a concentration of 0.10 mass%, the interfacial tension was 0.091 mN m^{-1} and it barely changed as the concentration increased, *i.e.*, the adsorption of surfactant molecules at the oil–water interface reached saturation, and the oil recovery for the nanoemulsion upon spontaneous impregnation was 30%.

Analysis of the droplet shape is an effective method for investigation of interfacial properties. Different configurations of a deformed drop (sitting, hanging) make it possible to determine the static interfacial tension. The hanging drop method is used to accurately determine the surface tension and interfacial tension, while the sitting drop method is used to characterize the wetting properties by measuring the contact angle. These approaches can be used to quantitatively determine the interfacial activity of system components, which is particularly important for the development of stable nanoemulsions and for the study of their interaction with various surfaces. The differences between the procedures are due to different physical conditions: a hanging drop in the equilibrium state reflects the balance of surface forces, whereas a sitting drop demonstrates the behaviour of a liquid on a solid substrate, which is critical for understanding of adhesion characteristics and wetting processes.

Tliba *et al.*[239] investigated the effect of various nanoemulsion formulations on the rock wettability by measuring the contact angles and found that hydrophilic rocks become oil-wet after interaction with oil due to the adsorption of polar components (Fig. 21).[239] The authors used various nanoemulsions containing crude oil and water with 0.05 mass% NaCl and 0.1 mass% Na_2CO_3 (oil : water = 1 : 9 v/v), and an active component, which was either SiO_2 NPs (0.01 mass%), or ammonium lauryl sulfate (ALS), or sodium olefin sulfonate (C14–16) (SOS), or their combinations. Testing of ALS and SOS separately showed moderate efficacy: the wetting angles were in the range of 105–120°, which corresponds to the transition to intermediate wettability. SiO_2 NPs also proved to have low efficiency. However, when they were used together with a surfactant, the contact angle sharply changed to 161–177°, which is indicative of switching to clear-cut hydrophilicity. The synergistic effect caused by combination of surfactant and SiO_2 NPs provided much higher efficiency compared to the efficiency of their separate use, which opens up new opportunities for the control of the reservoir filtration and storage properties.

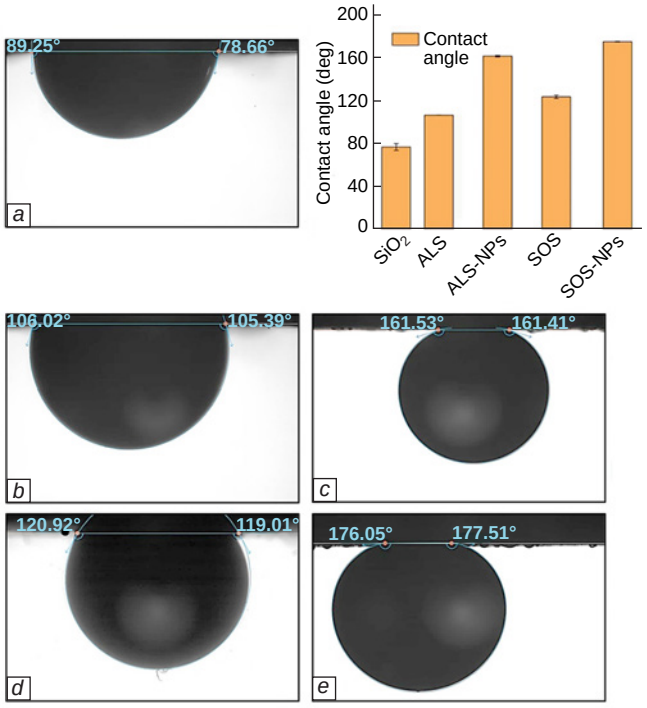

Figure 21. Measurement of the contact angle in the presence of (*a*) SiO_2 NPs, (*b*) ALS, (*c*) ALS–SiO_2 NPs, (*d*) SOS, and (*e*) SOS–SiO_2 NPs; diagram of the change in the wettability.[239] Copyright belongs to the Elsevier.

The experimental data reported by Pal *et al.*[237] demonstrate the variation of the cumulative oil recovery and pressure drop for the use of nanoemulsion stabilized by surfactant–polymer–NPs. n-Heptane and an aqueous solution containing gemini surfactant (14-6-14) (0.02–0.2 mass%), polyacrylamide (PAA, 0.01–0.1 mass%), and SiO_2 NPs (0.0–0.1 mass%) were mixed in 1 : 9 volume ratio, and the mixture was ultrasonicated. The study included simulation of secondary oil recovery methods: successive injection of water and brine (1.0 mass% NaCl) at a flow rate of 10 mL h^{-1}, which resulted in an early breakthrough of water because of the considerable viscosity difference between reservoir oil and the displacing aqueous phase. This provided extraction of 46–47% of the original oil in place. When a water cut of approximately 95% was achieved, a nanoemulsion plug was injected at a lower flow rate of 5 mL h^{-1} (tertiary oil recovery method, EOR). The proposed approach implements three main mechanisms for enhancement of oil recovery: reduction of IFT, alteration of the rock wettability, and emulsification. This resulted in a gradual increase in the oil recovery accompanied by a simultaneous decrease in the water cut, which was attributed to enhanced coalescence of mobilized, previously immobile, oil droplets to form a clear-cut oil bank, which is an indicator of effective displacement, where coalesced droplets form a single mobile front (Fig. 22).[237] The use of the surfactant–polymer–NP system decreased the residual oil saturation to 23.8%, with the nanoemulsion phase effectively preventing the back-flow and re-entrapment of oil by porous rock. The subsequent water flooding without stopping the process helped to maintain uniform displacement of the oil bank, thus providing additional production growth.

In recent years, researchers have proposed an innovative approach to assessing the wettability by measuring the zeta-

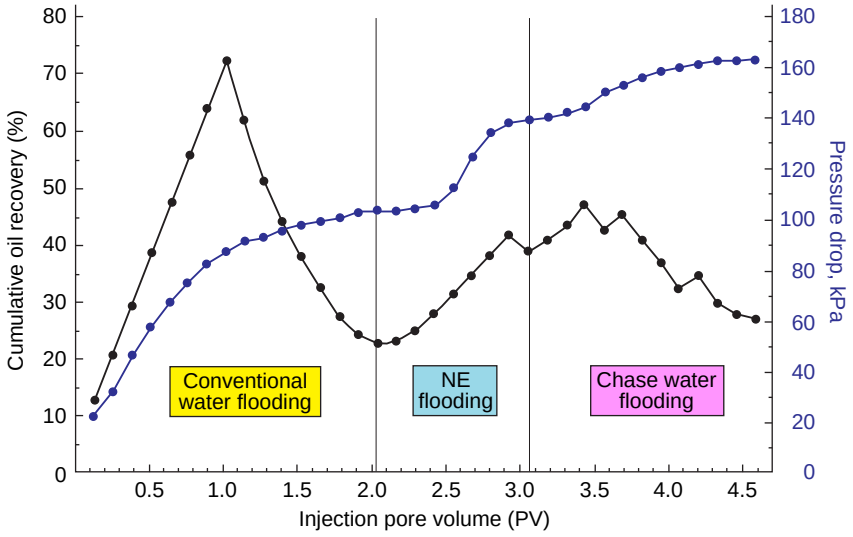

Figure 22. Cumulative oil recovery and pressure drop curves as functions of the injection pore volume for flooding with a surfactant–polymer–NP-stabilized nanoemulsion.[237] Copyright belongs to the Elsevier.

potential. This method overcomes the limitations of classical methods of wettability analysis developed six decades ago. Unlike the conventional methods, which do not allow *in situ* measurements, the new method based on zeta-potential measurement provides real-time monitoring of the wettability, which is especially important for investigation of dynamic processes that change the wettability characteristics. As shown by Bassioni и Taqvi,[240] this method opens up new prospects for interpreting the role of the surface charge of minerals in the control of reservoir wettability. The procedure was based on step-by-step addition of components (crude oil was added in 1 mL portions to an aqueous slurry of limestone, and water was added to crude oil-saturated limestone), with zeta-potential being measured after the addition of each portion. Analysis of the curves obtained in this way revealed clear patterns: initially, hydrophilic limestone had a potential of +29 mV, the gradual decrease in the potential reflected the adsorption of oil components, while the sharp drop from +10 to 0 mV after the addition of 40–45 mL of oil corresponded to the critical point of wettability transition. A particular benefit of this study is the comparison of various systems, including the use of polymers, which prevent oil adsorption; this made it possible to quantitatively evaluate the rate of wettability change and the critical points of phase transitions. Of considerable interest are the results reported by Cabaleiro *et al.*,[241] who studied nanoemulsions of phase change materials (PCM) with a droplet size of 25–180 nm and a zeta-potential reaching –80 mV. Phase change materials represent a class of functional substances able to accumulate and release large amounts of energy as they undergo phase transitions, mainly melting and crystallization (*e.g.*, paraffins and fatty acids). Thin nanoemulsions with long-term stability (PCME) were prepared by ultrasonic treatment at a constant surfactant (SDS) : technical grade paraffin (RT21HC) ratio of 1 : 8. The experiments identified two key benefits of these systems: a pronounced decrease in the surface tension and considerably improved wetting properties, manifested as a 52% decrease in the contact angles compared to water. These data confirm good prospects of PCME nanoemulsions for modification of wetting characteristics in various industrial processes.

Graphene-based Janus materials showed excellent interfacial behaviour owing to amphiphilic properties. Tabar *et al.*[153] synthesized a nanoemulsion by ultrasonic treatment of an aqueous dispersion of a nanohybrid of graphene quantum dots with MoS_2 quantum dots (GQDs/MQDs) for 10–15 min. Nanoemulsions with nanohybrid content of 10 mass%, 50 mass%, or 70 mass% were prepared by adding 0.3 mass% SDBS (anionic surfactant)/CTAB (cationic surfactant), 5.3 mass% n-decane, and 5.3 mass% 2-propanol to nanohybrids diluted in water (50 mL). The 10% GQDs/MQDs/CTAB and 50% GQDs/MQDs/SDBS nanoemulsions showed good stability and the ability to alter the reservoir rock wettability to water-wet, and the 10% GQDs/MQDs/CTAB nanoemulsion had the lowest IFT value (18.72 mN m^{-1}). The contact angle of 64.57° indicated that this nanohybrid has the most pronounced capacity, in the series of prepared nanohybrids, for altering the wettability of the reservoir rock from oil-wet to water-wet, while providing oil recovery efficiency of 22% of the original oil in place.

An ultralow IFT value (10^{-3} mN m^{-1}) was obtained[242] for a crude oil nanoemulsion (50–200 nm) upon the addition of 3.4×10^{-3} mass% of powdered NPs of organically intercalated montmorillonites (OMts), that is, montmorillonite (smectite group natural clay mineral) modified with organic compounds. The nanoemulsion was prepared by the PIC method and additionally stabilized by a gemini cationic surfactant (G16-2-16) and nonionic polyoxyethylene lauryl ether (Brij 30). The results of the study suggest a synergistic effect between gemini surfactant and OMts with ultralow interfacial tension.

The effect of salinity on the properties of nanoemulsions at various NaCl concentrations (0, 0.01, 0.02, and 0.05 M) was studied by Peng *et al.*[243] The authors showed a gradual decrease in IFT with increasing salinity due to the reduction in the repulsive barrier between oil droplets and emulsifier molecules, which facilitates adsorption of the nanoemulsion compared to oil droplets. The effect of temperature on the surface tension at the air–nanoemulsion interface was studied in a similar way;[237] the surface tension was found to decrease with increasing temperature due to the increase in the interface area/curvature, as this is favourable for the adsorption of surfactant molecules.[244]

The nontoxic and environmentally safe SiO_2 NP@montmorilant@xanthan nanocomposite with a 31–50 nm size was synthesized using montmorilant (nanoclay), xanthan gum, (a green surfactant extracted from the plant *Adinandra dumosa*), and SiO_2 nanoparticles for the use in EOR.[236] A nanoemulsion of crude oil containing SiO_2@montmorilant@xanthan prepared by ultrasonic treatment provided a decrease in IFT from 36 to 15.42 mN m^{-1} and a wettability shift for carbonate rocks from

150° to 33° in the presence of 250 ppm of the nanocomposite. In sandstones, the wettability shift from 140° to 34° occurred at 1000 ppm of the nanocomposite, with the additional oil recovery being 15.79%.

Miscibility is the ability of liquids to mutually dissolve each other to form a homogeneous system, which is especially important for evaluation of the interaction of nanoemulsions with reservoir oil in EOR processes and in the removal of contaminants. This feature is a measure of the efficiency of nanoemulsions on contact with hydrocarbons (reservoir oil), which determines their practical applicability. The miscibility is evaluated by a variety of methods, including visual analysis, rheological measurements, and spectroscopic studies. Kumar and Mandal[37] established that a nanoemulsion based on a light mineral oil, nonionic Tween 40 surfactant, and water in a concentration varying from 0.5 to 93 mass% has stable miscibility with crude oil for more than 48 h. This long-term compatibility is a critical factor for enhanced oil recovery. Pal and Mandal[58] demonstrated that a nanoemulsion system (<500 nm) containing dimeric surfactants, partially hydrolyzed polyacrylamide as a polymer, and SiO_2 NPs gives rise to a three-phase system: crude oil phase at the top (~5mL), mixed emulsion phase in the middle (~12.5 mL), and nanoemulsion phase at the bottom (~2.5 mL). The volume of the intermediate phase, representing a crude oil–emulsifier–nanoemulsion system, is the critical mixing characteristic. This volume is a quantitative measure of the efficiency of a nanoemulsion in displacing residual oil from the reservoir pore space, indicating high solubilization activity of the nanoemulsion. This effect is attributable to the exceptionally low interfacial tension between the nanoemulsion and oil,[245] which confirms the good prospects for the use of these systems in enhanced oil recovery processes.

5.3. Rheological properties

Rheology affects the permeation properties of nanoemulsions, such as migration, working volume, pore plugging, and displacement efficiency in porous media. The unique rheological properties of nanoemulsions, caused by their nanoscale nature and the specific state of interfaces, exceed those of macro- and microemulsion systems. Nanoemulsions show a complex rheological behaviour, which can be classified into three main types: Newtonian fluid, non-Newtonian fluid (pseudoplastic: liquefaction under shear, and dilatant: thickening under shear), and viscoelastic fluid. These rheological characteristics can be controlled and changed in accordance with the requirements by adjusting the volume fraction of the dispersed phase and the droplet size; by adding various components such as thickeners (polymers) and salts/depleting agents that cause gelation of the emulsion droplets; and by changing the temperature, which affects the viscosity and structure of the system. Wilking and Mason[246] investigated an O/W nanoemulsion consisting of 40 vol.% oil phase (polydimethylsiloxane, PDMS) and 60 vol.% aqueous phase containing 10–116 mm sodium lauryl sulfate (SDS). The authors showed that the nanoemulsion switches from the free-flowing liquid state to the elastic gel state. This structural transformation was achieved through multiple cycles of passing the premix emulsion through a microfluidic device with an inlet pressure of ~1 MPa. This transition was caused by intense droplet rupture, *i.e.*, generation of smaller droplets that induce stagnation in the nanoemulsion structure. Thermoreversible gels based on nanoemulsions (40–200 nm) containing polydimethylsiloxane (PDMS) silicone oil (33 vol.%), water (34 vol.%), sodium dodecyl sulfate (SDS) as a surfactant (200 mM), and poly(ethylene glycol) diacrylate (PEGDA) as a gelator (33 vol.%) were obtained[247] using a high-pressure homogenizer (104 MPa). The nanoemulsion showed a sharp thermoreversible transition from a low-viscosity liquid to a fractal-like colloidal gel formed by PDMS droplets with mesoscopic porosity and solid-like viscoelasticity with an elastic modulus approaching 100 kPa, which is perhaps the highest value recorded for emulsion-based systems. In addition, these nanoemulsions showed a thermoreversible response and the possibility of fixing the structure under UV irradiation.

De Castro Dantas *et al*.[19] obtained a nanoemulsion with a low content of the LONano oil (RNX95 surfactant, isopropyl alcohol co-surfactant, kerosene, and distilled water) by diluting a microemulsion of the same composition with water and stirring at 500 rpm followed by introduction of polyacrylamide. The authors achieved an increase in the apparent viscosity of nanoemulsions from 22.19 to 48.82 cP as the polyacrylamide content increased from 0.2 to 0.4 mass%, which is much higher than the viscosity of crude oil (14.799 cP). Presumably, a more viscous nanoemulsion system would preferably sweep the low-permeability zone, while avoiding the high-permeability channels in the reservoir, thus increasing the oil recovery factor upon the injection. Moreover, the surfactant present in the nanoemulsion competes with the polymer and migrates into micelles in the bulk phase, which leads to swelling and to increase in the system viscosity due to the decrease in the number of free water molecules and, hence, is favourable for the control of the mobility. The residual oil recovery was directly proportional to the percentage of the polymer in the nanoemulsion, ranging from 39.6 to 76.8%.

The interaction of SiO_2 nanoparticles with polymer chains gives micellar or supramolecular structures that are strong enough to maintain the nanoemulsion integrity, which results in increasing viscosity in high shear-rate regions.[69,248] The nanoemulsion has a potential to reduce the residual viscosity of heavy oil as a result of mass transfer between the droplets and heavy oil, which gives an oil/water emulsion. In this case, nanodroplets of the nanoemulsion serve as the surface tension gradient, permitting both interfacial turbulence and mass transfer.

An integrated analysis of the factors[249] determining the viscosity of nanoemulsions, particularly, mixing, aggregation of nanodroplets, and viscosity ratio between the dispersed and continuous phases demonstrated that nanoemulsions exhibit unique rheological properties owing to the capacity of the droplets for reversible deformation upon shear loads. Low interfacial tension ensures fast restoration of the spherical droplet shape after the end of treatment, which accounts for pronounced elastic properties. Comparative analysis shows that nanoemulsions are superior to microemulsions in terms of elasticity, which is quantitatively confirmed by elastic modulus values comparable to the Laplace pressure of undeformed droplets. A considerable contribution to the understanding of rheological transformations was made by Fryd and Mason,[250] who demonstrated the possibility of microemulsion transition into the highly elastic nanoscale state under the action of intense shear. This process is caused by cavitation-induced breakup of the droplets, followed by the formation of a stable spatial network of nanodroplets.

At the end of the Section addressing the rheological properties of nanoemulsions, we would like to mention the reservoir properties and permeability factor and rock properties. The heterogeneity of the rock plays an important role for the fabrication of nanoemulsions, because the emulsion stability,

relationship between the viscosity and mobility, flow rate, and, hence, the plugging ability depend on the pore size distribution and type and length of permeable regions. In a similar way, a contrast between the vertical and horizontal permeability is a crucial factor for choosing the way of emulsion supply through either injection or production wells, although it is generally believed that injection through a production well provides rapid and relatively economical plugging and eliminates cross-flow or undesirable locations. In the case of a low permeability contrast, arrangement of injection wells in elevated parts of the reservoir would be more appropriate than in the case of high contrast, since the probability of cross-flow into high-permeability areas is lower. Meanwhile, when the contrast is high, the arrangement of emulsion plugging sites near a producing well is achieved by generation of an optimal pressure drop between high- and low-permeability zones, which leads to effective plugging and flow.

Nanoemulsions exhibit a complex set of rheological properties, which are of prime importance for enhanced oil recovery techniques. Thus, their behaviour should vary depending on the composition and operation conditions. For example, the ultralow-permeability sandstone has very tight pore channels with poor connection between them. For rocks characterized by low porosity and ultralow permeability, pseudoplastic behaviour of nanoemulsions is preferred (*e.g.*, surfactant-stabilized crude oil in salt water).[251] Flooding with a nanoemulsion (mineral oil–Tween 40–water) of a sandstone with a porosity of 30.52% provided an additional oil recovery according to a power law model of the rheological behaviour.[37] Stable viscosity values with increasing shear rate and surfactant concentration attest to a better control of the nanoemulsion mobility (compared to emulsions the viscosity of which is unstable upon changes in the shear rate or surfactant concentration), which provides a better displacement efficiency upon injection of this nanoemulsion into a reservoir. A nanoemulsion (n-heptane–Tween 40–SiO_2 NPs–water)[252] with a clear-cut pseudoplastic behaviour synthesized by ultrasonic treatment provided an additional oil recovery of 34.94% relative to the crude oil extracted by water flooding of the sandstone (31.61% porosity, 381.70 mD permeability).

The use of nanoemulsions under field conditions requires further research to confirm their efficacy as observed on a laboratory scale. Table 4 presents compositions of the injected nanoemulsions, their significance and application prospects for particular reservoir conditions. In view of the enormous volumes of residual oil in reservoirs, the use of nanoemulsions could become a key factor for increasing oil production.

6. Simulation of nanoemulsion behaviour and field studies

6.1. Simulation of nanoemulsion behaviour

Laboratory experiments require a lot of time and resources, and experimental results can be obtained only on a core scale or using displacement models. Simulation can provide a lot of information about the phase behaviour of nanoemulsions at a reservoir or pore level.[253] Currently, methods of molecular dynamics (MD simulation) and computational fluid dynamics are widely used to simulate the phase behaviour and EOR applications of nanoemulsions.

Molecular dynamics simulation can be used to study microscopic systems comprising thousands of molecules. This method combines classical mechanics with quantum and statistical mechanics to describe changes in complex structures under various conditions.[254] In terms of statistical dynamics, all system characteristics such as viscosity and IFT can be found by calculating the potential energy according to positions of atoms.[255] The adsorption and self-assembly of emulsifier molecules at an oil–water interface and the properties of arising interfacial films can be studied using MD simulation. This is done within specialized program packages such as GROMACS, AMBER, and LAMMPS, which make it possible to reproduce an oil–water system and model the behaviour of emulsifier molecules. A recent review by Wang *et al*.[256] systematizes the key aspects of the application of MD simulation to the study of oil–water interfaces such as simulation principles, analysis of intermolecular interactions, and data processing algorithms to predict the properties of emulsions. Miyamoto *et al*.[257] investigated the adsorption of cellulose NPs at the octane–water interface. The dispersed cellulose chains aggregate over time to form microcrystals, while octane molecules form oil droplets (Fig. 23). The cellulose microcrystals interact with the surface of octane droplets through the corners and then gradually cover them, which is confirmed by increasing interaction energy. In addition, intermolecular hydrogen bonds are formed between adjacent cellulose chains, thus producing a viscoelastic film, which is favourable for stabilization of emulsions.

Table 4. Composition of nanoemulsions and results of their application for particular reservoir conditions.

Nanoemulsion composition (types of oil and aqueous phases, surfactant, polymer, NPs)	Type of rock	Rock characteristics	Oil recovery	Ref.
Liquid paraffin, water, polymer SL75, surfactant Brij30, clay NPs LAPONITE® RD	Artificial sandstone	Porosity: no data Gas permeability: 209 mD Pore volume: 4.88 mL	70% of the oil in place	235
Kerosene, water, polymer PAA, surfactant (RNX95 + isopropyl alcohol + sodium *p*-toluenesulfonate)	Natural sandstone	Porosity: ~ 36–41% Permeability: 100–300 mD Pore volume: 23–25 cm^3	90% of the oil in place	19
Xylene, sea water (total salinity of 44.5 g L^{-1}), surfactant Triton X-100 (octylphenol ethoxylate), ZrO_2 NPs	Compacted non-cemented silicate layer	Porosity: 29–31% Permeability: 16–18 mD	Additional 59.3% after water flooding	57

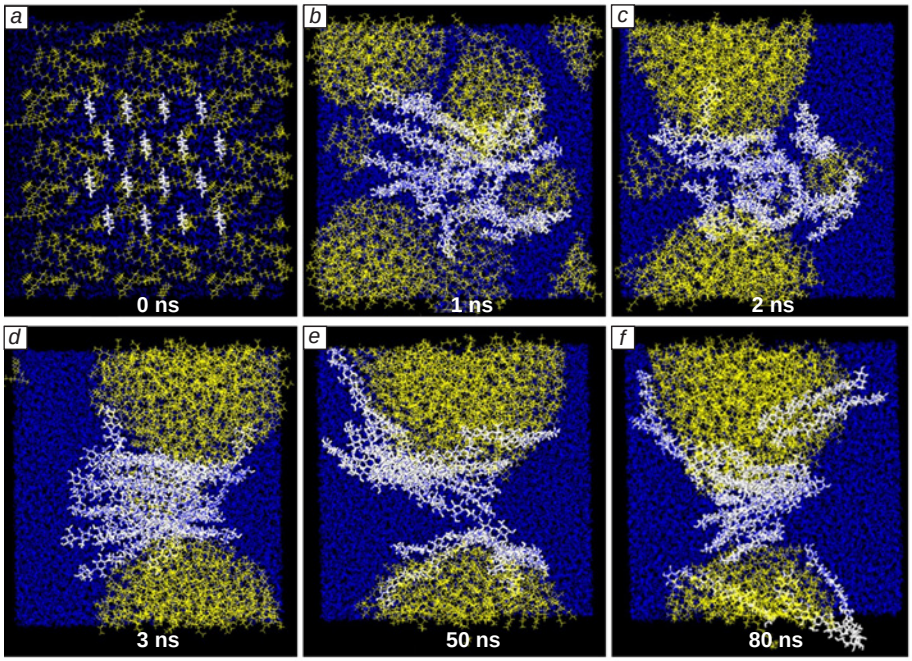

Figure 23. The results of MD simulation of a cellulose mini-crystal in O/W medium over time (indicated in the photographs) (designations: white lines are cellulose, blue lines are water, and yellow lines are octane).[257] Copyright belongs to Springer Netherlands.

Shi *et al*.[258] performed MD simulation to study the self-assembly of four types of surfactants at the oil–water interface. The results demonstrated the following hierarchy in terms of the ability to reduce interfacial tension: dimeric surfactants (gemini) possess the highest efficiency owing to the double hydrophobic-hydrophilic structure; anionic surfactants have moderate activity caused by electrostatic repulsion; zwitter-ionic surfactants have reduced activity due to charge neutralization; and nonionic surfactants are least active, as stabilization is achieved only due to steric effects. During micelle formation in aqueous solutions of various types of surfactants, enthalpy and entropy compensation phenomena were observed. Gemini surfactants and zwitter-ionic surfactants were highly prone to form micelles. These data are of practical importance for the selection of emulsifiers in oil production where the ability of surfactants to reduce the interfacial tension is the key feature. Unlike traditional experimental methods, MD simulation provides the unique possibility of real-time monitoring of structural changes in the emulsifier molecules, including their diffusion, penetration into the interfacial layer, and reorganization. This is especially valuable for the analysis of adsorption/desorption mechanisms and determination of the emulsion stability. Using MD simulation, Liu *et al*.[259] proposed a mechanism of asphaltene self-organization in crude oil–water systems. On water surfaces *in vacuo*, asphaltenes form ordered nanoaggregates, *i.e*., polycyclic aromatic structures are arranged perpendicular to the water surface, thus forming an analogue of a fence the stacks of which are asphaltene molecules. This orientation gives rise to a stable protective film that envelops water droplets and stabilizes the emulsion (Fig. 24). This study also demonstrated that ethyl cellulose demulsifier destroys this film, which leads to exposure of water droplets. This confirms the key role of asphaltene aggregates for the emulsion stability.

Computational fluid dynamics is a numerical simulation method for solving fluid flow and heat transfer problems in three dimensions, which makes it possible to model the hydrodynamics of two fluids with immiscible interfaces. The conservation equations are solved numerically by discretization of the geometric domain and using the finite element/volume method. This method can be applied to a number of properties of a liquid such as viscosity, density, IFT, *etc*.[95] Imani *et al*.[260] investigated the dynamics of oil droplets in pore constrictions by analyzing the effect of pore geometry, wettability, and droplet size. It was shown that overcoming the capillary resistance at a capillary number of above 0.0001 requires simultaneous increase in the pore channel radius to provide for effective migration of a

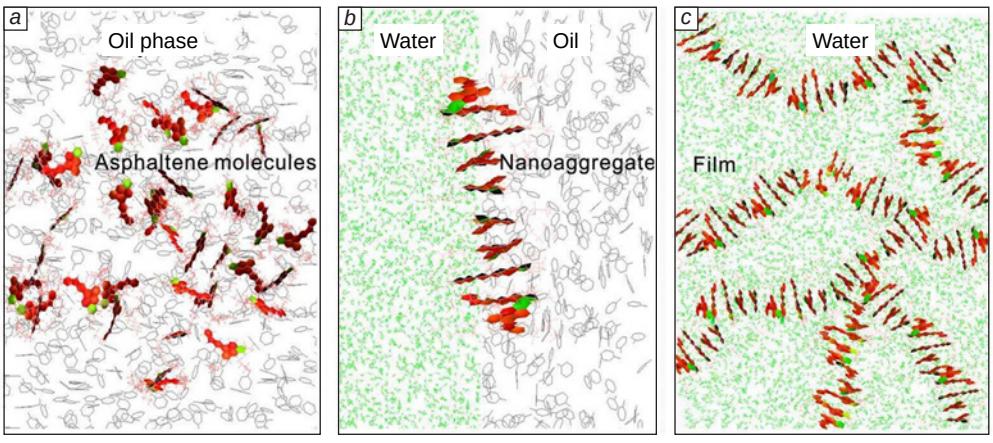

Figure 24. MD simulation of the formation of asphaltene protective film: (*a*) separate asphaltene molecule arranged perpendicular to the water surface, (*b*) ordered asphaltene nanoaggregate (fence), (*c*) protective film formed from interlaced aggregates, which stabilizes a water droplet at the oil–water interface.[259] Copyright belongs to the ACS Publications.

droplet. Munir and Du[261] used the Level Set method[262] for numerical simulation of the behaviour of nanoemulsion droplets in a constricted splitting channel. The study revealed the key role of three factors, that is, gravitational forces, surface tension, and wetting angle, on the ability of droplets to overcome the resistance and penetrate through the pore space. Rosengarten *et al*.[263] utilized the computational fluid dynamics to investigate the effect of the contact angle on the oil droplet dynamics in a channel constriction. They found that the droplet breaks up at a contact angle of less than 30°, while a plug forms at 150°. Zhang *et al*.[264] reported an analytical and numerical study of the minimum momentum needed for an oil droplet to squeeze through a constriction. The results showed that the minimum momentum can be achieved when the unsteady Young–Laplace pressure counterbalances the total loss of the minor pressure in the constriction, which is important for calculating the pressure that must be applied for reservoir flooding.

One example of fluid dynamic simulator is the CMG-STARTS program package, which makes it possible to model multiphase flows in an oil reservoir taking account of the change in IFT and capillary pressure and phase transitions.[265] This package is used to simulate the nanoemulsion flooding of oil fields on the basis of the results of laboratory experiments.

Although simulation is an advanced approach providing understanding of the phase behaviour of nanoemulsions and evaluation of the efficiency of oil production methods, there are still only few results, and the prediction accuracy inherent in the modern simulators is insufficient.[266] The nanoemulsion flow through a medium is a very complex process, and further development of simulation methods for nanoemulsions is a challenging and relevant problem.

6.2. Field pilot tests of nanoemulsions in hydrocarbon production

When it comes to oil reservoir conditions, it is important to consider the limitations. In a high-temperature and saline reservoir, the surfactant properties (solubility, activity of the molecule, *etc*.) that stabilize the nanoemulsions change.[48] A change in the surfactant activity leads to changing adsorption and distribution of surfactant molecules in the interfacial film, thus decreasing the film strength. These complex external conditions can lead to increasing size of nanoemulsion droplets and even to demulsification. In addition, nanoemulsions would migrate from injection wells to production wells during flooding, and this long-distance migration may take months. The Ostwald ripening of nanoemulsions can occur during flooding, resulting in an increase in the size of nanoemulsion droplets. Meanwhile, adsorption of particles/surfactants such as clay, colloids, asphaltenes, *etc*. on the nanoemulsion surface during migration may change the structure of nanoemulsions.

Currently, the use of nanoemulsions to increase the productivity in the field is not widespread, with only few pilot studies being available. The first field test of a combined fracturing fluid was performed[267] at the Sulige gas field in Changqing, western China. The addition of a nanoemulsion to the fracturing fluid characterized by low level of formation damage resulted in a considerable increase in the fluid flowback rate and, hence, increased the single-well daily gas production.

Liang *et al*.[268] found that nanoemulsions can reduce the invasion pressure in oil reservoirs, increase the effective volume, and make drag reduction more efficient. After laboratory testing and simulation of an oil reservoir,[269] a field pilot project was designed, constructed, and commissioned. The field tests confirmed the possibility of generating and maintaining the injection of an emulsion stabilized by solid particles in the field and of distributing the stabilized emulsion in the reservoir.

The mentioned pilot projects demonstrate that emulsion flooding can be used in both light and heavy oil reservoirs, as well as in gas fields.

7. Conclusion

In order to provide the applicability and the wide use of nanoemulsion technologies for enhanced oil recovery, quite a few promising aspects can be considered. The implementation of new strategies and methods can substantially increase the efficiency of emulsion flooding. For example, the introduction of nanoparticles and/or nanocomposites into a nanoemulsion may enhance the stability, change the interface properties, and increase the emulsion viscosity. This may improve the control over oil displacement, especially in heterogeneous reservoirs.

The full understanding of the interaction between the used nanoemulsions and the reservoir medium is still to be gained, as indicated by the discrepancies between laboratory (95% predictability) and field (60–70% predictability) results.[37] The solution of this problem requires achieving the following goals: standardization of stability tests for different types of reservoirs, development of smart nanoemulsions maintaining their properties for a long period of time, and generation of digital twins for predicting the behaviour of nanoemulsions.

The current studies of the mechanisms of action of nanoemulsions, whether in the enhanced oil recovery or in the wellbore cleanup, face pronounced methodological limitations. Although experimental data confirm the high potential of these techniques (providing, for example, a 15–25% increase in oil recovery under controlled laboratory conditions[270]), the fundamental understanding of the underlying physicochemical processes remains fragmentary. A problem is the absence of comprehensive theoretical models describing the behaviour of nanoscale droplets under real reservoir conditions. In particular, specific features of the interaction between nanoemulsions and various types of rocks (especially with pore size less than 1 μm),[45] adsorption/desorption dynamics at high temperatures and pressures, and chemical transformations of emulsion components in a reservoir have not been sufficiently addressed.

The simulation of these processes presents a particular challenge. This is related to both the lack of experimental data for model verification and the fundamental difficulties of considering the nanoscale effects. To overcome these limitations, it is necessary to develop new research approaches, including standardized testing methods and conduction of long-term field experiments.

The differences in approaches to the synthesis, component composition, and experimental conditions lead to a wide scatter of performance characteristics: the gain in oil recovery may vary from 12% to 30% even for similar types of reservoirs.[271,272] The main cause for this inconsistency is the lack of standardized testing protocols. The vast majority of tests use unique, non-standard protocols for the preparation of nanoemulsions. The differences in the recommended concentrations of key components are particularly noticeable: the content of surfactants varies from 0.1 to 5 mass%, the polymer content ranges from 0.01 to 1.2 mass%, and the salt concentration is from 1 to 15 mass%.[265] This data variability generates serious obstacles to the industrial implementation of the techniques.

The issue of the cost-effectiveness of using nanoemulsions in the oil and gas industry remains a subject of active debate among

experts. The main disagreements are concerned with the high energy intensity of their production, the need to use specialized equipment, and the ambiguity of the environmental impact of using nanoemulsions compared to conventional chemicals. According to investigation results, the synthesis of nanoemulsions actually requires considerable energy expenditures, which are on average 30–40% higher than those of the production of injectable fluids (emulsions, surfactant or polymer solutions).[194] However, this can be counterbalanced by much lower consumption of surfactants (by 50–60 vol.%) and enhanced stability of nanoemulsions under various reservoir conditions. Experimental laboratory data confirm that nanoemulsions demonstrate better oil displacement efficiency at lower concentrations of active components.[25]

The environmental aspect also requires thorough analysis. On the one hand, the energy-intensive production actually increases the carbon footprint. On the other hand, the new-generation biodegradable formulations may decrease the environmental load compared to traditional chemicals.[273] A final resolution of these contradictions requires further development of technologies, including the development of energy-efficient synthesis methods and integrated evaluation of the product life cycle. The transition to industrial implementation is possible only after thorough optimization of all stages from laboratory research to production scaling-up.

The use of nanoemulsions in the oil and gas industry raises legitimate concerns among experts regarding their potential impact on ecosystems and human health. The lack of long-term data on the behaviour of nanoscale components in the environment poses considerable risks, particularly regarding migration to groundwater and accumulation in living organisms.[64] The main concern is the possibility of delayed environmental consequences that may appear decades after the technologies are applied. To minimize the environmental risks, it is necessary to develop a comprehensive system for safety evaluation, including long-term monitoring and strict regulatory requirements. Only an interdisciplinary approach combining nanotoxicological studies with the development of nature conservation standards will ensure safe application of nanoemulsions in the oil and gas industry.

This review was written within the framework of the State Assignment of the Ministry of Science and Higher Education of the Russian Federation (FSRZ-2020-0012).

8. List of abbreviations and symbols

ALS — ammonium lauryl sulfate,
ASP — alkali–surfactant–polymer,
CNTs — carbon nanotubes,
CMG — computer modelling group
CTAB — cetyltrimethylammonium bromide,
EOR — enhanced oil recovery,
FESEM — field emission scanning electron microscopy,
GO — graphene oxide,
HLB — hydrophilic-lipophilic balance,
HLD — hydrophilic-lipophilic deviation,
IEA — international energy agency,
IFT — interfacial tension,
IUPAC — International Union of Pure and Applied Chemistry,
MD — molecular dynamics,
ME — membrane emulsification,
NE — nanoemulsion,
NP — nanoparticle,
O/W — oil-in-water,
PAA — polyacrylamide,
PCM — phase-change material,
PCME — phase-change material emulsion,
PDMS — polydimethylsiloxane,
PEGDA — polyethylene glycol diacrylate,
PIC — phase inversion composition,
PIT — phase inversion temperature,
PMES — poly(methyl ester sulfonate–acrylamide),
PV — pore volume,
SEM — scanning electron microscopy,
SBS — sodium benzene sulfonate,
SDBS — sodium dodecylbenzene sulfonate,
SDS — sodium dodecyl sulfate,
SOS — sodium olefin sulfonate,
TEM — transmission electron microscopy,
US — ultrasound,
UV — ultraviolet light,
W/O — water-in-oil.

9. References

1. Toril Bosoni. *Oil 2024: Analysis and Forecast to 2030*. (Paris: International Energy Agency (IEA), 2024); https://www.iea.org/reports/oil-2024
2. A.M.Al Sabagh, A.I.Khodair, B.M.El-Sadek, E.E.Badr, E.H.Kalboush. *Sci. Rep.*, **15** (1), 17166 (2025); https://doi.org/10.1038/s41598-025-99993-8
3. *Gosudarstvennyi Doklad o Sostoyanii i Ispol'zovanii Mineral'no-syr'evykh Resursov Rossiiskoi Federatsii v 2023 godu*. (*State Report on the State and Use of Mineral Resources of the Russian Federation in 2023*). (Moscow: Federal Agency for Subsoil Use (Rosnedra), 2024); https://www.rosnedra.gov.ru/data/File/doklad_msb_2023.pdf
4. X.Lyu, H.Liu, J.Tian, Q.Zheng, W.Zhao. *J. Pet. Sci. Eng.*, **208**, 109372 (2022); https://doi.org/10.1016/j.petrol.2021.109372
5. A.Abdi, B.Ranjbar, Y.Kazemzadeh, F.Aram, M.Riazi. *Sci. Rep.*, **14** (1), 11408 (2024); https://doi.org/10.1038/s41598-024-62255-0
6. H.Ali, H.Soleimani, N.Yahya, L.Khodapanah, M.Sabet, B.M.R.Demiral, T.Hussain, L.L.Adebayo. *J. Mol. Liq.*, **309**, 113095 (2020); https://doi.org/10.1016/j.molliq.2020.113095
7. N.Kumar, M.Augusto Sampaio, K.Ojha, H.Hoteit, A.Mandal. *Fuel*, **330**, 125633 (2022); https://doi.org/10.1016/j.fuel.2022.125633
8. A.Gandomkar, M.Ghorbani Sheykhneshin, H.R.Nasriani, P.Yazdkhasti, M.S.Safavi. *Chem. Eng. Res. Des.*, **188**, 462 (2022); https://doi.org/10.1016/j.cherd.2022.09.053
9. M.Tabaeh Hayavi, Y.Kazemzadeh, M.Riazi. *Chem. Phys. Lett.*, **806**, 139975 (2022); https://doi.org/10.1016/j.cplett.2022.139975
10. S.Huang, G.Jiang, C.Guo, Q.Feng, J.Yang, T.Dong, Y.He, L.Yang. *Chem. Eng. J.*, **487**, 150628 (2024); https://doi.org/10.1016/j.cej.2024.150628
11. A.Somoza, M.Flor García-Mayoral, A.Soto. *Fuel*, **346**, 128363 (2023); https://doi.org/10.1016/j.fuel.2023.128363
12. J.Liu, C.Sun, Z.Lun, Y.Li, X.Tang, Q.Zhang, P.Yang. *Sci. Rep.*, **14** (1), 8916 (2024); https://doi.org/10.1038/s41598-024-59637-9
13. J.Zhang, X.Wang, Q.Liang, M.Duan, S.Fang, C.Zhang, J.Chen. *J. Mol. Liq.*, **394**, 123805 (2024); https://doi.org/10.1016/j.molliq.2023.123805
14. W.Xiao, J.Ren, W.Pu, C.Yuan, L.Meng, L.Zheng, H.Zhao, Q.Cheng. *Fuel*, **352**, 129150 (2023); https://doi.org/10.1016/j.fuel.2023.129150
15. R.Sarbast, N.Salih, A.Préat. *Nanomaterials*, **12** (22), 4007 (2022); https://doi.org/10.3390/nano12224007

16. F.Navaie, E.Esmaeilnezhad, H.-J.Choi. *Polymers*, **14** (24), 5555 (2022); https://doi.org/10.3390/polym14245555
17. M.Rezaeizadeh, S.H.Hajiabadi, H.Aghaei, M.J.Blunt. *Adv. Colloid Interface Sci.*, **288**, 102345 (2021); https://doi.org/10.1016/j.cis.2020.102345
18. N.Kumar, A.Verma, A.Mandal. *J. Pet. Sci. Eng.*, **206**, 109042 (2021); https://doi.org/10.1016/j.petrol.2021.109042
19. T.N.De Castro Dantas, T.T.C.De Souza, A.A.Dantas Neto, M.C.P.D.A.Moura, E.L.De Barros Neto. *J. Surfactants Deterg.*, **20** (5), 1095 (2017); https://doi.org/10.1007/s11743-017-1992-2
20. J.H.Schulman, J.B.Montagne. *Ann. N.Y. Acad. Sci.*, **92** (2), 366 (1961); https://doi.org/10.1111/j.1749-6632.1961.tb44987.x
21. P.Calvo, J.L.Vila-Jato, M.J.Alonso. *J. Pharm. Sci.*, **85** (5), 530 (1996); https://doi.org/10.1021/js950474+
22. V.G.Babak, R.Gref, E.Dellacherie. *Mendeleev Commun.*, **8** (3), 105 (1998); https://doi.org/10.1070/MC1998v008n03ABEH000957
23. S.Slomkowski, J.V.Alemán, R.G.Gilbert, M.Hess, K.Horie, R.G.Jones, P.Kubisa, I.Meisel, W.Mormann, S.Penczek, R.F.T.Stepto. *Pure Appl. Chem.*, **83** (12), 2229 (2011); https://doi.org/10.1351/PAC-REC-10-06-03
24. A.Gupta, H.B.Eral, T.A.Hatton, P.S.Doyle. *Soft Matter*., **12** (11), 2826 (2016); https://doi.org/10.1039/C5SM02958A
25. J.Mariyate, A.Bera. *J. Mol. Liq.*, **353**, 118791 (2022); https://doi.org/10.1016/j.molliq.2022.118791
26. D.J.McClements. *Soft Matter*., **8** (6), 1719 (2012); https://doi.org/10.1039/C2SM06903B
27. H.Guo, J.N.Wilking, D.Liang, T.G.Mason, J.L.Harden, R.L.Leheny. *Phys. Rev. E*, **75** (4), 041401 (2007); https://doi.org/10.1103/PhysRevE.75.041401
28. M.Porras, C.Solans, C.González, J.M.Gutiérrez. *Colloids Surf. A: Physicochem. Eng. Asp.*, **324** (1–3), 181 (2008); https://doi.org/10.1016/j.colsurfa.2008.04.012
29. F.Shakeel, W.Ramadan. *Colloids Surf. B: Biointerfaces*, **75** (1), 356 (2010); https://doi.org/10.1016/j.colsurfb.2009.09.010
30. S.Talegaonkar, G.Mustafa, S.Akhter, Z.I.Iqbal. *J. Dispers. Sci. Technol.*, **31** (5), 690 (2010); https://doi.org/10.1080/01932690903120540
31. A.Forgiarini, J.Esquena, C.González, C.Solans. *Langmuir*, **17** (7), 2076 (2001); https://doi.org/10.1021/la001362n
32. N.Anton, J.-P.Benoit, P.Saulnier. *J. Controll. Release*, **128** (3), 185 (2008); https://doi.org/10.1016/j.jconrel.2008.02.007
33. P.P.Constantinides, M.V.Chaubal, R.Shorr. *Adv. Drug Deliv. Rev.*, **60** (6), 757 (2008); https://doi.org/10.1016/j.addr.2007.10.013
34. T.Tadros, P.Izquierdo, J.Esquena, C.Solans. *Adv. Colloid Interface Sci.*, **108**–**109**, 303 (2004); https://doi.org/10.1016/j.cis.2003.10.023
35. U.Sakulku, O.Nuchuchua, N.Uawongyart, S.Puttipipatkhachorn, A.Soottitantawat, U.Ruktanonchai. *Int. J. Pharm.*, **372** (1–2), 105 (2009); https://doi.org/10.1016/j.ijpharm.2008.12.029
36. L.-C.Peng, C.-H.Liu, C.-C.Kwan, K.-F.Huang. *Colloids Surf. A: Physicochem. Eng. Asp.*, **370** (1–3), 136 (2010); https://doi.org/10.1016/j.colsurfa.2010.08.060
37. N.Kumar, A.Mandal. *Energy Fuels*, **32** (6), 6452 (2018); https://doi.org/10.1021/acs.energyfuels.8b00043
38. V.V.Sergeev, K.Tanimoto, M.Abe, R.R.Sharapov, Y.V.Zeigman. *Nanotechnol. Constr.*, **12** (3), 166 (2020); https://doi.org/10.15828/2075-8545-2020-12-3-166-173
39. P.Pillai, R.K.Saw, A.Mandal. *J. Mol. Liq.*, **397**, 124189 (2024); https://doi.org/10.1016/j.molliq.2024.124189
40. J.Wang, Y.Li, F.Zhou, E.Yao, L.Zhang, H.Yang. *ACS Omega*, **5** (6), 2910 (2020); https://doi.org/10.1021/acsomega.9b03744
41. Y.Li, M.Wang, Z.Wei, Y.An, W.Qin, K.Bo, P.Cao, M.Guo. *J. Mol. Liq.*, **384**, 122273 (2023); https://doi.org/10.1016/j.molliq.2023.122273
42. B.Ding, S.H.Ahmadi, P.Babak, S.L.Bryant, A.Kantzas. *Langmuir*, **39** (20), 6975 (2023); https://doi.org/10.1021/acs.langmuir.3c00133
43. A.Sharifi, R.Miri, M.Riazi. *Fuel*, **353**, 129109 (2023); https://doi.org/10.1016/j.fuel.2023.129109
44. A.Mahboob, S.Kalam, M.S.Kamal, S.M.S.Hussain, T.Solling. *J. Pet. Sci. Eng.*, **208**, 109312 (2022); https://doi.org/10.1016/j.petrol.2021.109312
45. X.Hou, J.J.Sheng. *Geoenergy Sci. Eng.*, **221**, 211360 (2023); https://doi.org/10.1016/j.geoen.2022.211360
46. H.Xu, Y.Li, F.Zhou, H.Su, E.Yao, J.Hu, Z.Chen. *Chem. Eng. J.*, **470**, 144070 (2023); https://doi.org/10.1016/j.cej.2023.144070
47. N.M.Aljabri, N.Shi, A.Cavazos. *J. Pet. Sci. Eng.*, **208**, 109306 (2022); https://doi.org/10.1016/j.petrol.2021.109306
48. O.Massarweh, A.S.Abushaikha. *Energy Rep.*, **6**, 3150 (2020); https://doi.org/10.1016/j.egyr.2020.11.009
49. Z.Cao, H.Wang, T.Feng, X.Bu, C.Cui, F.Yang, C.Yu. *Ind. Crops Prod.*, **215**, 118704 (2024); https://doi.org/10.1016/j.indcrop.2024.118704
50. M.Kumari, B.Tomar, P.Singh, S.S.Tomar, T.Patle, S.S.Parihar. In *Advances in Environmental Engineering and Green Technologies*. (Eds V.D.Rajput, A.Singh, K.Ghazaryan, A.Alexiou, A.R.M.Said Al-Tawaha). (IGI Global, 2024). P. 176; https://doi.org/10.4018/979-8-3693-1890-4.ch009
51. S.Yousefi, W.Weisany, S.E.Hosseini, M.Ghasemlou. *Food Hydrocoll.*, **150**, 109655 (2024); https://doi.org/10.1016/j.foodhyd.2023.109655
52. M.Y.Koroleva, E.V.Yurtov. *Russ. Chem. Rev.*, **81** (1), 21 (2012); https://doi.org/10.1070/RC2012v081n01ABEH004219
53. N.M.Zadymova, Z.N.Skvortsova, Yu.D.Aleksandrov, I.Yu.Ilina. *Colloid J.*, **86** (6), 867 (2024); https://doi.org/10.1134/S1061933X24600647
54. W.Hu, Y.Wei, J.Bao. *Pet. Explor. Dev.*, **45** (4), 685 (2018); https://doi.org/10.1016/S1876-3804(18)30072-7
55. Y.Yao, M.Wei, W.Kang. *Adv. Colloid Interface Sci.*, **294**, 102477 (2021); https://doi.org/10.1016/j.cis.2021.102477
56. H.Hamedi, S.Zendehboudi, N.Rezaei, A.Azizi, F.Shahhoseini. *Langmuir*, **39** (23), 7995 (2023); https://doi.org/10.1021/acs.langmuir.2c03266
57. M.Jalilian, A.Tabzar, V.Ghasemi, O.Mohammadzadeh, P.Pourafshary, N.Rezaei, S.Zendehboudi. *Fuel*, **251**, 754 (2019); https://doi.org/10.1016/j.fuel.2019.02.122
58. N.Pal, A.Mandal. *Fuel*, **276**, 118138 (2020); https://doi.org/10.1016/j.fuel.2020.118138
59. A.F.Ibrahim, H.A.Nasr-El-Din. *SPE Res. Eval. Eng.*, **23** (02), 414 (2020); https://doi.org/10.2118/191251-PA
60. C.Wang, L.Zhong, Z.Cao, Y.Liu, J.Zou, Q.Wang. *Energy Fuels*, **34** (1), 95 (2020); https://doi.org/10.1021/acs.energyfuels.9b02796
61. D.Zhang, X.Du, X.Song, H.Wang, X.Li, Y.Jiang, M.Wang. *SPE J.*, **23** (03), 831 (2018); https://doi.org/10.2118/187953-PA
62. M.K.Al-Sakkaf, S.A.Onaizi. *Fuel*, **307**, 121845 (2022); https://doi.org/10.1016/j.fuel.2021.121845
63. Z.Li, D.Xu, Y.Yuan, H.Wu, J.Hou, W.Kang, B.Bai. *Adv. Colloid Interface Sci.*, **277**, 102119 (2020); https://doi.org/10.1016/j.cis.2020.102119
64. M.Adil, S.A.Onaizi. *Fuel*, **319**, 123667 (2022); https://doi.org/10.1016/j.fuel.2022.123667
65. H.H.W.B.Hansen, G.Kijanka, L.Ouyang, N.-T.Nguyen, H.An. *J. Mol. Liq.*, **399**, 124323 (2024); https://doi.org/10.1016/j.molliq.2024.124323
66. V.C.Santanna, F.D.S.Curbelo, T.N.Castro Dantas, A.A.Dantas Neto, H.S.Albuquerque, A.I.C.Garnica. *J. Pet. Sci. Eng.*, **66** (3–4), 117 (2009); https://doi.org/10.1016/j.petrol.2009.01.009
67. Z.Jeirani, B.Mohamed Jan, B.Si Ali, I.M.Noor, C.H.See, W.Saphanuchart. *J. Ind. Eng. Chem.*, **19** (4), 1304 (2013); https://doi.org/10.1016/j.jiec.2012.12.032
68. J.Yin, J.Wu, N.Wu, W.Liu, Y.Wang, C.Xian, W.Jia. *J. Mol. Liq.*, **405**, 125036 (2024); https://doi.org/10.1016/j.molliq.2024.125036
69. N.Kumar, A.Mandal. *J. Mol. Liq.*, **319**, 114087 (2020); https://doi.org/10.1016/j.molliq.2020.114087

70. A.Kaushik, D.Joshi, R.Kumar Saw, K.Bala Rathi, S.Mitra, A.Mandal. *Fuel*, **359**, 130500 (2024); https://doi.org/10.1016/j.fuel.2023.130500
71. S.A.Onaizi. *Sep. Purif. Technol.*, **281**, 119956 (2022); https://doi.org/10.1016/j.seppur.2021.119956
72. M.Kharazi, J.Saien. *J. Pet. Sci. Eng.*, **219**, 111090 (2022); https://doi.org/10.1016/j.petrol.2022.111090
73. A.Mandal, A.Samanta, A.Bera, K.Ojha. *Ind. Eng. Chem. Res.*, **49** (24), 12756 (2010); https://doi.org/10.1021/ie101589x
74. T.Sharma, G.S.Kumar, B.H.Chon, J.S.Sangwai. *J. Ind. Eng. Chem.*, **22**, 324 (2015); https://doi.org/10.1016/j.jiec.2014.07.026
75. A.Mandal, A. Bera. *Int. J. Chem. Mol. Eng.*, **6** (7), 537 (2012); https://doi.org/10.5281/ZENODO.1074477
76. H.Pei, G.Zhang, J.Ge, J.Zhang, Q.Zhang. *Colloids Surf. A: Physicochem. Eng. Asp.*, **484**, 478 (2015); https://doi.org/10.1016/j.colsurfa.2015.08.025
77. M.Li, W.Kang, Z.Li, H.Yang, R.Jia, Y.He, X.Kang, Z.Zheng, Y.Wang, B.Sarsenbekuly, M.Gabdullin. *Phys. Fluids*, **33** (7), 072002 (2021); https://doi.org/10.1063/5.0058759
78. Y.Guo, X.Zhang, X.Wang, L.Zhang, Z.Xu, D.Sun. *Langmuir*, **40** (2), 1364 (2024); https://doi.org/10.1021/acs.langmuir.3c03019
79. M.I.I.M.Noor, A.Islam, S.Saalah, C.C.Ken, S.M.Anisuzzaman, Z.Kamin. *IOP Conf. Ser. Mater. Sci. Eng.*, **606** (1), 012004 (2019); https://doi.org/10.1088/1757-899X/606/1/012004
80. Q.Sun, Z.-H.Zhou, L.Han, X.-Y.Zou, G.-Q.Li, Q.Zhang, F.Zhang, L.Zhang, L.Zhang. *Molecules*, **28** (4), 1672 (2023); https://doi.org/10.3390/molecules28041672
81. Z.Chen, M.Dong, M.Husein, S.Bryant. *Ind. Eng. Chem. Res.*, **57** (21), 7301 (2018); https://doi.org/10.1021/acs.iecr.8b00889
82. H.Li, H.Lu, Y.Zhang, D.Liu, J.Chen. *J. Mol. Liq.*, **336**, 116174 (2021); https://doi.org/10.1016/j.molliq.2021.116174
83. M.Yu.Koroleva, E.V.Yurtov. *Russ. Chem. Rev.*, **90** (3), 293 (2021); https://doi.org/10.1070/RCR4962
84. Z.Fajun, T.Zhexi, Y.Zhongqi, S.Hongzhi, W.Yanping, Z.Yufei. *Energy Sci. Eng.*, **8** (12), 4158 (2020); https://doi.org/10.1002/ese3.814
85. S.Mahdavi, A.Mousavi Moghadam. *Energy Fuels*, **35** (23), 19211 (2021); https://doi.org/10.1021/acs.energyfuels.1c02270
86. Z.Taherian, A.S.Dehaghani, S.Ayatollahi, R.Kharrat. *J. Pet. Sci. Eng.*, **205**, 108824 (2021); https://doi.org/10.1016/j.petrol.2021.108824
87. A.M.Sousa, H.A.Matos, M.J.Pereira. *Ind. Eng. Chem. Res.*, **61** (1), 1 (2022); https://doi.org/10.1021/acs.iecr.1c02744
88. S.Mohammadreza Shams, Y.Kazemzadeh, M.Riazi, F.B.Cortés. *J. Mol. Liq.*, **362**, 119783 (2022); https://doi.org/10.1016/j.molliq.2022.119783
89. M.Rayhani, M.Simjoo, M.Chahardowli. *J. Pet. Sci. Eng.*, **211**, 110123 (2022); https://doi.org/10.1016/j.petrol.2022.110123
90. H.Garmsiri, S.Jahani, M.Sharifi, Y.Kazemzadeh, M.Riazi, R.Azin. *J. Dispers. Sci. Technol.*, 1 (2023); https://doi.org/10.1080/01932691.2023.2288094
91. M.Shafiei, Y.Kazemzadeh, G.M.Shirazy, M.Riazi. *J. Mol. Liq.*, **364**, 120028 (2022); https://doi.org/10.1016/j.molliq.2022.120028
92. J.S.U.Tabaniag, M.Q.D.Abad, C.J.R.Morcelos, G.V.B.Geraldino, J.L.M.Alvarado, E.C.R.Lopez. *J. Eng. Appl. Sci.*, **70** (1), 154 (2023); https://doi.org/10.1186/s44147-023-00322-5
93. X.Hao, Y.Elakneswaran, M.Shimokawara, Y.Kato, R.Kitamura, N.Hiroyoshi. *Energy Fuels*, **38** (2), 979 (2024); https://doi.org/10.1021/acs.energyfuels.3c04034
94. J.Qiao, S.Cheng, W.Song, C.Jian, W.Wang, D.Zhang, Y.Xu. *Energy Fuels*, **33** (5), 3881 (2019); https://doi.org/10.1021/acs.energyfuels.8b03975
95. F.Goodarzi, S.Zendehboudi. *Can. J. Chem. Eng.*, **97** (1), 281 (2019); https://doi.org/10.1002/cjce.23336
96. S.Maaref, S.Ayatollahi, N.Rezaei, M.Masihi. *Ind. Eng. Chem. Res.*, **56** (15), 4549 (2017); https://doi.org/10.1021/acs.iecr.7b00432
97. N.Rezaei, A.Firoozabadi. *Energy Fuels*, **28** (3), 2092 (2014); https://doi.org/10.1021/ef402223d
98. J.S.Lim, S.F.Wong, M.C.Law, Y.Samyudia, S.S.Dol. *J. Appl. Sci.*, **15** (2), 167 (2015); https://doi.org/10.3923/jas.2015.167.172
99. L.Yu, M.Dong, B.Ding, Y.Yuan. *Chem. Eng. Sci.*, **189**, 165 (2018); https://doi.org/10.1016/j.ces.2018.05.033
100. Tharwat F.Tadros. *An Introduction to Surfactants*. (Berlin, Boston: Walter de Gruyter GmbH, 2014)
101. M.Soleimani Zohr Shiri, W.Henderson, M.R.Mucalo. *Materials*, **12** (12), 1896 (2019); https://doi.org/10.3390/ma12121896
102. S.Chowdhury, S.Shrivastava, A.Kakati, J.S.Sangwai. *Ind. Eng. Chem. Res.*, **61** (1), 21 (2022); https://doi.org/10.1021/acs.iecr.1c03301
103. R.A.Gonçalves, K.Holmberg, B.Lindman. *J. Mol. Liq.*, **375**, 121335 (2023); https://doi.org/10.1016/j.molliq.2023.121335
104. W.Faisal, F.Almomani. *Chemosphere*, **291**, 133099 (2022); https://doi.org/10.1016/j.chemosphere.2021.133099
105. A.F.Belhaj, K.A.Elraies, S.M.Mahmood, N.N.Zulkifli, S.Akbari, O.S.Hussien. *J. Pet. Explor. Prod. Technol.*, **10** (1), 125 (2020); https://doi.org/10.1007/s13202-019-0685-y
106. R.Sarkar, A.Pal, A.Rakshit, B.Saha. *J. Surfactants Deterg.*, **24** (5), 709 (2021); https://doi.org/10.1002/jsde.12542
107. M.S.Kamal. *J. Surfactants Deterg.*, **19** (2), 223 (2016); https://doi.org/10.1007/s11743-015-1776-5
108. A.Shalan, S.H.Kadhim. *Univ. Thi-Qar J. Sci.*, **10** (2), 33 (2023); https://doi.org/10.32792/utq/utjsci/v10i2.1069
109. X.Deng, M.S.Kamal, S.Patil, S.M.Shakil, E.A.Shalabi, A.Hassan. In *GOTECH,* SPE-219216-MS, (SPE: Dubai, UAE, 2024); https://doi.org/10.2118/219216-MS
110. W.C.Griffin. *J. Soc. Cosmet. Chem*., (1), 311 (1949)
111. M.Kawaguchi. *Adv. Colloid Interface Sci.*, **233**, 186 (2016); https://doi.org/10.1016/j.cis.2015.06.005
112. E.I.Lysakova, A.D.Skorobogatova, A.L.Neverov, M.I.Pryazhnikov, V.Ya.Rudyak, A.V.Minakov. *J. Mol. Liq.*, **411**, 125448 (2024); https://doi.org/10.1016/j.molliq.2024.125448
113. B.Wei, L.Romero-Zerón, D.Rodrigue. *J. Pet. Explor. Prod. Technol.*, **4** (2), 113 (2014); https://doi.org/10.1007/s13202-013-0087-5
114. S.Kumar, A.Mandal. *Polymer*, **120**, 30 (2017); https://doi.org/10.1016/j.polymer.2017.05.051
115. M.Chung, D.Kim, A.E.Herr. *Analyst*, **139** (22), 5635 (2014); https://doi.org/10.1039/C4AN01179A
116. N.Kumar, A.Mandal. *Eur. Polym. J.*, **109**, 265 (2018); https://doi.org/10.1016/j.eurpolymj.2018.09.058
117. J.Wang, Y.Sun, J.Zhou, Y.Liu, H.Liang, J.Sun, G.Liu, M.Di Serio, R.Vitiello. *J. Mol. Liq.*, **379**, 121694 (2023); https://doi.org/10.1016/j.molliq.2023.121694
118. H.Zheng, H.Liu, K.Tong. *ACS Omega*, **9** (10), 11243 (2024); https://doi.org/10.1021/acsomega.3c06390
119. X.Chen, Y.-Q.Li, Z.-Y.Liu, J.Trivedi, W.-B.Gao, M.-Y.Sui. *Pet. Sci.*, **20** (1), 619 (2023); https://doi.org/10.1016/j.petsci.2022.11.002
120. F.Afolabi, S.M.Mahmood, N.Yekeen, S.Akbari, H.Sharifigaliuk. *J. Pet. Sci. Eng.*, **208**, 109358 (2022); https://doi.org/10.1016/j.petrol.2021.109358
121. M.Yu. Koroleva, E.V.Yurtov. *Russ. Chem. Rev.*, **91** (5), RCR5024 (2022); https://doi.org/10.1070/RCR5024
122. N.Kumar, A.Mandal. *J. Mol. Liq.*, **266**, 147 (2018); https://doi.org/10.1016/j.molliq.2018.06.069
123. S.Davoodi, M.Al-Shargabi, D.A.Wood, V.S.Rukavishnikov, K.M.Minaev. *Fuel*, **324**, 124669 (2022); https://doi.org/10.1016/j.fuel.2022.124669
124. W.Wang, X.Dong, H.Liu, Y.Peng, Z.Chen, Y.Li, Y.Guo. Fly Ash Nanoparticle-Stabilized Emulsions for Improve Mobility Control Application. In *Day 2 Tue, June 07, 2022*; SPE: Madrid, Spain, 2022; p D021S004R003; https://doi.org/10.2118/209646-MS
125. S.Kinra, R.Pal. *Colloids Interfaces*, **7** (2), 36 (2023); https://doi.org/10.3390/colloids7020036

126. A.Pal, R.Pal. *Nanomaterials*, **12** (14), 2391 (2022); https://doi.org/10.3390/nano12142391
127. T.Zhao, J.Chen, Y.Chen, Y.Zhang, J.Peng. *J. Dispers. Sci. Technol.*, **42** (6), 934 (2021); https://doi.org/10.1080/01932691.2020.1721297
128. A.I.A.Mohamed, I.A.Hussein, A.S.Sultan, G.A.Al-Muntasheri. *J. Pet. Sci. Eng.*, **160**, 302 (2018); https://doi.org/10.1016/j.petrol.2017.10.077
129. H.S.Hagar, S.R.Jufar, J.H.Lee, N.Al-mahbashi, M.B.Alameen, S.Kwon, A.H.Jagaba, U.Rathnayake. *Case Stud. Chem. Environ. Eng.*, **8**, 100503 (2023); https://doi.org/10.1016/j.cscee.2023.100503
130. B.Aldemir Dikici, F.Claeyssens. *Front. Bioeng. Biotechnol.*, **8**, 875 (2020); https://doi.org/10.3389/fbioe.2020.00875
131. M.Zhao, K.Liu, X.Meng, Z.Ma, C.Dai. *Fuel*, **371**, 131985 (2024); https://doi.org/10.1016/j.fuel.2024.131985
132. M.Chi, J.Cui, J.Hu, J.Fan, S.Du, P.Xiao, S.Hu, S.Sun. *J. Anal. Appl. Pyrolysis*, **181**, 106603 (2024); https://doi.org/10.1016/j.jaap.2024.106603
133. R.He, S.Sun, J.Cui, M.Chi, Z.Wang, S.Hu. *Phys. Chem. Chem. Phys.*, **25** (37), 25780 (2023); https://doi.org/10.1039/D3CP03400C
134. Y.Meng, W.Sun, H.Yang, W.Wang, N.Jin, Y.Zhao, X.Zhang, H.Lü. *Colloids Surf. A: Physicochem. Eng. Asp.*, **592**, 124603 (2020); https://doi.org/10.1016/j.colsurfa.2020.124603
135. H.Wu, K.Hou, G.Xu, G.Li, J.Chang, T.Luan, W.Shao, J.Hou. *ACS Appl. Nano Mater.*, **7** (2), 1835 (2024); https://doi.org/10.1021/acsanm.3c05079
136. H.Jia, J.Dai, L.Miao, X.Wei, H.Tang, P.Huang, H.Jia, J.He, K.Lv, D.Liu. *Colloids Surf. A: Physicochem. Eng. Asp.*, **622**, 126658 (2021); https://doi.org/10.1016/j.colsurfa.2021.126658
137. J.Hou, J.Du, H.Sui, L.Sun. *Front. Chem. Sci. Eng.*, **16** (8), 1165 (2022); https://doi.org/10.1007/s11705-021-2120-4
138. L.Niedner, G.Kickelbick. *Nanoscale*, **16** (15), 7396 (2024); https://doi.org/10.1039/D3NR04907H
139. T.L.Rasool, A.A.Mohammed, V.Ravankhah. *Iraqi J. Chem. Pet. Eng.*, **25** (1) (2024)
140. H.Jia, H.Wu, X.Wei, Y.Han, Q.Wang, J.Song, J.Dai, H.Yan, D.Liu. *Colloids Surf. A: Physicochem. Eng. Asp.*, **603**, 125278 (2020); https://doi.org/10.1016/j.colsurfa.2020.125278
141. Z.Yan, Z.Xu, J.Yu, M.Jaroniec. *J. Colloid Interface Sci.*, **501**, 164 (2017); https://doi.org/10.1016/j.jcis.2017.04.050
142. H.Jia, J.He, Y.Xu, T.Wang, L.Zhang, B.Wang, X.Jiang, X.Li, X.Zhang, K.Lv. *Colloids Surf. A: Physicochem. Eng. Asp.*, **638**, 128333 (2022); https://doi.org/10.1016/j.colsurfa.2022.128333
143. E.Nourafkan, Z.Hu, D.Wen. *J. Colloid Interface Sci.*, **519**, 44 (2018); https://doi.org/10.1016/j.jcis.2018.02.032
144. A.S.Dibaji, A.Rashidi, S.Baniyaghoob, A.Shahrabadi. *Chem. Eng. Res. Des.*, **186**, 599 (2022); https://doi.org/10.1016/j.cherd.2022.08.034
145. R.Ma, M.Zeng, D.Huang, J.Wang, Z.Cheng, Q.Wang. *J. Colloid Interface Sci.*, **601**, 106 (2021); https://doi.org/10.1016/j.jcis.2021.05.104
146. W.Tang, C.Zou, H.Liang, C.Da, Z.Zhao. *J. Pet. Sci. Eng.*, **214**, 110458 (2022); https://doi.org/10.1016/j.petrol.2022.110458
147. C.Soldano, A.Mahmood, E.Dujardin. *Carbon*, **48** (8), 2127 (2010); https://doi.org/10.1016/j.carbon.2010.01.058
148. L.A.Chernozatonskii, P.B.Sorokin, A.A.Artukh. *Russ. Chem. Rev.*, **83** (3), 251 (2014); https://doi.org/10.1070/RC2014v083n03ABEH004367
149. S.Tajik, A.Shahrabadi, A.Rashidi, M.Jalilian, A.Yadegari. *Colloids Surf. A: Physicochem. Eng. Asp.*, **556**, 253 (2018); https://doi.org/10.1016/j.colsurfa.2018.08.029
150. L.Rong, A.Santra, G.Ross, R.C.Advincula. *MRS Commun.*, **13** (3), 445 (2023); https://doi.org/10.1557/s43579-023-00354-1
151. L.Fu, K.Liao, B.Tang, L.Jiang, W.Huang. *Nanomaterials*, **10** (6), 1013 (2020); https://doi.org/10.3390/nano10061013
152. A.Roy, D.Kabra, G.Pareek, K.Kumari, P.P.Kashyap, S.Naik, U.Chadha, S.K.Selvaraj. *Nano Express*, **4** (2), 022002 (2023); https://doi.org/10.1088/2632-959X/acdc40
153. M.AfzaliTabar, A.Rashidi, M.Alaei, H.Koolivand, S.Pourhashem, S.Askari. *J. Mol. Liq.*, **307**, 112984 (2020); https://doi.org/10.1016/j.molliq.2020.112984
154. R.Khoramian, A.Ramazani S.A., M.Hekmatzadeh, R.Kharrat, E.Asadian. *ACS Appl. Nano Mater.*, **2** (9), 5730 (2019); https://doi.org/10.1021/acsanm.9b01215
155. X.Chen, X.Song, J.Huang, C.Wu, D.Ma, M.Tian, H.Jiang, P.Huang. *Energy Fuels*, **31** (12), 13439 (2017); https://doi.org/10.1021/acs.energyfuels.7b02672
156. J.Kim, L.J.Cote, F.Kim, W.Yuan, K.R.Shull, J.Huang. *J. Am. Chem. Soc.*, **132** (23), 8180 (2010); https://doi.org/10.1021/ja102777p
157. M.Elshawaf. In *All Days*. (Dammam, Saudi Arabia: SPE, 2018). P. SPE-192245-MS; https://doi.org/10.2118/192245-MS
158. H.Radnia, A.R.Solaimany Nazar, A.Rashidi. *J. Pet. Sci. Eng.*, **175**, 868 (2019); https://doi.org/10.1016/j.petrol.2019.01.034
159. V.B.Souza, C.R.E.Mansur. *Energy Fuels*, **29** (12), 7855 (2015); https://doi.org/10.1021/acs.energyfuels.5b01996
160. M.Tang, X.Wang, F.Wu, Y.Liu, S.Zhang, X.Pang, X.Li, H.Qiu. *Carbon*, **71**, 238 (2014); https://doi.org/10.1016/j.carbon.2014.01.034
161. M.AfzaliTabar, M.Alaei, R.Ranjineh Khojasteh, F.Motiee, A.M.Rashidi. *Sci. Iran*, **24** (6), 3491 (2017); https://doi.org/10.24200/sci.2017.4428
162. R.Goyat, J.Singh, A.Umar, Y.Saharan, A.A.Ibrahim, S.Akbar, S.Baskoutas. *Waste Manag. Res. J. Sustain. Circ. Econ.*, **42** (8), 0734242X231223914 (2024); https://doi.org/10.1177/0734242X231223914
163. M.Alaei, M.AfzaliTabar, A.Rashidi. *Nashrieh Shimi Va Mohandesi Shimi Iran*, **40** (4), 215 (2022)
164. N.S.K.Abu Zaid, Mustafa.S.Nasser, S.A.Onaizi. *J. Mol. Liq.*, **393**, 123617 (2024); https://doi.org/10.1016/j.molliq.2023.123617
165. M.Tang, T.Wu, X.Xu, L.Zhang, F.Wu. *Mater. Res. Bull.*, **60**, 118 (2014); https://doi.org/10.1016/j.materresbull.2014.08.019
166. X.Li, D.Zhu, X.Wang. *J. Colloid Interface Sci.*, **310** (2), 456 (2007); https://doi.org/10.1016/j.jcis.2007.02.067
167. D.Zhu, X.Li, N.Wang, X.Wang, J.Gao, H.Li. *Curr. Appl. Phys.*, **9** (1), 131 (2009); https://doi.org/10.1016/j.cap.2007.12.008
168. S.Chakraborty, I.Sarkar, A.Ashok, I.Sengupta, S.K.Pal, S.Chakraborty. *Powder Technol.*, **335**, 285 (2018); https://doi.org/10.1016/j.powtec.2018.05.004
169. E.M.Hotze, T.Phenrat, G.V.Lowry. *J. Environ. Qual.*, **39** (6), 1909 (2010); https://doi.org/10.2134/jeq2009.0462
170. M.J.Vold. *J. Colloid Sci.*, **9** (5), 451 (1954); https://doi.org/10.1016/0095-8522(54)90032-X
171. K.P.Velikov, O.D.Velev. In *Colloid Stability and Application in Pharmacy*. Ed. T.F.Tadros. (Wiley, 2007). P. 277; https://doi.org/10.1002/9783527631117.ch9
172. J.Feng, Y.Yin. *Adv. Mater.*, **31** (38), 1802349 (2019); https://doi.org/10.1002/adma.201802349
173. A.V.Nushtaeva, P.M.Kruglyakov. *Colloid J.*, **65** (3), 341 (2003); https://doi.org/10.1023/A:1024262924419
174. N.J.Hadia, Y.H.Ng, L.P.Stubbs, O.Torsæter. *Nanomaterials*, **11** (3), 707 (2021); https://doi.org/10.3390/nano11030707
175. X.Li, W.Chen, C.Zou. *Powder Technol.*, **361**, 957 (2020); https://doi.org/10.1016/j.powtec.2019.10.106
176. J.Tang, P.J.Quinlan, K.C.Tam. *Soft Matter*., **11** (18), 3512 (2015); https://doi.org/10.1039/C5SM00247H
177. A.A.Umar, I.B.M.Saaid, A.A.Sulaimon, R.B.M.Pilus. *J. Pet. Sci. Eng.*, **165**, 673 (2018); https://doi.org/10.1016/j.petrol.2018.03.014
178. J.-X.Liu, H.-J.Zhu, P.Wang, J.-M.Pan. *Pet. Sci.*, **18** (5), 1551 (2021); https://doi.org/10.1016/j.petsci.2021.10.001
179. J.Frelichowska, M.-A.Bolzinger, Y.Chevalier. *J. Colloid Interface Sci.*, **351** (2), 348 (2010); https://doi.org/10.1016/j.jcis.2010.08.019
180. T.Liang, J.-R.Hou, M.Qu, J.-X.Xi, I.Raj. *Pet. Sci.*, **19** (2), 882 (2022); https://doi.org/10.1016/j.petsci.2021.11.011

181. E.Yazdani Sadati, E.Sahraei. *J. Pet. Explor. Prod. Technol.*, **9** (4), 2613 (2019); https://doi.org/10.1007/s13202-019-0679-9
182. M.M.Yousufi, I.B.Dzulkarnain, M.E.M.Elhaj, S.Ahmed. *Processes*, **11** (9), 2672 (2023); https://doi.org/10.3390/pr11092672
183. I.Kim, A.J.Worthen, K.P.Johnston, D.A.DiCarlo, C.Huh. *J. Nanoparticle Res.*, **18** (4), 82 (2016); https://doi.org/10.1007/s11051-016-3395-0
184. Y.Zan, J.Liu, Z.Zhao, Y.Wei, N.Yang, H.Zhang, X.Wang, Y.Kang. *ACS Appl. Bio Mater.*, **8** (1), 652 (2025); https://doi.org/10.1021/acsabm.4c01501
185. M.Luo, G.K.Olivier, J.Frechette. *Soft Matter*., **8** (47), 11923 (2012); https://doi.org/10.1039/c2sm26890f
186. G.Kaptay. *Colloids Surf. A: Physicochem. Eng. Asp.*, **282**–**283**, 387 (2006); https://doi.org/10.1016/j.colsurfa.2005.12.021
187. R.Aveyard, B.P.Binks, J.H.Clint. *Adv. Colloid Interface Sci.*, **100**–**102**, 503 (2003); https://doi.org/10.1016/S0001-8686(02)00069-6
188. B.R.Midmore. *Colloids Surf. Physicochem. Eng. Asp.*, **132** (2–3), 257 (1998); https://doi.org/10.1016/S0927-7757(97)00094-0
189. P.J.P.Espitia, C.A.Fuenmayor, C.G.Otoni. *Compr. Rev. Food Sci. Food Saf.*, **18** (1), 264 (2019); https://doi.org/10.1111/1541-4337.12405
190. H.Feng, W.Kang, H.Wu, Z.Li, J.Chen, Q.Zhou, B.Bai. *J. Dispers. Sci. Technol.*, **39** (8), 1214 (2018); https://doi.org/10.1080/01932691.2017.1391699
191. Y.Yang, W.-F.Pu. *J. Dispers. Sci. Technol.*, **41** (7), 1065 (2020); https://doi.org/10.1080/01932691.2019.1614044
192. S.Shi, Y.Wang, L.Wang, Y.Jin, T.Wang, J.Wang. *J. Dispers. Sci. Technol.*, **36** (5), 660 (2015); https://doi.org/10.1080/01932691.2014.905954
193. H.Schubert, K.Ax, O.Behrend. *Trends Food Sci. Technol.*, **14** (1–2), 9 (2003); https://doi.org/10.1016/S0924-2244(02)00245-5
194. A.Gupta, H.B.Eral, T.A.Hatton, P.S.Doyle. *Soft Matter*., **12** (5), 1452 (2016); https://doi.org/10.1039/C5SM02051D
195. Z.Wang, M.A.Neves, H.Isoda, M.Nakajima. *Jpn. J. Food Eng.*, **16** (4), 263 (2015); https://doi.org/10.11301/jsfe.16.263
196. M.A.Saad, M.Kamil, N.H.Abdurahman, R.M.Yunus, O.I.Awad. *Processes*, **7** (7), 470 (2019); https://doi.org/10.3390/pr7070470
197. J.Hong, Z.Wang, J.Li, Y.Xu, H.Xin. *Energy Fuels*, **37** (14), 9914 (2023); https://doi.org/10.1021/acs.energyfuels.3c00809
198. F.Souas, A.Safri, A.Benmounah. *Pet. Res.*, **6** (2), 116 (2021); https://doi.org/10.1016/j.ptlrs.2020.11.001
199. M.Shafiei, Y.Kazemzadeh, D.A.Martyushev, Z.Dai, M.Riazi. *Sci. Rep.*, **13** (1), 4100 (2023); https://doi.org/10.1038/s41598-023-31379-0
200. A.M.Al-Sabagh, M.M.Emara, M.R.Noor El-Din, W.R.Aly. *Egypt. J. Pet.*, **20** (2), 17 (2011); https://doi.org/10.1016/j.ejpe.2011.06.005
201. E.Jafarbeigi, F.Salimi, E.Kamari, M.Mansouri. *Pet. Sci.*, **19** (4), 1779 (2022); https://doi.org/10.1016/j.petsci.2021.12.022
202. S.M.T.Gharibzahedi, S.M.Jafari. In *Nanoemulsions*. (Elsevier, 2018). P. 233; https://doi.org/10.1016/B978-0-12-811838-2.00009-6
203. M.H.V.Bahrun, Z.Kamin, N.I.R.Idris, M.A.N.Aladin, A.Bono. *Synthesis and Optimization of Surfactant-Stabilized Palm Oil-Based Nanoemulsion for Enhanced Oil Recovery*. (Almaty, Kazakhstan, 2022). P. 030006; https://doi.org/10.1063/5.0099698
204. M.A.N.Aladin, M.H.V.Bahrun, Z.Kamin, Z.Zakaria, A.Bono. *J. Teknol.*, **86** (3), 1 (2024); https://doi.org/10.11113/jurnalteknologi.v86.20811
205. N.Pal, N.Kumar, A.Mandal. *Langmuir*, **35** (7), 2655 (2019); https://doi.org/10.1021/acs.langmuir.8b03364
206. M.K.Al-Sakkaf, S.A.Onaizi. *Fuel*, **361**, 130604 (2024); https://doi.org/10.1016/j.fuel.2023.130604
207. K.Meleson, S.Graves, T.G.Mason. *Soft Mater.*, **2** (2–3), 109 (2004); https://doi.org/10.1081/SMTS-200056102
208. S.Kotta, A.W.Khan, S.H.Ansari, R.K.Sharma, J.Ali. *Drug Deliv.*, **22** (4), 455 (2015); https://doi.org/10.3109/10717544.2013.866992
209. T.Z.Soofiani, M.Nasr Esfahany, M.G.Rasteiro, P.Ferreira. *Iran. Polym. J.*, **31** (11), 1409 (2022); https://doi.org/10.1007/s13726-022-01088-y
210. R.Gupta, D.Rousseau. *Food Funct.*, **3** (3), 302 (2012); https://doi.org/10.1039/c2fo10203j
211. N.H.Che Marzuki, R.A.Wahab, M.Abdul Hamid. *Biotechnol. Biotechnol. Equip.*, **33** (1), 779 (2019); https://doi.org/10.1080/13102818.2019.1620124
212. T.M.Ho, F.Abik, K.S.Mikkonen. *Crit. Rev. Food Sci. Nutr.*, **62** (18), 4908 (2022); https://doi.org/10.1080/10408398.2021.1879727
213. F.Ganachaud, J.L.Katz. *ChemPhysChem*, **6** (2), 209 (2005); https://doi.org/10.1002/cphc.200400527
214. Z.Li, H.Wu, M.Yang, J.Jiang, D.Xu, H.Feng, Y.Lu, W.Kang, B.Bai, J.Hou. *Energy Fuels*, **32** (3), 3119 (2018); https://doi.org/10.1021/acs.energyfuels.7b03720
215. Z.Li, W.Kang, B.Bai, H.Wu, C.Gou, Y.Yuan, D.Xu, Y.Lu, J.Hou. *Energy Fuels*, **33** (9), 8279 (2019); https://doi.org/10.1021/acs.energyfuels.9b01796
216. G.T.Vladisavljević. *Colloids Surf. A: Physicochem. Eng. Asp.*, **579**, 123709 (2019); https://doi.org/10.1016/j.colsurfa.2019.123709
217. J.Mugabi, K.Naohiro, Y.Hiroki, M.Miki, N.Igura, M.Shimoda. *J. Chem. Eng. Jpn.*, **52** (3), 259 (2019); https://doi.org/10.1252/jcej.18we074
218. O.Alliod, E.Almouazen, G.Nemer, H.Fessi, C.Charcosset. *J. Pharm. Sci.*, **108** (8), 2708 (2019); https://doi.org/10.1016/j.xphs.2019.03.026
219. Y.Liu, Q.Jiang, K.Zhou, Q.Gu, Z.Zhong, W.Jing, Y.Fan, W.Xing. *Appl. Surf. Sci.*, **665**, 160364 (2024); https://doi.org/10.1016/j.apsusc.2024.160364
220. K.Juraij, A.Niroula, Y.Greish, P.K.S.Mural, A.Nazir, M.Z.Iqbal. *J. Membr. Sci.*, **717**, 123622 (2025); https://doi.org/10.1016/j.memsci.2024.123622
221. S.Gehrmann, H.Bunjes. *J. Pharm. Sci.*, **106** (8), 2068 (2017); https://doi.org/10.1016/j.xphs.2017.04.066
222. Z.Toprakcioglu, P.K.Challa, D.B.Morse, T.Knowles. *Sci. Adv.*, **6** (6), eaay7952 (2020); https://doi.org/10.1126/sciadv.aay7952
223. E.Chiesa, R.Dorati, S.Pisani, B.Conti, G.Bergamini, T.Modena, I.Genta. *Pharmaceutics*, **10** (4), 267 (2018); https://doi.org/10.3390/pharmaceutics10040267
224. C.Priest, M.D.Reid, C.P.Whitby. *J. Colloid Interface Sci.*, **363** (1), 301 (2011); https://doi.org/10.1016/j.jcis.2011.07.060
225. K.Schroën, O.Bliznyuk, K.Muijlwijk, S.Sahin, C.C.Berton-Carabin. *Curr. Opin. Food Sci.*, **3**, 33 (2015); https://doi.org/10.1016/j.cofs.2014.11.009
226. I.F.Guha, S.Anand, K.K.Varanasi. *Nat. Commun.*, **8** (1), 1371 (2017); https://doi.org/10.1038/s41467-017-01420-8
227. S.Anand, V.Galavan, M.U.Mulik. *Adv. Sci.*, **11** (15), 2307443 (2024); https://doi.org/10.1002/advs.202307443
228. M.M.Fryd, T.G.Mason. *J. Phys. Chem. Lett.*, **1** (23), 3349 (2010); https://doi.org/10.1021/jz101365h
229. J.Feng, M.Roché, D.Vigolo, L.N.Arnaudov, S.D.Stoyanov, T.D.Gurkov, G.G.Tsutsumanova, H.A.Stone. *Nat. Phys.*, **10** (8), 606 (2014); https://doi.org/10.1038/nphys3003
230. M.Sagir, M.Mushtaq, M.S.Tahir, M.B.Tahir, A.R.Shaik. *Surfactants for Enhanced Oil Recovery Applications*. (Cham: Springer International Publishing, 2020); https://doi.org/10.1007/978-3-030-18785-9
231. M.K.Al-Sakkaf, S.A.Onaizi. *Fuel*, **344**, 128052 (2023); https://doi.org/10.1016/j.fuel.2023.128052
232. S.A.Onaizi. *Nanomaterials*, **12** (10), 1673 (2022); https://doi.org/10.3390/nano12101673
233. P.Cui, H.Zhang, S.Yuan. *Chem. Phys. Lett.*, **845**, 141315 (2024); https://doi.org/10.1016/j.cplett.2024.141315

234. P.Kundu, K.Arora, Y.Gu, V.Kumar, I.M.Mishra. *Can. J. Chem. Eng.*, **97** (7), 2039 (2019); https://doi.org/10.1002/cjce.23481
235. Y.Zhao, F.Peng, Y.Ke. *RSC Adv.*, **11** (4), 1952 (2021); https://doi.org/10.1039/D0RA06080A
236. M.J.Nazarahari, A.K.Manshad, M.Ali, J.A.Ali, A.Shafiei, S.M.Sajadi, S.Moradi, S.Iglauer, A.Keshavarz. *Fuel*, **298**, 120773 (2021); https://doi.org/10.1016/j.fuel.2021.120773
237. N.Pal, N.Kumar, R.K.Saw, A.Mandal. *J. Pet. Sci. Eng.*, **183**, 106464 (2019); https://doi.org/10.1016/j.petrol.2019.106464
238. F.Goodarzi, J.Kondori, N.Rezaei, S.Zendehboudi. *J. Mol. Liq.*, **295**, 111357 (2019); https://doi.org/10.1016/j.molliq.2019.111357
239. L.Tliba, M.Edokali, T.Moore, O.Choudhry, P.W.J.Glover, R.Menzel, A.Hassanpour. *J. Mol. Liq.*, **424**, 127021 (2025); https://doi.org/10.1016/j.molliq.2025.127021
240. G.Bassioni, S.Taha Taqvi. *J. Chem.*, **2015**, 1 (2015); https://doi.org/10.1155/2015/743179
241. D.Cabaleiro, S.Hamze, F.Agresti, P.Estellé, S.Barison, L.Fedele, S.Bobbo. *Energies*, **12** (17), 3334 (2019); https://doi.org/10.3390/en12173334
242. F.Peng, Y.Ke, Y.Zhao, X.Hu, X.Zhao. *RSC Adv.*, **9** (24), 13378 (2019); https://doi.org/10.1039/C8RA10595B
243. F.Peng, Y.Ke, S.Lu, Y.Zhao, X.Hu, Q.Deng. *RSC Adv.*, **9** (26), 14692 (2019); https://doi.org/10.1039/C9RA01383K
244. M.C.Teixeira, P.Severino, T.Andreani, P.Boonme, A.Santini, A.M.Silva, E.B.Souto. *Saudi Pharm. J.*, **25** (2), 231 (2017); https://doi.org/10.1016/j.jsps.2016.06.004
245. A.O.Gbadamosi, R.Junin, M.A.Manan, A.Agi, A.S.Yusuff. *Int. Nano Lett.*, **9** (3), 171 (2019); https://doi.org/10.1007/s40089-019-0272-8
246. J.N.Wilking, T.G.Mason. *Phys. Rev. E*, **75** (4), 041407 (2007); https://doi.org/10.1103/PhysRevE.75.041407
247. M.E.Helgeson, S.E.Moran, H.Z.An, P.S.Doyle. *Nat. Mater.*, **11** (4), 344 (2012); https://doi.org/10.1038/nmat3248
248. J.Foroozesh, S.Kumar. *J. Mol. Liq.*, **316**, 113876 (2020); https://doi.org/10.1016/j.molliq.2020.113876
249. R.Pal. *Fluids*, **1** (2), 11 (2016); https://doi.org/10.3390/fluids1020011
250. M.M.Fryd, T.G.Mason. *Annu. Rev. Phys. Chem.*, **63** (1), 493 (2012); https://doi.org/10.1146/annurev-physchem-032210-103436
251. Z.Sun, M.Li, S.Yuan, X.Hou, H.Bai, F.Zhou, X.Liu, M.Yang. *Energy*, **291**, 130226 (2024); https://doi.org/10.1016/j.energy.2023.130226
252. N.Kumar, A.Mandal. *Colloids Surf. A: Physicochem. Eng. Asp.*, **601**, 125043 (2020); https://doi.org/10.1016/j.colsurfa.2020.125043
253. D.Pradilla, W.Vargas, O.Alvarez. *Chem. Eng. Res. Des.*, **95**, 162 (2015); https://doi.org/10.1016/j.cherd.2014.10.016
254. H.Niu, W.Wang, Z.Dou, X.Chen, X.Chen, H.Chen, X.Fu. *Adv. Colloid Interface Sci.*, **311**, 102813 (2023); https://doi.org/10.1016/j.cis.2022.102813
255. D.Zare, J.R.Allison, K.M.McGrath. *Biomacromolecules*, **17** (5), 1572 (2016); https://doi.org/10.1021/acs.biomac.5b01709
256. Z.Wang, Y.Xu, Y.Liu, X.Liu, Z.Rui. *Arab. J. Sci. Eng.*, **45** (9), 7161 (2020); https://doi.org/10.1007/s13369-020-04840-9
257. H.Miyamoto, D.M.Rein, K.Ueda, C.Yamane, Y.Cohen. *Cellulose*, **24** (7), 2699 (2017); https://doi.org/10.1007/s10570-017-1290-1
258. P.Shi, H.Zhang, L.Lin, C.Song, Q.Chen, Z.Li. *RSC Adv.*, **9** (6), 3224 (2019); https://doi.org/10.1039/C8RA09670H
259. J.Liu, Y.Zhao, S.Ren. *Energy Fuels*, **29** (2), 1233 (2015); https://doi.org/10.1021/ef5019737
260. G.Imani, L.Zhang, M.J.Blunt, C.Xu, Y.Guo, H.Sun, J.Yao. *Int. J. Multiph. Flow*., **153**, 104107 (2022); https://doi.org/10.1016/j.ijmultiphaseflow.2022.104107
261. B.Munir, D.Du. *Eur. Phys. J. Plus*., **137** (11), 1266 (2022); https://doi.org/10.1140/epjp/s13360-022-03494-w
262. E.Olsson, G.Kreiss, S.Zahedi. *J. Comput. Phys.*, **225** (1), 785 (2007); https://doi.org/10.1016/j.jcp.2006.12.027
263. G.Rosengarten, D.J.E.Harvie, J.Cooper-White. *Appl. Math. Model.*, **30** (10), 1033 (2006); https://doi.org/10.1016/j.apm.2005.06.011
264. Z.Zhang, C.Drapaca, D.Gritsenko, J.Xu. *Phys. Fluids*, **30** (10), 102004 (2018); https://doi.org/10.1063/1.5045495
265. N.Kumar, N.Pal, A.Mandal. *J. Pet. Sci. Eng.*, **202**, 108579 (2021); https://doi.org/10.1016/j.petrol.2021.108579
266. N.Pal, A.Mandal. *J. Taiwan Inst. Chem. Eng.*, **122**, 1 (2021); https://doi.org/10.1016/j.jtice.2021.04.022
267. J.Wang, F.-J.Zhou. *Pet. Sci.*, **18** (1), 219 (2021); https://doi.org/10.1007/s12182-020-00482-6
268. X.Liang, T.Liang, F.Zhou, S.Yuan. In *Proceedings of the 8th Unconventional Resources Technology Conference*. (American Association of Petroleum Geologists: Online, 2020); https://doi.org/10.15530/urtec-2020-2899
269. R.D.Kaminsky, R.C.Wattenbarger, J.P.Lederhos, S.A.Leonardi. In *SPE Annual Technical Conference and Exhibition*. (Florence, Italy: SPE, 2010). P. SPE-135284-MS; https://doi.org/10.2118/135284-MS
270. G.Ren, B.Li, D.Lu, W.Di, L.Ren, L.Tian, P.Zhang, J.He, D.Sun. *J. Mol. Liq.*, **342**, 117469 (2021); https://doi.org/10.1016/j.molliq.2021.117469
271. D.Liu, J.Xu, H.Zhao, X.Zhang, H.Zhou, D.Wu, Y.Liu, P.Yu, Z.Xu, W.Kang, M.Fan. *Colloids Surf. A: Physicochem. Eng. Asp.*, **637**, 128235 (2022); https://doi.org/10.1016/j.colsurfa.2021.128235
272. H.Wu, Y.Luo, G.Li, Y.Yuan, J.Chang, N.Kang, J.Hou. *J. Mol. Liq.*, **425**, 127190 (2025); https://doi.org/10.1016/j.molliq.2025.127190
273. M.K.Adhikari, C.K.Yadav, S.Chaudhary, D.Nath, A.Bhattarai. *Next Research*, **2** (2), 100305 (2025); https://doi.org/10.1016/j.nexres.2025.100305